

NATIONAL TRANSPORTATION SAFETY BOARD

Office of Research and Engineering
Washington, D.C. 20594

September 23, 2016

Aircraft Performance Radar & Cockpit Visibility Study

by John O'Callaghan

Location: Moncks Corner, South Carolina
Date: July 7, 2015
Time: 11:00 Eastern Daylight Time (EDT) / 15:00 Coordinated Universal Time (UTC)
Aircraft: Cessna 150M, registration N3601V
Lockheed-Martin F-16CM, registration 96-0085
NTSB#: ERA15MA259A (C150)
ERA14MA259B (F-16)

CONTENTS

A. ACCIDENT 1

B. GROUP 1

C. SUMMARY 1

D. DETAILS OF THE INVESTIGATION 2

I. The accident airplanes 2

The Lockheed-Martin F-16 2

The Cessna 150M 2

II. Radar data 3

Description of ARSR and ASR radar data 3

Primary and secondary radar returns 3

Recorded radar data 4

Presentation of the radar data 5

Radar data uncertainty and estimates of C150 performance based on radar data 5

III. F-16 CSMU data and estimated collision geometry 7

Introduction 7

F-16 trajectory based on CSMU and radar data 7

Estimated collision time, location, and geometry 9

Winds computed from F-16 CSMU data 11

IV. Cockpit visibility study 11

Azimuth and elevation angles of “target” aircraft relative to “viewer” aircraft 11

Azimuth and elevation angles of airplane structures from laser scans 12

Results: azimuth and elevation angle calculations 13

V. Cockpit Display of Traffic Information (CDTI) Study 19

Introduction 19

NTSB CDTI simulation description 20

NTSB CDTI simulation results 21

E. CONCLUSIONS 22

F. REFERENCES 25

G. GLOSSARY 26

Acronyms 26

English symbols 27

Greek symbols 27

FIGURES

APPENDIX A: Computing the Azimuth and Elevation Angles of Airplane Cockpit Windows and other Structures from Laser Scans

APPENDIX B: Creating Geometrically Correct Cockpit Window “Masks” in Microsoft Flight Simulator X (FSX)

NATIONAL TRANSPORTATION SAFETY BOARD

Office of Research and Engineering
Washington, D.C. 20594

September 23, 2016

Aircraft Performance Radar & Cockpit Visibility Study

by John O'Callaghan

A. ACCIDENT

Location: Moncks Corner, South Carolina

Date: July 7, 2015

Time: 11:01 Eastern Daylight Time (EDT) / 15:01 Coordinated Universal Time (UTC)

Aircraft: Cessna 150M, registration N3601V (C150)

Lockheed-Martin F-16CM, registration 96-0085 (F-16)

NTSB#: ERA15MA259A (C150)

ERA14MA259B (F-16)

B. GROUP

Not Applicable

C. SUMMARY

On July 7, 2015, about 11:01 EDT¹, a Cessna 150M, N3601V, and a Lockheed Martin F-16CM, operated by the US Air Force, collided in midair near Moncks Corner, South Carolina. The private pilot and passenger aboard the Cessna died, and the Cessna was destroyed during the collision. The damaged F-16 continued to fly for about 2.5 minutes, during which the pilot activated the airplane's ejection system. The F-16 pilot ejected safely and incurred minor injuries, and the F-16 was destroyed after its subsequent collision with terrain and postimpact fire. Visual meteorological conditions (VMC) prevailed at the time of the accident. No flight plan was filed for the Cessna, which departed from Berkeley County Airport, Moncks Corner, South Carolina (KMKS), about 10:57, and was destined for Grand Strand Airport, North Myrtle Beach, South Carolina. The personal flight was conducted under the provisions of 14 Code of Federal Regulations (CFR) Part 91. The F-16 was operating on an instrument flight rules (IFR) flight plan and had departed from Shaw Air Force Base, Sumter, South Carolina, about 10:20.

This *Aircraft Performance Radar & Cockpit Visibility Study* presents the results of using Charleston Air Force Base / International Airport (KCHS) Surveillance Radar (ASR) data and recorded data from the F-16 to calculate the position and orientation of each airplane in the minutes preceding the collision. This information is then used to estimate the approximate location of each airplane in the other airplane's field of view (the "visibility study"), and to estimate the Cockpit Display of Traffic Information (CDTI) data that could have been presented to the pilots had the airplanes been equipped to provide this information. As described further in Section D-V, CDTI uses the Federal

¹ All times in this *Study* are in EDT based on a 24-hour clock, unless otherwise noted.

Aviation Administration (FAA) Automatic Dependent Surveillance – Broadcast (ADS-B) system to drive a traffic situation display in the cockpits of appropriately-equipped aircraft.

The sections that follow present the radar data and F-16 recorded data used in this *Study*, and describe the methods used to calculate aircraft speeds, orientation (pitch, yaw and roll angles), CDTI information, and cockpit visibility from this data. The results of these calculations are presented in the Figures and Tables described throughout the *Study*.

D. DETAILS OF THE INVESTIGATION

I. The accident airplanes

The Lockheed-Martin F-16

The F-16 is a single-seat, single-turbofan-powered fighter airplane. Figure 1 shows diagrams of the F-16, taken from Reference 1. A photograph of an F-16CM based at Shaw Air Force Base (AFB) with a paint scheme identical to the accident airplane (except for lettering) is shown in Figure 2. The geometry of this airplane was measured with a laser scanner in support of the cockpit visibility study described in Section D-IV and Appendix A.

The F-16 was equipped with a crash survivable memory unit (CSMU) and a digital flight control system seat data recorder (SDR) that recorded numerous flight data parameters. These devices were recovered from the accident F-16 and sent to the NTSB laboratory for data readout, as described in Reference 2. The data from the CSMU, including the airplane's pitch, roll, and heading angles, is used in the present *Study* to compute a more precise flight path than that available from radar data, and to evaluate the visibility of the C150 from the F-16 cockpit. These calculations are described in Sections D-III and D-IV.

The Cessna 150M

The C150 is a single-engine, two-seat high-wing airplane with a conventional tail. Figure 3 is a pre-accident photograph of the accident airplane (N3601V), and Figure 4 shows a 3-view image of the C150, taken from Reference 3. Table 1 provides some dimensions of the airplane, as well as relevant mass properties for N3601V on the accident flight. The empty weight of the airplane is based on the airplane weight and balance documentation found in the C150 wreckage. The pilot and passenger weights and takeoff fuel load were provided by the NTSB Investigator In Charge (IIC) in Reference 4. The full fuel load is an assumption, supported in part by security video depicting the pilot adding 15 gallons of fuel to the airplane. The amount of fuel in the airplane prior to this fueling is unknown.

Aerodynamic information for the C150 (such as the lift coefficient (C_L) as a function of angle of attack (α)) was provided to the NTSB by Textron Aviation (Textron). This information is used along with the gross weight and wing area shown in Table 1 in the analysis of the radar data for the C150 to estimate the pitch and roll angles throughout the flight (see Section D-II).

The geometry of an exemplar C150M that was made available to the NTSB by the Aircraft Owners and Pilots Association (AOPA) was measured with a laser scanner in support of the cockpit visibility study described in Section D-IV and Appendix A.

Item	Value
<i>Reference dimensions (from References 3 & 5):</i>	
Wing area	158.96 ft. ² (160 ft. ² used in <i>Study</i> calculations)
Wing span	33.3 ft.
<i>Mass properties for N3601V:</i>	
Empty weight	1127 pounds
Pilot weight	180 pounds
Passenger weight	195 pounds
Baggage weight (assumed)	41 pounds
Fuel weight	135 pounds (full fuel = 22.5 gallons @ 6 lb./gal.)
Total gross weight	1678 pounds

Table 1. Relevant geometry and mass properties for N3601V.

II. Radar data

Description of ARSR and ASR radar data

In general, two types of radar are used to provide position and track information, both for aircraft cruising at high altitudes between airport terminal airspaces, and those operating at low altitude and speeds within terminal airspaces.

Air Route Surveillance Radars (ARSRs) are long range (250 nmi) radars used to track aircraft cruising between terminal airspaces. ARSR antennas rotate at 5 to 6 RPM, resulting in a radar return every 10 to 12 seconds. Airport Surveillance Radars (ASRs) are short range (60 nmi) radars used to provide air traffic control services in terminal areas. ASR antennas rotate at about 13 RPM, resulting in a radar return about every 4.6 seconds. The FAA ASR radar at KCHS received returns from both airplanes involved in this accident.

Primary and secondary radar returns

A radar detects the position of an object by broadcasting an electronic signal that is reflected by the object and returned to the radar antenna. These reflected signals are called *primary returns*. Knowing the speed of the radar signal and the time interval between when the signal was broadcast and when it was returned, the distance, or range, from the radar antenna to the reflecting object can be determined. Knowing the direction the radar antenna was pointing when the signal was broadcast, the direction (or bearing, or azimuth) from the radar to the object can be determined. Range and azimuth from the radar to the object define the object's position. In general, primary returns are not used to measure the altitude of sensed objects, though some ARSRs do have height estimation capability. ASRs do not have height estimation capabilities.

The strength or quality of the return signal from the object depends on many factors, including the range to the object, the object's size and shape, and atmospheric conditions. In addition, any object in the path of the radar beam can potentially return a signal, and a reflected signal contains no information about the identity of the object that reflected it. These difficulties make

distinguishing individual aircraft from each other and other objects (e.g., flocks of birds) based on primary returns alone unreliable and uncertain.

To improve the consistency and reliability of radar returns, aircraft are equipped with transponders that sense beacon interrogator signals broadcast from radar sites, and in turn broadcast a response signal. Thus, even if the radar site is unable to sense a weak reflected signal (primary return), it will sense the response signal broadcast by the transponder and be able to determine the aircraft position. The response signal can also contain additional information, such as the identifying “beacon code” for the aircraft, and the aircraft’s pressure altitude (also called “Mode C” altitude). Transponder signals received by the radar site are called *secondary returns*.

The C150 was flying according to Visual Flight Rules (VFR, as opposed to Instrument Flight Rules, or IFR), broadcasting a “1200” transponder beacon code. The F-16 was on an IFR flight plan and was assigned and using a transponder beacon code of 5526.

Recorded radar data

Recorded data from the KCHS ASR was obtained from the FAA, and includes the following parameters:

- UTC time of the radar return, in hours, minutes, and seconds. EDT = UTC – 4 hours.
- Transponder beacon code associated with the return (secondary returns only)
- Transponder reported altitude in hundreds of feet associated with the return (secondary returns only). The transponder reports pressure altitude. The altitude recorded in the file depends on the site recording the data; some sites record both pressure altitude, and pressure altitude adjusted for altimeter setting (MSL altitude). Others record just the adjusted altitude. The KCHS file contains both altitudes, with the MSL altitude being 200 ft. higher than the pressure altitude². The resolution of this data is ± 50 ft.
- Slant Range from the radar antenna to the return, in nmi. The accuracy of this data is $\pm 1/16$ nmi or about ± 380 ft.
- Azimuth relative to magnetic north from the radar antenna to the return³. The KCHS ASR azimuth is reported in Azimuth Change Pulses (ACPs). ACP values range from 0 to 4096, where 0 = 0° magnetic and 4096 = 360° magnetic. Thus, the azimuth to the target in degrees would be:

$$(\text{Azimuth in degrees}) = (360/4096) \times (\text{Azimuth in ACPs}) = (0.08789) \times (\text{Azimuth in ACPs})$$

The accuracy of azimuth data is ± 2 ACP or $\pm 0.176^\circ$.

To determine the latitude and longitude of radar returns from the range and azimuth data recorded by the radar, the geographic location of the radar antenna must be known. The coordinates of the KCHS ASR antenna are:

32° 52' 28.3" N latitude; 080° 02' 29.0" W longitude; elevation 124 feet

² The altimeter setting for the time and location of the accident was 30.15 “Hg, resulting in a pressure altitude about 213 ft. lower than true altitude above Mean Sea Level (MSL).

³ The nominal magnetic variation used by the CHS ASR to determine magnetic azimuth is 7° W, though in this *Study* a magnetic variation of 6.93° W is used to better align the F-16 radar track with speed and track information recorded on the airplane.

Presentation of the radar data

To calculate performance parameters from the radar data (such as ground speed, track angle, pitch and roll angles, etc.), it is convenient to express the position of the airplane in rectangular Cartesian coordinates. The Cartesian coordinate system used in this *Study* is centered on the KCHS ASR antenna, and its axes extend east, north, and up from the center of the Earth. The data from the KCHS ASR are converted into this coordinate system using the WGS84 ellipsoid model of the Earth.

Figure 5 presents the KCHS ASR returns for the C150 and the F-16 near the accident site, plotted in terms of nautical miles north and east of the ASR antenna, and at two different scales.⁴ The Figure also presents the F-16 track derived from ground speed and track angle data recorded on the F-16 CSMU, as well as the adjustments made to the radar track of the C150 and the CSMU track of the F-16 in order to force a collision, and to reduce the “noise” in the C150 performance calculations resulting from position uncertainty in the radar data (see “Estimates of C150 performance based on radar data,” below).

The content of radio communications between the F-16 (call sign “DEATH41”) and Air Traffic Control (ATC) (designated “WEST” in the communications) are also annotated in Figure 5, at the locations along the F-16 track where they occurred.⁵

Figure 6 is similar to Figure 5, but presents the data over a Google Earth image of the area, and without the radio communication annotations.

Radar data uncertainty and estimates of C150 performance based on radar data

The boxes surrounding the KCHS ASR returns in Figures 5b and 6b represent the (nominal) uncertainty in the radar return location; the sensed location is at the center of the box, but uncertainties in range and azimuth could place the actual location anywhere within the box. Note that the uncertainty boxes only depict potential point-to-point, random errors in the radar range and azimuth data, and do not account for “bias” errors in the radar data that may shift the entire radar track away from the true track. The slight offset of the C150 track from the KMKS runway 23 extended centerline during the airplane’s initial climb is evidence of some bias error in the radar data. Evidence of bias errors observed in other cases are the offsets between the tracks of the same aircraft recorded by different radar sensors.

Random point-to-point uncertainty or error in airplane position and altitude leads to unrealistic noisiness in aircraft performance parameters, such as speed and track angle, calculated using the “raw” (i.e., uncorrected) radar data.⁶ To reduce the noisiness and obtain a better estimate of the C150’s performance, in this *Study* the C150 radar data is smoothed using a running-average algorithm. There are other smoothing techniques that can result in a reasonable fit of the raw radar data (i.e., that keep each radar return within its uncertainty box), and each of these will produce slightly different performance calculation results. Figures 5 and 6 show the smoothed track used in

⁴ Several Figures in this *Study* have an “a” and a “b” version, which present the same information but at different scales, or with different background images. When the *Study* refers to a Figure with two or more versions without specifying the version, all versions are meant to be included in the reference.

⁵ The C150 was not in communication with ATC.

⁶ A constant bias error in the radar track does not contribute to noise in speed and other performance calculations.

this *Study* to compute the performance parameters for the C150. The smoothed C150 track has also been shifted slightly so as to align the initial climb of the airplane with the KMKS runway 23 extended centerline, and to force a collision with the F-16 (see further discussion of this point in Section D-III). The final C150 track used as the basis for the C150 performance calculations and the cockpit visibility study is the line labeled “C150 smoothed track shifted to force collision” in Figures 5 and 6. The final F-16 track used for the cockpit visibility study is the line labeled “F-16 integrated track shifted to force collision,” and is described further in Section D-III.

Many performance parameters for the F-16, including altitude, speed, and Euler angles (pitch, roll, and heading), are recorded on the CSMU, and hence do not need to be computed from the radar data. However, the radar data is the only source of performance information for the C150, including the Euler angles required for the cockpit visibility study.

If the position (latitude, longitude, and altitude) of an airplane is known as a function of time, then its orientation (i.e., the Euler angles) can also be estimated as long as the following are true:

- The motion of the air mass relative to the Earth, i.e., the wind, is known;
- The lift coefficient of the airplane as a function of angle of attack is known;
- The gross weight of the airplane is known;
- The sideslip angle and lateral acceleration are negligible (i.e., coordinated flight).

The wind in the vicinity of the accident was computed from the ground speed, ground track, airspeed, and heading recorded on the F-16 CSMU (see Section D-III). Based on these calculations, a constant wind from 125° (true) at 7 knots is assumed for the C150 performance calculations (see Figure 12).

The KCHS and KMKS Meteorological Aerodrome Reports (METARs) surrounding the time of the accident are shown in Tables 2 and 3, respectively:

Parameter \ Report	KCHS METAR 09:56 EDT	KCHS METAR 10:56 EDT	KCHS METAR 11:56 EDT
Sky condition	4000 ft. few	4000 ft. scattered	3500 ft. scattered
Visibility	10 statute miles	10 statute miles	10 statute miles
Winds	240° @ 5 kt.	220° @ 7 kt.	230° @ 8 kt.
Temperature / Dew Point	29°C / 22°C	30°C / 22°C	31°C / 21°C
Altimeter setting	30.16 "Hg	30.15 "Hg	30.15 "Hg

Table 2. Weather observations at KCHS surrounding the time of the accident.

Parameter \ Report	KMKS METAR 10:35 EDT	KMKS METAR 10:55 EDT	KMKS METAR 11:15 EDT
Sky condition	clear	2600 ft. scattered	clear
Visibility	10 statute miles	10 statute miles	7 statute miles
Winds	calm	calm	calm
Temperature / Dew Point	30°C / 22°C	30°C / 22°C	31°C / 22°C
Altimeter setting	30.16 "Hg	30.15 "Hg	30.15 "Hg

Table 3. Weather observations at KMKS surrounding the time of the accident.

The F-16 CSMU recorded a static air temperature of 25°C at 1600 ft. Based on this data and the METARs shown in Tables 2 and 3, a temperature profile of 25°C at 1600 ft. increasing linearly to 30° C at 0 ft. is assumed in this *Study* (the temperature profile influences the calculated calibrated airspeed presented below).

As noted above, aerodynamic data for the C150 was provided by Textron Aviation. A gross weight of 1678 lb. (see Table 1) is assumed in the C150 performance calculations.

The position coordinates of an airplane as a function of time define its velocity and acceleration components. In coordinated flight, these components lie almost entirely in the plane defined by the airplane's longitudinal and vertical axes. Furthermore, any change in the *direction* of the velocity vector is produced by a change in the lift vector, either by increasing the magnitude of the lift (as in a pull-up), or by changing the direction of the lift (as in a banked turn). The lift vector also acts entirely in the aircraft's longitudinal-vertical plane, and is a function of the angle between the aircraft longitudinal axis and the velocity vector (the angle of attack, α). These facts allow the equations of motion to be simplified to the point that a solution for the airplane orientation can be found given the additional information about wind and the airplane lift curve (i.e., C_L vs. α).

The results of the C150 performance calculations are presented along with the F-16 performance parameters recorded by the CSMU in Section D-III. The limited accuracy of the radar-based performance calculations should be considered when drawing conclusions based on these calculations. It is generally preferable to regard performance calculations based on smoothed radar data as qualitative indicators of the area of the performance envelope in which an aircraft was operating, rather than as quantitative and precise measurements of performance parameters (such as the F-16 performance parameters recorded by the CSMU). This caveat must also be borne in mind when considering the results of the cockpit visibility calculations described in Section D-IV, which depend on the pitch, roll, and heading angles computed from the radar data.

III. F-16 CSMU data and estimated collision geometry

Introduction

The F-16 CSMU recorded many performance parameters of interest, but not all. Most significantly, the airplane latitude and longitude coordinates are not recorded. In addition, wind speed and direction, which are used in the C150 radar-based performance calculations, are not recorded. However, the F-16 trajectory and winds can be computed from other parameters that are recorded on the CSMU. This Section describes these calculations, and presents the results along with the results of the C150 performance calculations described above. In addition, an estimate of the collision geometry that is consistent with the CSMU data and time and place of the collision is presented.

F-16 trajectory based on CSMU and radar data

The CSMU recorded ground speed and track angle. These parameters can be used to compute the *changes* in the F-16's north and east positions as a function of time, resulting in a ground track of the correct "shape," but that still needs to be anchored to reference points on the Earth in order to specify the airplane's location.

In this *Study*, the KCHS ASR data is used initially to "anchor" the F-16 ground track. It is possible to locate the track such that the airplane positions are consistent with the F-16 radar uncertainty boxes. However, this initial anchoring places the F-16 well east of the accident location and does not result in a collision with the C150 at the proper time. Consequently, the ground track is shifted

so as to force a collision with the C150 at a time and place consistent with the end of the CSMU and radar data, and with the location of the C150 debris field. As will be seen, the shifted track lies outside the uncertainty boxes of the F-16 radar data. A solution that is consistent with the CSMU data and the time and place of the collision, and that also lies within the F-16 uncertainty boxes, was not found. As a result, in this *Study* consistency with the radar uncertainty boxes is sacrificed in favor of consistency with the CSMU ground track and ground speed, the end of the recorded data, the location of the C150 debris field, and the altitudes and rates of climb of both airplanes.

The north and east velocities of the F-16 can be computed from the ground speed and ground track recorded on the CSMU as follows:

$$V_E = V_G \cos \psi_G \quad [1]$$

$$V_N = V_G \sin \psi_G \quad [2]$$

Where:

V_G = ground speed

ψ_G = ground track (measured from true north)

V_E = east component of ground speed

V_N = north component of ground speed

The F-16 east and north positions relative to a reference point are given by:

$$E(t) = \int_0^t V_E dt + E_0 \quad [3]$$

$$N(t) = \int_0^t V_N dt + N_0 \quad [4]$$

Where:

t = time

$E(t)$ = east position at time t

E_0 = east position at time 0 (initial east position)

$N(t)$ = north position at time t

N_0 = north position at time 0 (initial north position)

As described above, the initial coordinates (E_0, N_0) are determined after the integration so as to place the integrated track within the F-16 radar uncertainty boxes, as far as possible. The result of these calculations is shown in Figures 5 and 6 as the lines labeled “F-16 integrated track matched to ASR data.” As shown in Figures 5b and 6b, the integrated track lies within the F-16 radar uncertainty boxes, except for the point at 11:00:27.0, which lies just to the west of the uncertainty box boundary.

Note that the radius of curvature of the F-16’s left turn just before the collision is tighter for the track computed from Equations [1] – [4] than that indicated by the F-16 radar data; near the point of collision, the integrated track has turned slightly “inside” the radar track. In order to fit the integrated track to the uncertainty boxes, the integrated track has to lie on the southeast corner of the uncertainty box associated with the radar return at 11:00:54.6. However, this placement is too far east to be consistent with a collision with the C150. This problem is solved if the integrated track is shifted to the location indicated by the line labeled “F-16 integrated track shifted to force

collision” in Figures 5 and 6. However, in this case the integrated track lies outside all of the F-16 radar uncertainty boxes. A track for the F-16 could be constructed by smoothing the radar returns for that airplane, such as was done for the C150 as described above; however, the ground speed and track that would be implied by that radar-based track would be inconsistent with the ground speed and ground track parameters recorded on the CSMU. Since the recorded CSMU parameters are much more accurate than any radar-based calculation, the solution that is based on the integrated track is preferred in this *Study* to one based solely on the radar.

Estimated collision time, location, and geometry

The north and east positions of the C150 and F-16 are presented as a function of time in Figure 7. This Figure presents the KCHS ASR raw radar returns for each airplane, along with the smoothed and shifted tracks for the C150, and the integrated and shifted tracks for the F-16. Note that the last CSMU ground speed and ground track data were recorded at 11:00:55.03 (as indicated by the end of the “F-16 integrated track matched to ASR data” line in Figure 7). The last radar return from the C150 was received at 11:00:54.8, and the last radar return from the F-16 prior to the collision was received at 11:00:54.6. Radar returns from the F-16 resumed at 11:01:13.1 (18.5 seconds later, after the collision had occurred and as the disabled F-16 was descending and flying south, as shown in Figures 5 and 6). Since the time between the ASR radar returns averages about 4.7 seconds, had the collision not occurred, the next radar return from the C150 would have been expected at about 11:00:59.5, and the next return from the F-16 would have been expected at about 11:00:59.3. Consequently, the collision likely occurred between 11:00:55.3 (the end of the CSMU data) and 11:00:59.3 (the time of the earliest radar return that would have been expected had the collision not occurred).

Extrapolating the C150 and F-16 east, north, and altitude trajectories to a common point within this time window results in the following time and coordinates for the collision:

Time of collision = 11:00:56.6 EDT KCHS ASR time
 East coordinate = 2.55 nmi east of KCHS ASR
 North coordinate = 17.17 nmi north of KCHS ASR
 Altitude = 1466 ft. MSL

The extrapolation of the F-16 integrated track to this point is illustrated in Figure 7 as the line labeled “F-16 track shifted to force collision.” The extrapolation of the C150 smoothed-radar track to this point is illustrated in Figure 7 as the line labeled “C150 smoothed track shifted to force collision.”

The content of radio communications between the F-16 and Air Traffic Control (ATC) are also annotated in Figure 7, as rotated green text centered on vertical, dashed green lines that intersect the x axis of the plot at the times that the communications occurred. These annotations also appear on many subsequent plots of data vs. time.

The C150 and F-16 altitudes as a function of time are presented in Figure 8. The KCHS ASR Mode C returns, and the associated 50 ft. Mode C uncertainty bands, are presented in this Figure, along with the recorded CSMU MSL altitude. The C150 altitude used in this *Study* for performance and cockpit visibility calculations is the line labeled “C150 smoothed Mode C altitude, extrapolated to

force collision.” The F-16 altitude used in this *Study* for the cockpit visibility calculations is the line labeled “F-16 MSL altitude extrapolated to force collision.”

Note that the F-16 Mode C and CSMU altitude data suggest a slight descent during the F-16’s left turn toward the south just prior to the collision (the F-16 reached a 32° left bank angle at about 11:00:38 – see Figure 11). This descent is maintained in the extrapolation of the F-16 altitude to the estimated collision time of 11:00:56.6. Per the CSMU data, during the turn the F-16 autopilot was on in altitude hold and heading select modes (see Reference 2); consequently, the descent during the turn may appear surprising. NTSB asked Lockheed-Martin whether the autopilot would have been expected to maintain the 1600 ft. altitude recorded prior to the turn during the turn itself, at the recorded flight conditions. Lockheed-Martin indicated⁷ that at an airspeed of about 240 KCAS, the F-16 was flying at a relatively high α , and that the higher α demanded by a level 32° banked turn would trigger the airplane’s α – protection algorithms and prevent the autopilot from maintaining altitude. Consequently, the descent during the turn is expected.

Figure 9 shows the true airspeed, calibrated airspeed, ground speed, and rate of climb calculated from the smoothed radar data for the C150, along with the F-16 calibrated airspeed and ground speed recorded on the CSMU, extrapolated to the estimated collision time. The F-16 true airspeed and rate of climb computed from the CSMU data is also shown. Figure 9 indicates that at the time of the collision, the ground speed of the F-16 was about 245 knots, and the ground speed of the C150 was about 68 knots. The F-16 was descending at about 150 ft./min. and the C150 was climbing at about 520 ft./min.

Figure 10 shows the separation distance between the two airplanes and the closure rate. The Figure indicates that the closure rate was about 255 knots at the time of the collision.

The angle between the velocity vectors of the airplanes can be determined by comparing the ground track angles shown in Figure 11. This Figure presents the pitch, roll, heading, and ground track angles for the C150 calculated from the smoothed radar data, and the same angles for the F-16 recorded by the CSMU, extrapolated to the estimated collision time. The track angle of the F-16 at the time of the collision was about 197°, and the track angle of the Cessna was about 109°. Therefore, the collision angle (the smallest angle between the longitudinal axes of the aircraft at the time of impact) is about 88° (197°- 109°), with the C150 climbing into the F-16 from the right, and the F-16 descending into the C150 from the left.

According to the NTSB factual report of the accident (Reference 6), “the lower aft engine cowling of the F-16 was ... recovered in the immediate vicinity of the Cessna’s aft fuselage,” (i.e., near the collision point and C150 debris field). In addition, “the F-16’s engine augments was recovered about 1,500 ft. southwest.” The location of these parts of the F-16 near the collision point (and the continued crippled flight of the F-16 towards the south) is consistent with the C150 impacting the F-16’s lower, aft fuselage.

The yaw, pitch and roll angles plotted in Figure 11 are used along with the (colliding) airplane tracks shown in Figures 5 and 6 in the cockpit visibility study presented in Section D-IV.

⁷ Lockheed-Martin provided a brief analysis of the autopilot performance in an email to NTSB dated 7/27/2016.

Winds computed from F-16 CSMU data

Airspeed, ground speed, and wind are related as follows:

$$\vec{V}_W = \vec{V}_G - \vec{V}_T \quad [5]$$

Where \vec{V}_T is the true airspeed vector, \vec{V}_G is the ground speed vector, and \vec{V}_W is the wind vector. The east and north components of \vec{V}_G are given by Equations [1] and [2]. The east and north components of \vec{V}_T are also given by these Equations, with V_G replaced with the true airspeed V_T , and ψ_G replaced by the true heading ψ_T (assuming level, coordinated flight; Equations [1] and [2] do not yield the correct east and north components of airspeed at large sideslip or bank angles). The east and north components of ground speed and airspeed can be used in Equation [5] to compute the east and north components of the wind. Finally, the east and north components of the wind can be used to compute the wind speed and direction.

The results of the wind calculation for the 1.5 minutes preceding the collision are shown in Figure 12. Note that the large increase in the wind speed at about 11:00:35 is not realistic, and is the result of errors introduced into the calculation by the large bank angle that develops at that time. The red lines in Figure 12 show the constant wind estimate used in this *Study* based on the results of the wind calculation (wind from 125° true at 7 knots).

IV. Cockpit visibility study

Azimuth and elevation angles of “target” aircraft relative to “viewer” aircraft

Once the position and orientation of each airplane has been determined, their positions in the body axis system of the other airplane can be calculated. These relative positions then determine where the “target” aircraft will appear in the field of view of the pilot of the “viewer” aircraft.

For this *Study*, the relative positions of the two aircraft (and the visibility of each from the other) were calculated beginning when the C150 was detected by the KCHS ASR, and then at 1-second intervals up to the collision.

The “visibility angles” from the “viewer” airplane to the “target” airplane correspond to the angular coordinates of the line of sight between the airplanes, measured in a coordinate system fixed to the viewer airplane (the viewer’s “body axis” system), and consist of the azimuth angle and elevation angle (see Figure 13). The azimuth angle is the angle between the x-axis and the projection of the line of sight onto the x-y plane. The elevation angle is the angle between the line of sight itself, and its projection onto the x-y plane. At 0° elevation, 0° azimuth is straight ahead, and positive azimuth angles are to the right. 90° azimuth would be out the right window parallel to the y axis of the airplane. At 0° azimuth, 0° elevation is straight ahead, and positive elevation angles are up. 90° elevation would be straight up parallel to the z axis. The azimuth and elevation angles depend on both the position (east, north, and altitude coordinates) of the viewer and target airplanes, and the orientation (yaw, pitch, and bank angles) of the viewer. The azimuth and elevation angles of points on the target away from its CG also depend on the orientation of the target.

The position and Euler angles of the F-16 are based on data recorded on the CSMU and so are known relatively precisely; however, the position and Euler angles of the C150 are determined from the smoothed radar data, and so are sensitive to how that data is smoothed. Since the uncertainty in the radar data allows some flexibility in the smoothing (see the discussion in Section D-II), there is uncertainty in the Euler angles determined from any particular smoothing. Consequently, the azimuth and elevation angles presented below should be considered analytical estimates rather than exact measurements.

Azimuth and elevation angles of airplane structures from laser scans

The target airplane will be visible from the viewer airplane unless a non-transparent part of the viewer's structure lies in the line of sight between the two airplanes. To determine if this is the case, the azimuth and elevation coordinates of the boundaries of the viewer's transparent structures (windows) must be known, as well as the coordinates of the viewer's structure visible from the cockpit (such as the wings and wing struts). If the line of sight passes through a non-transparent structure (such as the instrument panel, a window post, or a wing), then the target airplane will be obscured from the viewer.

For this *Study*, the azimuth and elevation angles of the window boundaries and wings of the F-16 and C150 were determined from the interior and exterior dimensions of exemplar airplanes, as measured using a FARO laser scanner.⁸ The laser scanner produces a "point cloud" generated by the reflection of laser light off of objects in the laser's path, as the scanner sweeps through 360° of azimuth and approximately 150° of elevation. The 3-dimensional coordinates of each point in the cloud are known, and the coordinates of points from multiple scans (resulting from placing the scanner in different positions) are "merged" by the scanner software⁹ into a common coordinate system. By placing the scanner in a sufficient number of locations so that the scanner can "see" every part of the airplane, the complete exterior and interior geometry of the airplane can be defined.

In this *Study*, the scanner was placed in several locations to scan the exterior of the airplanes, and in the pilot seats to scan the interior of the airplanes.¹⁰ The scanner software was then used to identify the points defining the outline of the cockpit windows (from the interior scans) and exterior structures visible from the cockpit (from the exterior scans). The coordinates were transformed into the airplane's body axis system and, ultimately, into azimuth and elevations angles from the pilot's eye position. The transformation method is described in Appendix A.

The azimuth and elevation angles of the viewer airplane's windows and other structures are very sensitive to the pilot's eye location in the cockpit. If the pilot moves his head forward or aft, or from a position centered over his seat to one close to a window surface, the view out the window (and the azimuth and elevation angles of all the airplane's structures) change substantially. This potential variability in the pilot's eye position, and the consequent variability in the location of the window edges and airplane structures in the pilot's field of view, is by far the greatest source of uncertainty as to whether the target aircraft is obscured or not at a given time.

⁸ Specifically, the FARO "Focus 3D" scanner; see <http://www.faro.com/en-us/products/3d-surveying/faro-focus3d/overview>.

⁹ FARO SCENE software: see <http://faro-3d-software.com/>.

¹⁰ Two scans each from the pilot and co-pilot seats of the C150 were performed: one with the other seat empty, and one with the other seat occupied (to measure the obstruction to vision presented by the occupant).

To evaluate the effect of varying eye position on the visibility of the target airplane, the azimuth and elevation angles of the cockpit windows and other airplane structures were computed for a matrix of eye positions displaced from the nominal eye positions, as described below. The “nominal” eye positions were estimated by scanning a person seated in the exemplar aircraft, in the usual flying position (seated upright with the head centered over the seat).

In addition to the calculation of the visibility angles, this *Study* presents recreations of possible views from the pilots’ seats (including simulation-based depictions of the outside world) constructed assuming the nominal eye positions as defined above.

Results: azimuth and elevation angle calculations

The azimuth and elevation angles from the “viewer” airplanes to the “target” airplanes are shown as a function of time in Figure 14. In the top plot, the F-16 is the “viewer” and the C150 is the “target,” and in the bottom plot, the C150 is the “viewer” and the F-16 is the “target.”

Plots of the “target” airplane elevation angle vs. azimuth angle are shown in Figure 15a, along with the azimuth and elevation coordinates of the “viewer” airplane cockpit windows and other structures, for the nominal pilot eye positions. Figure 15b presents photographs of the cockpits that help identify the cockpit structures depicted in gray in Figure 15a. The red lines in Figure 15a indicate the coordinates of the “target” aircraft, which change with time. The times corresponding to selected coordinates are indicated by the time labels. If the red lines pass through a shaded area of the plots, the “target” airplane is obscured from view by the “viewer” airplane structure.

The azimuth and elevation angles of the sun are also of interest, because sun glare can affect a pilot’s ability to see other aircraft. The azimuth (relative to true north) and altitude angles of the sun at 11:00:00 EDT on July 7, 2015 at the accident site were 98.96° and 56.47° , respectively.¹¹ These angles place the sun predominantly behind the F-16, and so would not have been in the field of view of the F-16 pilot. To compute the location (azimuth and elevation angles) of the sun in the C150 pilot’s field of view, the coordinates of the sun in earth coordinates were computed (using the sun angles and an assumed very large distance to the sun), and then transformed into the C150 body axis coordinates using the C150 Euler angles. The azimuth and elevation angles of the sun were then computed from its body axis coordinates.

The results of these calculations are shown in Figure 16, and indicate that the sun would have been located above the C150’s windows and behind airplane structure throughout the flight.

As noted above, the azimuth and elevation angles of the window and cockpit structures are sensitive to the position of the pilot’s eyes in the cockpit. To determine how these angles change as the pilot’s eye position changes (e.g., by leaning in different directions, or by a seat height adjustment), plots similar to Figure 15 were generated for the 27 different eye positions shown in Table 4. The positions are expressed as displacements from the nominal eye position along the three airplane body axes ($\{\Delta x_b, \Delta y_b, \Delta z_b\}$ ¹²):

¹¹ This sun position was determined using the <http://www.susdesign.com/sunangle/> website.

¹² The body axis system origin is at the center of gravity of the airplane. The $+z_b$ axis lies in the plane of symmetry, and at zero pitch and roll angles is parallel to the gravity vector, pointing down. The $+x_b$ axis is also in the plane of symmetry and is normal to the $+z_b$ axis, pointing forward. The $+y_b$ axis is normal to the $+x_b$ and $+z_b$ axes, pointing to towards the right wingtip.

Case name	Δx_b from nominal, in. (+ forward, - aft)	Δy_b from nominal, in. (+ right, - left)	Δz_b from nominal, in. (+ down, - up)
CCD	0	0	+1.5
FCD	+3	0	+1.5
ACD	-3	0	+1.5
FLD	+3	-3	+1.5
CLD	0	-3	+1.5
ALD	-3	-3	+1.5
FRD	+3	+3	+1.5
CRD	0	+3	+1.5
ARD	-3	+3	+1.5
CCC (nominal)	0	0	0
FCC	+3	0	0
ACC	-3	0	0
FLC	+3	-3	0
CLC	0	-3	0
ALC	-3	-3	0
FRC	+3	+3	0
CRC	0	+3	0
ARC	-3	+3	0
CCU	0	0	-1.5
FCU	+3	0	-1.5
ACU	-3	0	-1.5
FLU	+3	-3	-1.5
CLU	0	-3	-1.5
ALU	-3	-3	-1.5
FRU	+3	+3	-1.5
CRU	0	+3	-1.5
ARU	-3	+3	-1.5

Table 4. Matrix of eye positions for cockpit structure azimuth and elevation angle calculations.

The results of the calculations are presented in Figure 18 for the F-16, and in Figure 19 for the C150. The times associated with the trajectory of the “target” airplane in these figures is depicted by the color of the trajectory line, starting with green at 10:57:40, and progressing to red at 11:01:00. A color legend for these lines is shown in Figure 17.

As shown in Figures 18 and 19, variations in the pilot’s eye position from the nominal position affects the times at which the target airplane may have become obscured by the viewer airplane’s structure. For example, Figure 19 shows that the F-16 would become obscured by the C150’s left wing strut slightly sooner if the pilot’s eyes were aft of the nominal position. Specifically, if the pilot’s eyes were 3” aft and 1.5” above the nominal position, then the F-16 would become obscured by the strut about 1.5 seconds sooner than otherwise.

Similarly, if the F-16 pilot’s eyes were 1.5” lower than the nominal position, then the C150 would become obscured by the F-16 instrument panel about 1.2 seconds earlier than with the pilot’s eyes in the nominal position.

While these differences in time of obscuration are relatively small, Figures 18 and 19 underscore the fact that scanning for traffic visually can be more effective if the pilot moves his head as well as redirecting his eyes, since head movements may bring otherwise obscured aircraft into view.

Simulated views from the F-16 and C150 cockpits

While Figures 15-19 depict where the “target” airplanes could have appeared in the “viewer” airplanes’ windows, they do not provide a sense of the background against which the targets would appear, and against which the pilot of each airplane would have to see the target. To provide a rough approximation of these backgrounds and how the view from each cockpit evolved over time, the views were recreated in the *Microsoft Flight Simulator X (FSX)* simulation program, using airplane and sky graphics inherent in *FSX*, and terrain textures based on *Microsoft Visual Earth* satellite imagery.¹³

The cockpit structure of each airplane at the nominal pilot’s eye point (based on the laser scans) was constructed in *FSX* as semi-transparent instrument panels that “mask” the view from each cockpit (see Appendix B); the cockpit geometry built into the airplane models used in the simulation was not used. Airplane models were only used to represent the exterior “target” airplane geometry in the recreated views. The airplane models were chosen based on their color resemblance to the accident airplanes, and are freely provided by *FSX* enthusiasts.¹⁴ The position (latitude, longitude, and altitude) and attitude (heading, pitch, and roll) of each airplane was recreated in *FSX* using the *FS Recorder* program developed by Matthias Neusinger,¹⁵ based on the final estimated position and attitude data for each airplane described in Sections D-II and D-III.

FSX contains inherent options to customize the time, date, and weather depiction in the simulation. The time and date were set to those of the accident (11:00 EDT on July 7, 2015), which results in the correct placement of the sun in the sky. The sky conditions were selected to match those of the 10:55 EDT METAR from KMKS: 2600 ft. scattered and 10 miles visibility (see Table 3). Of course, the clouds depicted in the simulation are only a generic representation of the reported sky condition, and do not recreate the clouds in the skies over KMKS on the day of the accident precisely. However, this presentation of the sky is likely more “realistic” and representative of the accident conditions than a clear, cloudless sky with unlimited visibility.

The view depicted by *FSX* depends on the “camera” settings. In this *Study*, the *FSX* camera is equivalent to the pilot’s eyes: the view from the cockpit depends on the camera’s position, orientation (where it’s pointed), and its “field of view” (i.e., the range of azimuth and elevation angles that can be “seen” by the camera). The widest field of view available in *FSX* is 90° horizontally and about 62° vertically.¹⁶ Consequently, if the camera is pointed straight ahead (0° azimuth), then only azimuth angles between -45° and +45° will be visible in that view. If objects of interest (e.g., the target airplane) are beyond this range, then to “see” them the camera will have to be rotated away from 0° azimuth toward the object. However, in this case, a portion of the view straight-ahead will be lost, which may be unsatisfactory for the purpose of giving the viewer a good sense of the airplane’s direction of travel and general situation relative to the outside world.

To see objects beyond $\pm 45^\circ$ of azimuth while at the same time preserving a field of view of at least $\pm 45^\circ$ of azimuth about the direction of travel, the view from two co-located cameras can be joined

¹³ See <https://www.bing.com/mapspreview?v=2&cp=44.023938~-99.71&style=h&lvl=4&tilt=-89.875918865193&dir=0&alt=7689462.6842358>

¹⁴ The F-16 model used is the “F-16 Fighting Falcon FSX & P3D” by Kirk Olsson; see <http://www.rikoooo.com/en/downloads/viewdownload/18/740>.

The C150 model used is the “FS Insider Just Flight Cessna 152;” see <http://www.justflight.com/microsoft-c152>.

¹⁵ See <http://www.fs-recorder.net/>.

¹⁶ These values are for an *FSX* window with an aspect ratio of 1.6, at “zoom” setting of 0.3.

side-by-side: the first camera pointed away from 0° azimuth to capture the object, and the second camera pointed in such a way that the boundaries of the fields of view of the cameras coincide at a particular azimuth angle. For example, if one camera is rotated to -75° azimuth, the left boundary of its field of view will be at $-75^\circ - 45^\circ = -120^\circ$, and the right boundary will be at $-75^\circ + 45^\circ = -30^\circ$. If the second camera is rotated to $+15^\circ$ azimuth, its left boundary will be at $+15^\circ - 45^\circ = -30^\circ$ (coinciding with the right boundary of the first camera), and its right boundary will be at $+15^\circ + 45^\circ = 60^\circ$. Setting the views from the cameras side-by-side, a continuous field of view from -120° to $+60^\circ$ is obtained.

However, discontinuities (kinks) in straight lines may appear at the boundary of these views when they are viewed side-by-side on a flat surface (such as a computer screen), because the viewer will be viewing both from the same angle, whereas the view on the left is intended to be viewed at an angle rotated 90° from that on the right. The discontinuities can be removed if each view is presented on a separate surface (monitor), and then the surfaces are joined at a 90° angle. However, this solution may be impractical (and is impossible for presenting screenshots of these views in a single document), and so the line discontinuities at the boundaries of the views may simply need to be tolerated, as they are in the present *Study*.

As shown in Figure 15, the C150 remained within $\pm 15^\circ$ of azimuth and between -20° and 0° of elevation of the F-16 pilot's field of view for its entire flight. Consequently, a single camera pointed straight ahead and with a horizontal field of view of $\pm 45^\circ$ is sufficient to depict the C150 and the direction of travel of the F-16. However, the F-16 approached the C150 from an azimuth angle of about -75° ; consequently, for the C150 two cameras are needed to depict both the approach of the F-16, and the view in the C150's direction of travel. Based on these observations, the F-16 cockpit view was recreated using a single camera pointed at 0° azimuth, and the C150 cockpit view was recreated using two cameras, pointed at -75° and $+15^\circ$, respectively. The elevation angles for all cameras was 0° .

Screenshots of the F-16 cockpit recreation are presented in Figures 20a-i, and screenshots of the C150 cockpit recreation are presented in Figures 21a-i. The times of the screenshots correspond roughly to the events listed in Table 5, with some substitutions and additions. In lieu of the "C150 radar contact" event at 10:57:40.7, a screenshot at 10:58:05 is included corresponding to the first CDTI information that would have been provided to either airplane about the other (had either airplane had been equipped with a CDTI). Screenshots at 11:00:18 and 11:00:35 EDT are included in lieu of the ATC communication events at 11:00:16 and 11:00:33 to partially account for the time necessary for the communication to occur (2 seconds added), and because a CDTI aural alert would have been triggered at 11:00:35 (had the airplanes been equipped). Screenshots at 11:00:49 and 11:00:56 are also included to portray the rapid growth in size of the target airplanes in the seconds before the collision.

Images of what a CDTI could have displayed to the pilots are also included as insets in Figures 20 and 21. These CDTI displays and alerts are described in more detail in Section D-V.

A measure of the size of the "target" airplane in the field of view of the "viewer" is the difference in azimuth and elevation angles between different points on the "target." For this *Study*, the azimuth and elevation angles of the nose, tail, center, and left and right wingtips of the targets were computed (the angles plotted in Figures 14-19 correspond to the center of the targets). The difference in azimuth and elevation angles between the nose and the tail of the targets are

presented as a function of time in Figure 22 as the lines labeled “ Δ azimuth, fuselage” and “ Δ elevation, fuselage.” The difference in angles between the left and right wingtips are presented as the lines labeled “ Δ azimuth, wings” and “ Δ elevation, wings.” In these calculations, the nose, tail, and wingtips are assumed to lie in a plane, and so the airplanes in this representation have zero thickness. Hence, the information in Figure 22 does not represent the size of the area of the target presented to the viewer (which is what makes the target visible), but only the extent of a subset of dimensions that contribute to the area. Nonetheless, Figure 22 does provide a measure of the target size, and of the very sudden increase in size (called the “blossom” effect) within a few seconds of the collision. Reference 7 indicates that on average, in ideal conditions people can see an object that spans at least 0.01° of the field of view, when looking directly at the object. However, the actual visual detection threshold depends on many factors, including viewer age, contrast, illumination, color, and the viewer’s focus. Consequently, Figure 22 should not be used to determine a specific time at which the pilots “should” have been able to see the other airplane.

Figure 22a also indicates the time (10:59:13) at which the airplanes were 10 statute miles (8.69 nautical miles) apart. Before this time, the airplanes would have been separated by more than 10 miles, and presumably invisible to each other given the 10 mile visibility reported in the KMKS 10:55 EDT METAR (see Table 3).

The dark gray shaded areas in Figure 22 indicate the times where the center of the target appears obscured by the viewer airplane’s structure (with the viewer pilot’s eyes at the nominal position), consistent with Figures 14-19. In these areas, the viewer pilot may not have been able to see the target airplane unless he moved his head from the nominal position (see Figures 18 and 19).

Figures 20 - 22 indicate that each airplane would have remained a relatively small object in the other airplane’s windows (spanning less than 0.5° of the field of view) until about 5 seconds before the collision, and subsequently grown in size suddenly (the “blossom” effect). The WEST controller first alerted the F-16 pilot about the C150 at 11:0016, about 40 seconds prior to the collision. For several brief periods after this time, the C150 may have been obscured from the F-16 pilot’s field of view behind the F-16 Head-Up Display (HUD) support structure or the instrument panel; between these times, the C150 would have appeared predominantly in the transparent area of the HUD, on the horizon between ground and sky. Primary flight data is projected onto the HUD as translucent green lines and text; it is not known how this projected information may have affected the visibility of the C150. In the last 3 to 4 seconds before the collision, the C150 may have been mostly obscured by the HUD support structure and the instrument panel.

In the 40 seconds prior to the collision, the F-16 would have remained in the C150 pilot’s field of view until about 1 second before the collision, when the F-16 may have become obscured by the C150’s left wing strut.

These circumstances underscore the difficulty in seeing airborne traffic (the foundation of the “see and avoid” concept), even when the airplanes are not obscured from view, and one of the pilots is alerted to the presence of the other airplane. The CDTI images presented here indicate that CDTI systems could have alerted each pilot to the presence of the other airplane, and presented precise bearing, range, and altitude information about each target, up to two minutes and 50 seconds prior to the collision. Such timely and information-rich traffic presentations would likely have enabled each pilot to avoid the other airplane using only slight course and / or altitude adjustments, and without the need for aggressive maneuvering. The CDTI displays are discussed further below.

Time HH:MM:SS EDT	Time before collision MM:SS	Event	Distance North of CHS ASR, nmi		Distance East of CHS ASR, nmi		Altitude, ft. MSL		Ground speed, knots		Ground track, deg. true		Separation distance, nmi	Closure rate, knots
			F-16	C150	F-16	C150	F-16	C150	F-16	C150	F-16	C150		
10:57:40.7	03:15.9	C150 radar contact	22.00	18.27	15.64	-0.06	1566	222	272	59	253	223	16.14	222
10:58:56.6	02:00.0	2 min prior to collision	20.29	17.69	10.27	0.38	1564	701	266	67	253	84	10.22	332
10:59:56.6	01:00.0	1 min prior to collision	18.98	17.56	6.17	1.49	1564	1083	255	62	252	110	4.89	304
11:00:13.0	00:43.6	CA alarm	18.63	17.45	5.06	1.76	1560	1183	254	71	252	110	3.50	308
11:00:16.0	00:40.6	1st traffic advisory to F-16	18.56	17.43	4.86	1.82	1568	1194	253	71	252	109	3.25	308
11:00:26.0	00:30.6	1st turn instruction to F-16	18.35	17.36	4.19	2.00	1595	1236	252	69	252	111	2.40	299
11:00:33.0	00:23.6	2nd turn instruction to F-16	18.20	17.31	3.72	2.13	1573	1279	253	68	252	109	1.83	293
11:00:53.0	00:03.6	Traffic altitude call to F-16	17.40	17.20	2.65	2.49	1477	1436	245	69	207	108	0.26	264
11:00:56.6	00:00.0	Collision	17.17	17.17	2.55	2.55	1467	1466	245	68	197	108	0.00	255

Table 5. Events of interest leading up to the collision.

V. Cockpit Display of Traffic Information (CDTI) Study

Introduction

According to a 2007 “Fact Sheet” published by the FAA,¹⁷ the “Next Generation Air Transportation System” (NextGen) program “is a wide ranging transformation of the entire national air transportation system - not just certain pieces of it - to meet future demands and avoid gridlock in the sky and in the airports. It moves away from legacy ground based technologies [such as radar] to a new and more dynamic satellite based technology.” A key component of NextGen is the surveillance of aircraft through the Global Positioning System (GPS) satellite constellation instead of by ground radar. This GPS-based surveillance is enabled through the “Automatic Dependent Surveillance – Broadcast” (ADS-B) system. As described in the FAA fact sheet,

Automatic Dependent Surveillance Broadcast (ADS-B) is, quite simply, the future of air traffic control. As the backbone of the NextGen system, it uses GPS satellite signals to provide air traffic controllers and pilots with much more accurate information that will help keep aircraft safely separated in the sky and on runways. Aircraft transponders receive GPS signals and use them to determine the aircraft’s precise position in the sky, which is combined with other data and broadcast out to other aircraft and air traffic control facilities. When properly equipped with ADS-B, both pilots and controllers will, for the first time, see the same real-time displays of air traffic, substantially improving safety.

After January 1, 2020, ADS-B Out equipment (that broadcasts the airplane’s position to ATC and other aircraft) is required to be installed on all aircraft in the National Airspace System (NAS) operating above 10,000 ft. and within or above Class B and C airspace, with certain exceptions (see 14 CFR 91.225).

The ADS-B capabilities that enhance a pilot’s awareness of airborne traffic in his vicinity are described in Advisory Circular (AC) 20-172B, “Airworthiness Approval for ADS-B In Systems and Applications.” Per the AC,

ADS-B In refers to an appropriately equipped aircraft’s ability to receive and display other aircraft’s ADS-B information and ground station broadcast information, such as TIS-B [Traffic Information Services – Broadcast] and ADS-R [Automatic Dependent Surveillance – Rebroadcast]. The information can be received by an appropriately equipped aircraft on either or both of two radio frequency (RF) links: 1090 ES or 978 MHz UAT. The received information is processed by onboard avionics and presented to the flight crew on a display.

ADS-B In avionics enable a number of aircraft surveillance applications. The applications most relevant to this accident are the enhanced visual acquisition (EVAcq) and ADS-B Traffic Advisory System (ATAS) applications. AC 20-172B describes these applications as follows:

The enhanced visual acquisition application (EVAcq) ... displays ADS-B traffic on a plan view (bird’s eye view) relative to own-ship. This application is designed to support only the display and alerting of ADS-B traffic, including ADS-R, TIS-B, and TCAS [Traffic Collision Avoidance System] derived traffic. ... The traffic information assists the flight crew in visually acquiring traffic out the window while airborne. EVAcq does not relieve the pilot of see and avoid responsibilities under 14 CFR 91.113b. This application is expected to improve both safety and efficiency by providing the flight crew enhanced traffic awareness. ...

ADS-B Traffic Advisory System (ATAS) is an Automatic Dependent Surveillance-Broadcast (ADS-B) In application intended to reduce the number of mid-air collisions and near mid-air collisions involving general

¹⁷ See:

http://web.archive.org/web/20150403151639/http://www.faa.gov/news/fact_sheets/news_story.cfm?newsid=8145

aviation aircraft. Previously known as Traffic Situation Awareness with Alerts (TSAA), the name ATAS has been used in this AC as well TSO-C195b to be more consistent with existing traffic advisory systems. ATAS provides voice annunciations to flight crews to draw attention to alerted traffic and also adds visual cues to the underlying basic traffic situation awareness application (e.g., Enhanced Visual Acquisition [EVAcq] or Basic Airborne Situation Awareness [AIRB]) in installations where a Traffic Display is available. The ATAS application uses ADS-B information, and where available Automatic Dependent Surveillance-Rebroadcast (ADS-R) and Traffic Information Service-Broadcast (TIS-B) information to provide the flight crew with indications of nearby aircraft in support of their see-and-avoid responsibility. ATAS is the only ADS-B application with an aural-only implementation (via an annunciator panel). All other applications require a traffic display as defined by the CDTI [Cockpit Display of Traffic Information] requirements.

NTSB CDTI simulation description

The cockpit display that presents traffic information to the pilot in a plan or “birds eye” view as stated in the EVAcq and ATAS application descriptions is the Cockpit Display of Traffic Information, or CDTI. For this accident, simulated CDTI displays for both the F-16 and C150 were created based on the TIS-B information¹⁸ that would have been displayed to the pilots of each aircraft assuming that both aircraft were equipped with:

- ADS-B In capability
- Avionics capable of running the ATAS application
- A CDTI for displaying traffic information
- An audio system capable of annunciating the ATAS aural alerts

In addition, the simulation assumes that at least one ADS-B Out equipped aircraft was operating in the vicinity of the two accident aircraft, in order to trigger the broadcast of TIS-B information from a ground station (aircraft equipped only with ADS-B In cannot trigger the broadcast of this information; therefore, if no ADS-B Out equipped aircraft were in the vicinity, the TIS-B information would not have been available for display on either airplane’s CDTI).

AC 20-172B also describes the symbol requirements for the CDTI, which are more completely defined in RTCA document DO-317B, “Minimum Operational Performance Standards (MOPS) for Aircraft Surveillance Applications (ASA) System.” These requirements specify that, among other things,

- The position of the ownship symbol should allow the display of traffic in all directions around the ownship, and indicate the direction of travel of the ownship (in the NTSB simulations, the ownship symbol is a white triangle with the direction of motion towards the top of the display (12 o’clock position)).
- Traffic symbols that are not proximate (i.e., not within 6 nmi and ± 1200 ft. of the ownship) should be cyan-colored and open (not filled). In the NTSB simulations, these symbols are open cyan-colored arrowheads.

¹⁸ This information was provided to the NTSB by the FAA, based on the FAA’s recorded radar data for the event, and filtering algorithms that would have selected traffic targets for TIS-B uplinks within a moving 15 nmi radius and ± 3500 ft “hockey puck” of the accident aircraft (the service volume associated with an ADS-B Out equipped aircraft co-located with the accident aircraft). Note that the TIS-B information is based on recorded radar data with an update rate of once every 4.5 seconds, and not on 1 sample-per-second, GPS-based, ADS-B Out data from the aircraft themselves. Consequently, the quality of TIS-B data is degraded compared to ADS-B or ADS-R data by the inherent position uncertainties and slower update rate of the radar.

- Traffic symbols that are proximate should be cyan and filled. In the NTSB simulations, these symbols are filled cyan arrowheads.
- Traffic that generates an ATAS alert should be displayed with yellow symbols enclosed in a circle. In the NTSB simulation, these symbols are filled yellow arrowheads enclosed in a yellow circle.

DO-317B also specifies the aural annunciations that should accompany an ATAS traffic alert. The components of the annunciation include the alert “Traffic,” followed by the relative traffic bearing expressed as a clock position (e.g., “two o’clock”), the relative altitude (“high,” “low,” or “same altitude”), the range to the target in nautical miles, and optionally, the vertical tendency¹⁹ (e.g., “descending”). The example of a complete annunciation given in DO-317B is “Traffic, two o’clock, high, two miles, descending.” The aural annunciation is provided both when a traffic target first generates an ATAS alert (by the algorithm predicting that the ownship will penetrate a “protected airspace zone” (PAZ) around the target), and again when the algorithm predicts that the ownship will penetrate a smaller, “collision airspace zone” (CAZ) around the target.²⁰ The NTSB simulations incorporate these elements of the aural annunciation of ATAS alerts.

It should be noted that while the simulation images presented below are representative of a CDTI that complies with the DO-317B MOPS, they do not duplicate the implementation or presentation of any particular operational display exactly. The actual images presented to a pilot depend on the range scale and background graphics selected by the pilot (which could reflect various implementations and combinations of moving maps, terrain elevation data, and weather information, rather than the simple black background presented below).

NTSB CDTI simulation results

The NTSB simulation of a CDTI display for the F-16 indicates that at 10:58:05, an open cyan target representing the C150 would have appeared at the F-16’s 12 o’clock position (i.e., straight ahead; see Figure 20a), 15 nmi from and 1300 ft. below the F-16, and would have been the only target within that range from that time up to the time of the collision at 11:00:56.6. As the aircraft approached each other, the C150 target would have been shown turning left from west to east and then approaching the F-16 from the F-16’s 12 o’clock position, slightly to the right of the F-16’s flight path, and climbing. The heading depicted by the C150 symbol as the aircraft converged would have indicated that the C150’s projected flight path would cross the F-16’s flight path from right to left (as viewed from the F-16). At 10:59:47, the C150 symbol would have changed from an open cyan arrowhead to a filled cyan arrowhead, as the C150 closed within 6 nmi horizontally and 600 ft. vertically of the F-16.

At 11:00:35, as the F-16 banked into its left turn towards the south, it would have received an ATAS alert associated with the C150, which by then had closed within 2 nmi horizontally and 300 ft. vertically. As shown in Figure 20f, at this time the C150 symbol would have changed to a filled yellow arrowhead, enclosed by a yellow circle. At the same time, an audio alert of “Traffic, 12 o’clock, low, 2 miles” would have been annunciated. As the F-16 continued in its left turn, the C150 target would have rotated to the right side of the F-16’s projected course, with its heading still projected to intercept that course (see Figure 20g). At 11:00:56, less than one second before the

¹⁹ The vertical tendency will only be annunciated when the computed rate of climb or descent is at least 500 ft./min.

²⁰ Per DO-317B, the size of the PAZ depends on the closure rate between the aircraft, increasing as the closure rate increases. The size of the CAZ is constant at a 500 ft. radius and a height of ± 2000 ft.

collision, the F-16 would have received a second ATAS aural alert of “Traffic, 2 o’clock, same altitude, zero miles” and the C150 symbol would have depicted the C150 100 ft. below the F-16 (see Figure 20i).

The NTSB simulation of a CDTI display for the C150 indicates that at 10:58:05, an open cyan target representing the F-16 would have appeared at the C150’s 8 o’clock position, 15 nmi from and 1300 ft. above the C150, and would have been one of two targets within that range from that time up to the time of the collision at 11:00:56.6 (see Figure 21a). The other target would have appeared between the C150’s 12 and 1 o’clock position, about 11 nmi from and 1300 ft. above the C150. As the C150 turned left from west to east, the F-16 target would have rotated to the C150’s 11 o’clock position and been depicted flying towards the C150, and the other aircraft would have rotated to the C150’s 3 o’clock position and been depicted flying away from the C150 (see Figure 21b). At 10:59:47, the F-16 symbol would have changed from an open cyan arrowhead to a filled cyan arrowhead, as the F-16 closed within 6 nmi horizontally and 600 ft. vertically of the C150.

At 11:00:35, as the F-16 banked into its left turn towards the south, the C150 would have received an ATAS alert associated with the F-16, which by then had closed within 2 nmi horizontally and 300 ft. vertically. As shown in Figure 21f, at this time the F-16 symbol would have changed to a filled yellow arrowhead, enclosed by a yellow circle. At the same time, an audio alert of “Traffic, 11 o’clock, high, 1 mile” would have been annunciated.²¹ The C150 would not have received a second ATAS aural alert for the F-16,²² but the F-16 symbol would have remained in alert status (filled yellow arrowhead enclosed by a yellow circle) until the collision. The CDTI display for the C150 at 11:00:56, one second before the collision, is shown in Figure 21i.²³

E. CONCLUSIONS

This *Aircraft Performance Radar & Cockpit Visibility Study* presents the results of using the KCHS ASR and F-16 CSMU data to calculate the position and orientation of each aircraft in the minutes preceding the collision. This information is then used to estimate the approximate location of each airplane in the other airplane’s windows during the same period, and to simulate the traffic information that could have been presented to the pilots, had the airplanes been equipped with CDTI displays.

The position, speed, track angle, separation distance, and closure rate of both airplanes at the times of events of interest are summarized in Table 5. Detailed position, attitude, speed, and convergence information is presented in Figures 5-11. The azimuth and elevation angles of each airplane in the fields of view of the pilots are presented in Figures 14-19, and recreations of the out-the-window views from each airplane at significant times are presented in Figures 20 and 21.

²¹ The different aural annunciations of “2 miles” for the F-16 and “1 mile” for the C150, even for the same encounter geometry at 1100:35, is the result of slight differences in the computed range to the target for the F-16 and C150, and the way the range is discretized for aural alerts. The TIS-B data for the F-16 resulted in range to the C150 of 1.85 nmi at 11:00:35, which is rounded to 2 miles for the aural alert. The TIS-B data for the C150 resulted in a range to the F-16 of 1.74 nmi at 11:00:35, which is rounded to 1 mile for the aural alert.

²² The second aural alert provided to the F-16 was caused by the ATAS algorithms for the F-16 predicting that the F-16 would penetrate the CAZ around the C150. The ATAS algorithms for the C150 did not predict a similar penetration of the CAZ around the F-16, so no second aural alert was issued. The difference in the predictions is likely the result of the uncertainty in and relatively low sample rate of the radar data upon which the TIS-B information is based.

²³ The appearance of the F-16 symbol passing slightly behind the C150 “ownship” symbol in Figure 21i is likely the result of small errors in the TIS-B data stemming from the low sample rate and uncertainties in the radar data, and the smoothing and extrapolation functions used in the FAA tracker and DO-317B ATAS algorithms.

Figures 20 and 21 also present the traffic information that could have been presented on CDTI displays (had the airplanes been so equipped).

The information cited above indicates that when the WEST controller first alerted the F-16 pilot about the C150 at 11:00:16 (about 40 seconds before the collision), the C150 was climbing through about 1200 ft. on a ground track of about 109° (true), at a ground speed of about 71 kt. At the same time, the F-16 was level at about 1600 ft. on a ground track of about 252° (true) and a ground speed of about 250 kt. The airplanes were 3.25 nmi apart, closing at about 308 kt.

The F-16 began a left turn to the south (following the WEST controller's instructions) at 11:00:35. At 11:00:33, when the controller began speaking the instruction that included the phrase "turn left heading 180 immediately," the airplanes were about 1.8 nmi apart and closing at about 293 kt. The C150 was 300 ft. below the F-16 and climbing.

As the F-16 turned, it began a slow descent from 1600 ft. because the airplane's α – protection system precluded the autopilot from maintaining a level, 32° banked turn at the F-16's flight condition.

The airplanes collided at 11:00:56.6, at an altitude of about 1466 ft., and with a closure rate of about 255 kt., at a collision angle of about 88°. The location certain F-16 engine parts near the collision point (and the continued crippled flight of the F-16 towards the south) is consistent with the C150 impacting the F-16's lower, aft fuselage.

The cockpit visibility part of this *Study* indicates that each airplane would have remained a relatively small object in the other airplane's windows (spanning less than 0.5° of the field of view²⁴) until about 5 seconds before the collision, and subsequently grown in size suddenly (the "blossom" effect). The WEST controller first alerted the F-16 pilot about the C150 at 11:00:16, about 40 seconds prior to the collision. For several brief periods after this time, the C150 may have been obscured from the F-16 pilot's field of view behind the F-16 Head-Up Display (HUD) support structure or the instrument panel; between these times, the C150 would have appeared predominantly in the transparent area of the HUD, on the horizon between ground and sky. In the last 3 to 4 seconds before the collision, the C150 may have been mostly obscured by the HUD support structure and the instrument panel.

In the 40 seconds prior to the collision, the F-16 would have remained in the C150 pilot's field of view until about 1 second before the collision, when the F-16 may have become partially obscured by the C150's left wing strut.

While the visibility of a target airplane in the viewer pilot's field of view is sensitive to movements of the pilot's head, the variations in eye position examined in this *Study* changed the timing of the obscurations of the target aircraft by less than +/-1.5 seconds at any given point. Nonetheless, the results indicate that looking for traffic can be more effective if the pilot moves his head as well as redirecting his eyes, since head movements may bring otherwise obscured aircraft into view.

The circumstances of this accident underscore the difficulty in seeing airborne traffic (the foundation of the "see and avoid" concept), even when the airplanes are not obscured from view, and even when one of the pilots is alerted to the presence of the other airplane by ATC.

²⁴ 0.5° of the field of view is equivalent to the diameter of a penny viewed from about 7 ft. away.

The CDTI simulations indicate that, had the airplanes been equipped with a CDTI, the system could have alerted each pilot to the presence of the other airplane, and presented precise bearing, range, and altitude information about each target, up to two minutes and 50 seconds prior to the collision. Such timely and information-rich traffic presentations would likely have enabled each pilot to avoid the other airplane using only slight course and / or altitude adjustments, and without the need for aggressive maneuvering.

John O'Callaghan
National Resource Specialist - Aircraft Performance
Office of Research and Engineering

F. REFERENCES

1. Lockheed Martin Corporation, *Guide for USAF F-16 Mishap Investigations*, Contract No. F42620-01-D-0058, Document # 16PR1304G, dated 15 February 2015. Copyright © 2015 Lockheed Martin Corporation. All rights reserved.
2. National Transportation Safety Board, Office of Research and Engineering, *Flight Data Recorder Group Chairman's Factual Report, Lockheed-Martin F-16CM, Moncks Corner, South Carolina, July 07, 2015, NTSB Accident # ERA15MA259AB*. (Washington, D.C., July 26, 2016). (Contact NTSB at pubinq@ntsb.gov).
3. Textron Aviation, *1975 Cessna Model 150 Owner's Manual*, Document # D1033-13, Copyright © 1985 Cessna Aircraft Company, Wichita, Kansas.
4. Internal NTSB emails from IIC to Aircraft Performance Specialist, dated 7/16/2015 & 7/21/2015.
5. Textron Aviation, *Cessna Aircraft Company Report No. S-150M-0 (76): Model 150M Basic Data*, dated 22 January 1975. (Textron proprietary document)
6. National Transportation Safety Board, *Factual Report: Lockheed-Martin F-16CM, 96-0085, and Cessna 150M, N3601V, Moncks Corner, South Carolina, July 07, 2015, NTSB Accident # ERA15MA259AB*. (Contact NTSB at pubinq@ntsb.gov).
7. Velasco e Cruz, A., *Historical Roots of 20/20 as a (Wrong) Standard Value of Normal Visual Acuity*, Optometry and Vision Science Journal, Vol. 67, No.8, p. 661, March 30, 1990. Copyright © American Academy of Optometry.

G. GLOSSARY

Acronyms

AC	Advisory Circular
ACP	Azimuth Change Pulses
ADS-B	Automatic Dependent Surveillance – Broadcast
ADS-R	Automatic Dependent Surveillance – Rebroadcast
AFB	Air Force Base
AOPA	Aircraft Owners and Pilots Association
ARSR	Air Route Surveillance Radar
ASA	Aircraft Surveillance Applications
ASR	Airport Surveillance Radar
ATAS	ADS-B Traffic Advisory System
ATC	Air Traffic Control
ATCT	Air Traffic Control Tower
C150	Cessna model 150M airplane
CAZ	Collision Airspace Zone
CDTI	Cockpit Display of Traffic Information
CFR	Code of Federal Regulations
CG	Center of Gravity
CSMU	Crash survivable memory unit
DEATH41	Accident F-16 call sign
EDT	Eastern Daylight Time
EVAcq	Enhanced visual acquisition
F-16	Lockheed-Martin model F-16CM airplane
FAA	Federal Aviation Administration
FSX	Microsoft Flight Simulator X computer program
GPS	Global Positioning System
HUD	Head-Up Display
IFR	Instrument Flight Rules
IIC	Investigator In Charge
KCHS	Charleston Air Force Base / International Airport, Charleston, South Carolina
KMKS	Berkeley County Airport, Moncks Corner, South Carolina
MAC	Mean Aerodynamic Chord
METAR	Meteorological Terminal Air Report
MOPS	Minimum Operational Performance Standards
MSL	Mean Sea Level
NAS	National Airspace System
NextGen	Next Generation Air Transportation System
NTSB	National Transportation Safety Board
PAZ	Protection Airspace Zone
RPM	Revolutions Per Minute
SDR	Seat Data Recorder
TCAS	Traffic Collision Avoidance System
TIS-B	Traffic Information Services – Broadcast
TSAA	Traffic Situation Awareness with Alerts
UTC	Universal Coordinated Time
VMC	Visual Meteorological Conditions
VFR	Visual Flight Rules
WEST	Abbreviation of KCHS ATCT West radar position controlling accident F-16

English symbols

C_L	Lift coefficient
E	Distance east of KCHS ASR antenna
E_0	Distance east of KCHS ASR antenna at time = 0
N	Distance north of KCHS ASR antenna
N_0	Distance north of KCHS ASR antenna at time = 0
t	Time
\vec{V}	Airspeed vector
V_G	Ground speed
\vec{V}_G	Groundspeed vector
V_E	East component of ground speed
V_N	North component of ground speed
V_T	True airspeed
\vec{V}_T	True airspeed vector
\vec{V}_W	Wind speed vector
x_b	Component along airplane x-body axis
y_b	Component along airplane y-body axis
z_b	Component along airplane z-body axis

Greek symbols

α	Angle of attack
β	Sideslip angle
γ	Flight path angle
Δ	Change in quantity following Δ
θ	Pitch angle
ϕ	Roll angle
ψ	Heading angle (true)
ψ_G	Ground track angle (true)

FIGURES

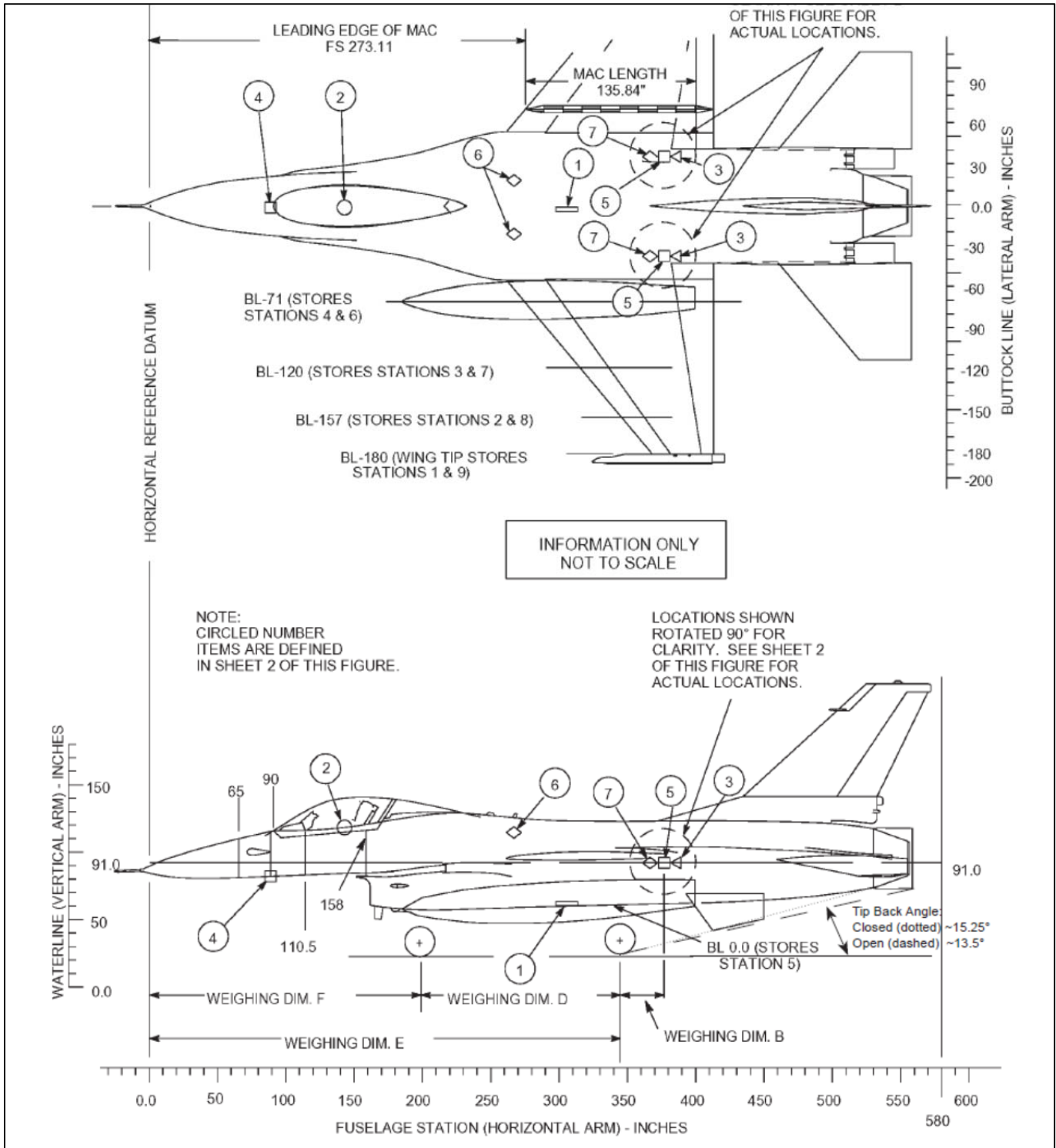


Figure 1. F-16CM diagrams, from Reference 1.



Figure 2. Photograph of F-16CM at Shaw AFB, with a paint scheme identical to that of accident F-16 (except for lettering).



Figure 3. Pre-accident photograph of N3601V.

* Maximum height of airplane with nose gear depressed, all tires and nose strut properly inflated, and optional flashing beacon installed.

** Maximum wing span if optional conical camber wing tips and optional strobe lights are installed. If standard wing tips without strobe lights are installed, wing span is 32'-8 1/2".

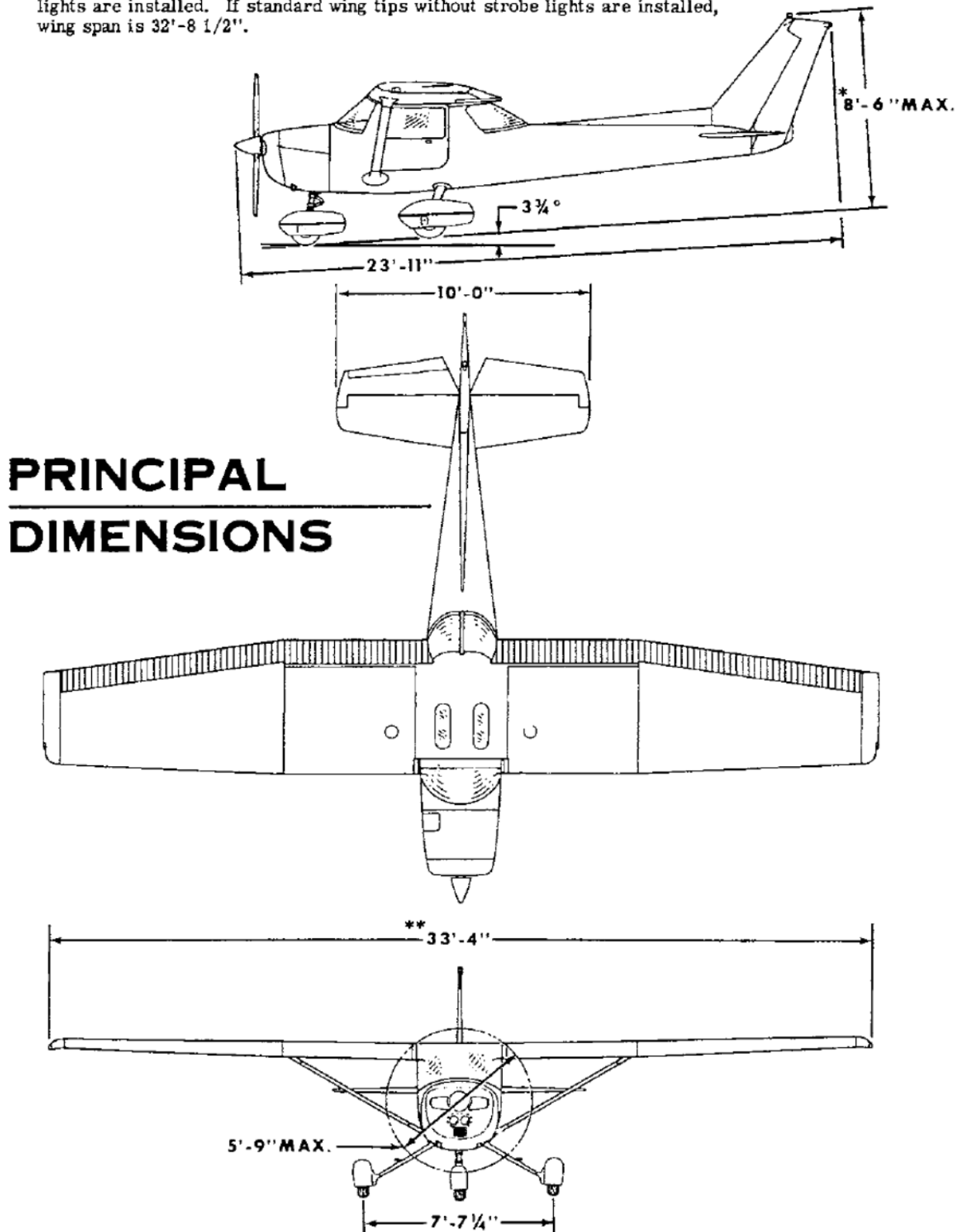
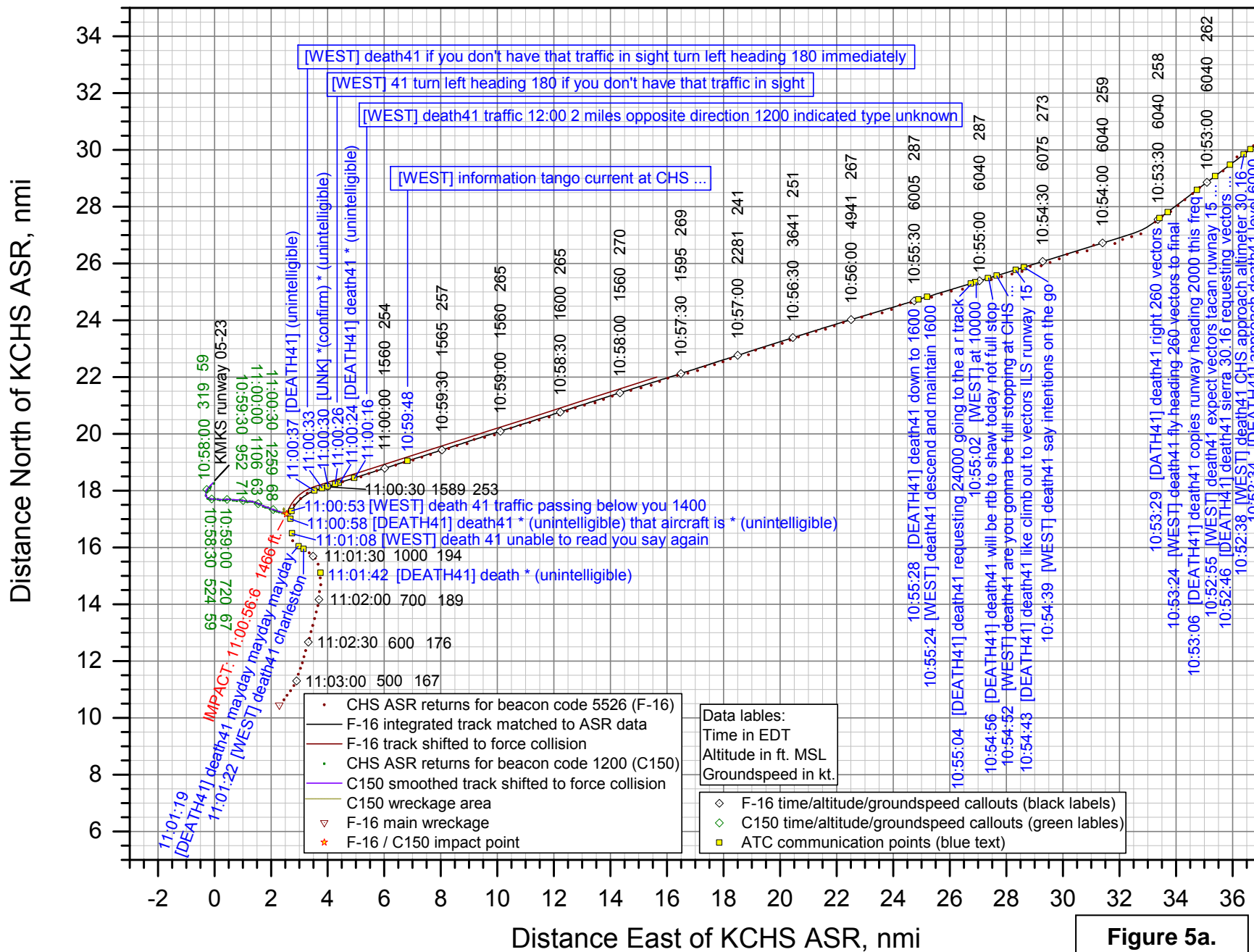


Figure 4. 3-view of Cessna 150M, from Reference 3.

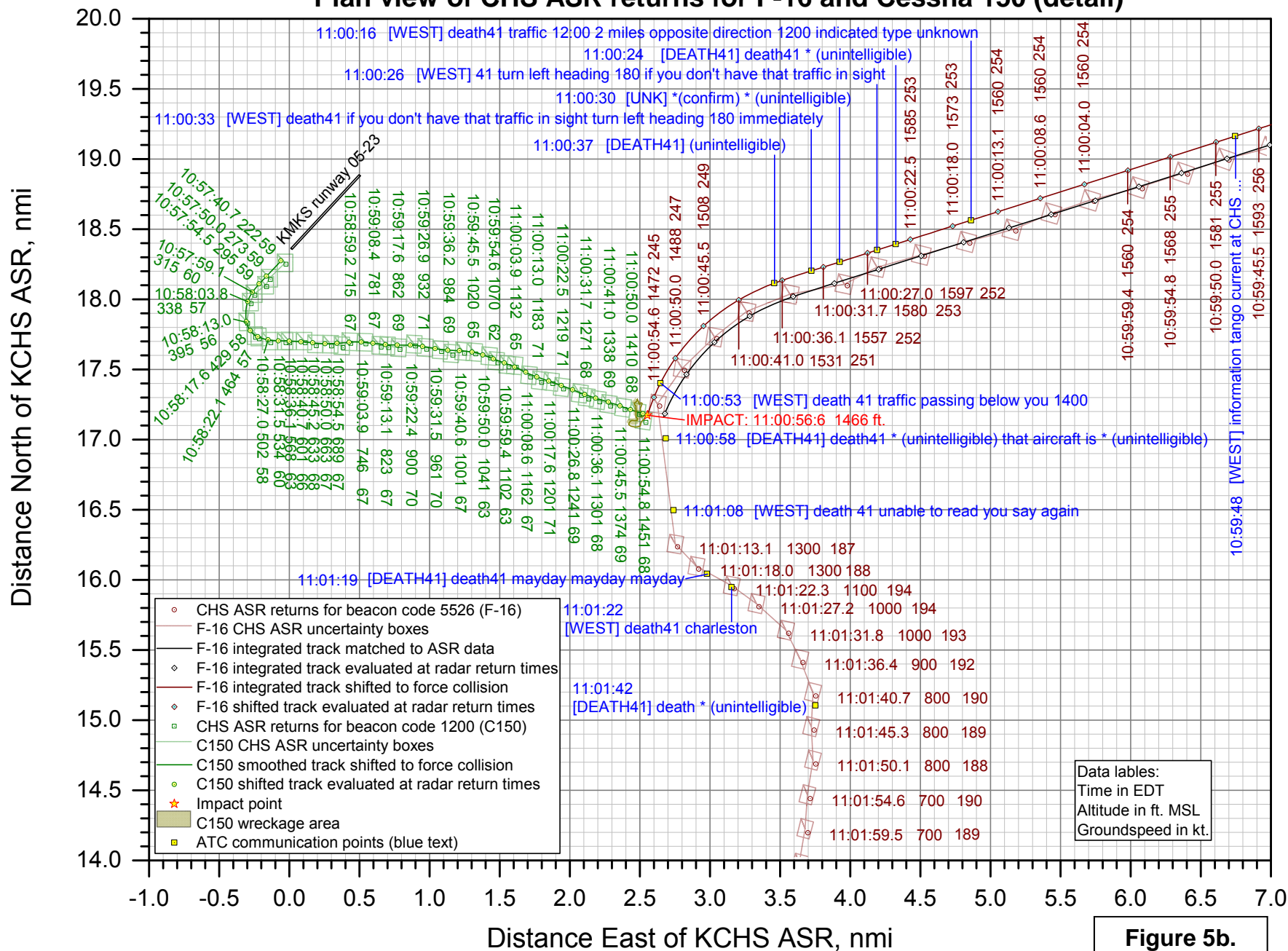
ERA15FA259AB: Midair collision, F-16 / C150, Moncks Corner, SC, 7/7/2015

Plan view of CHS ASR returns for F-16 and Cessna 150



ERA15FA259AB: Midair collision, F-16 / C150, Moncks Corner, SC, 7/7/2015

Plan view of CHS ASR returns for F-16 and Cessna 150 (detail)



ERA15FA259AB: Midair collision, F-16 / C150, Moncks Corner, SC, 7/7/2015

Plan view of CHS ASR returns for F-16 and Cessna 150

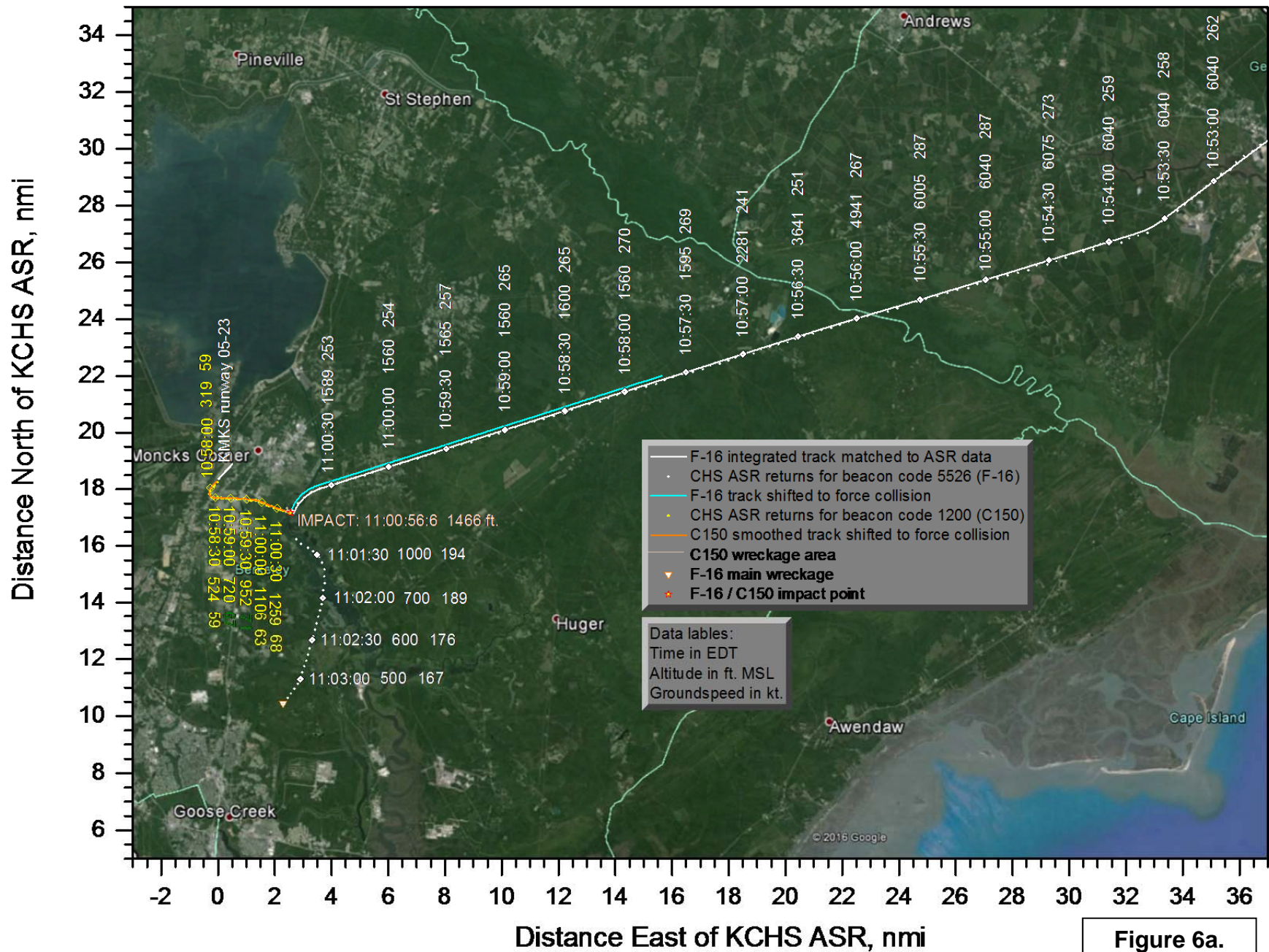


Figure 6a.

ERA15FA259AB: Midair collision, F-16 / C150, Moncks Corner, SC, 7/7/2015

Plan view of CHS ASR returns for F-16 and Cessna 150 (detail)

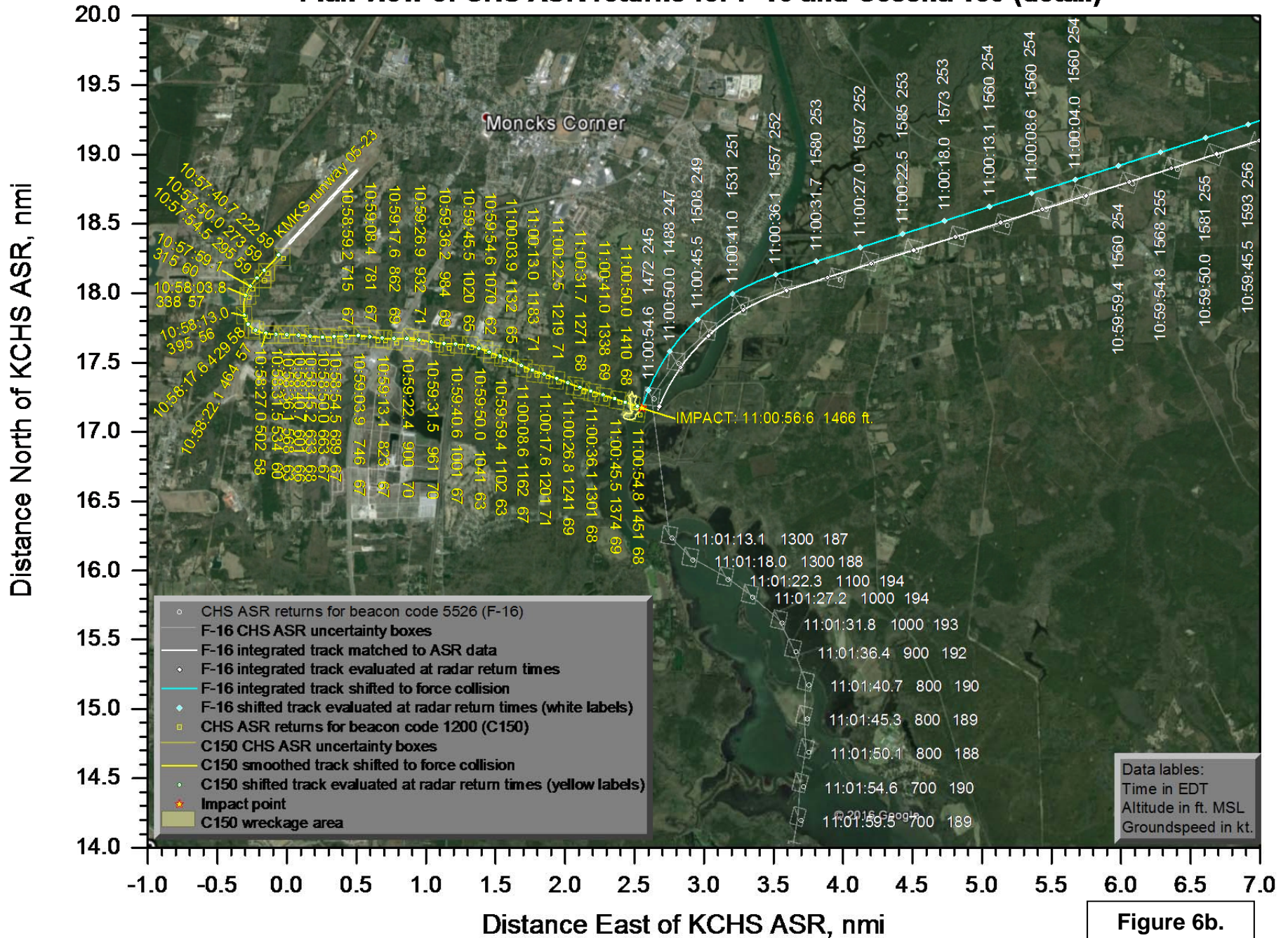
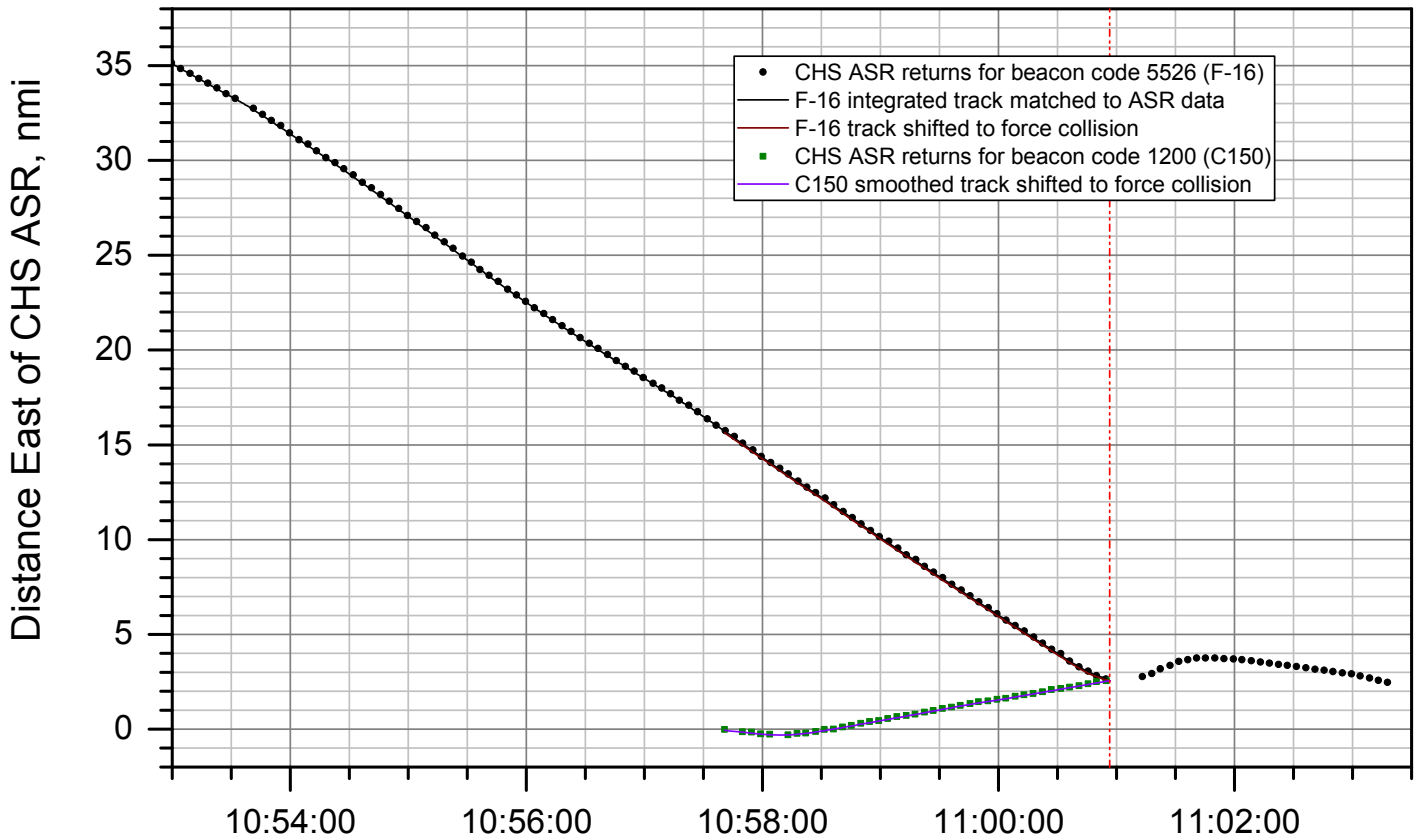
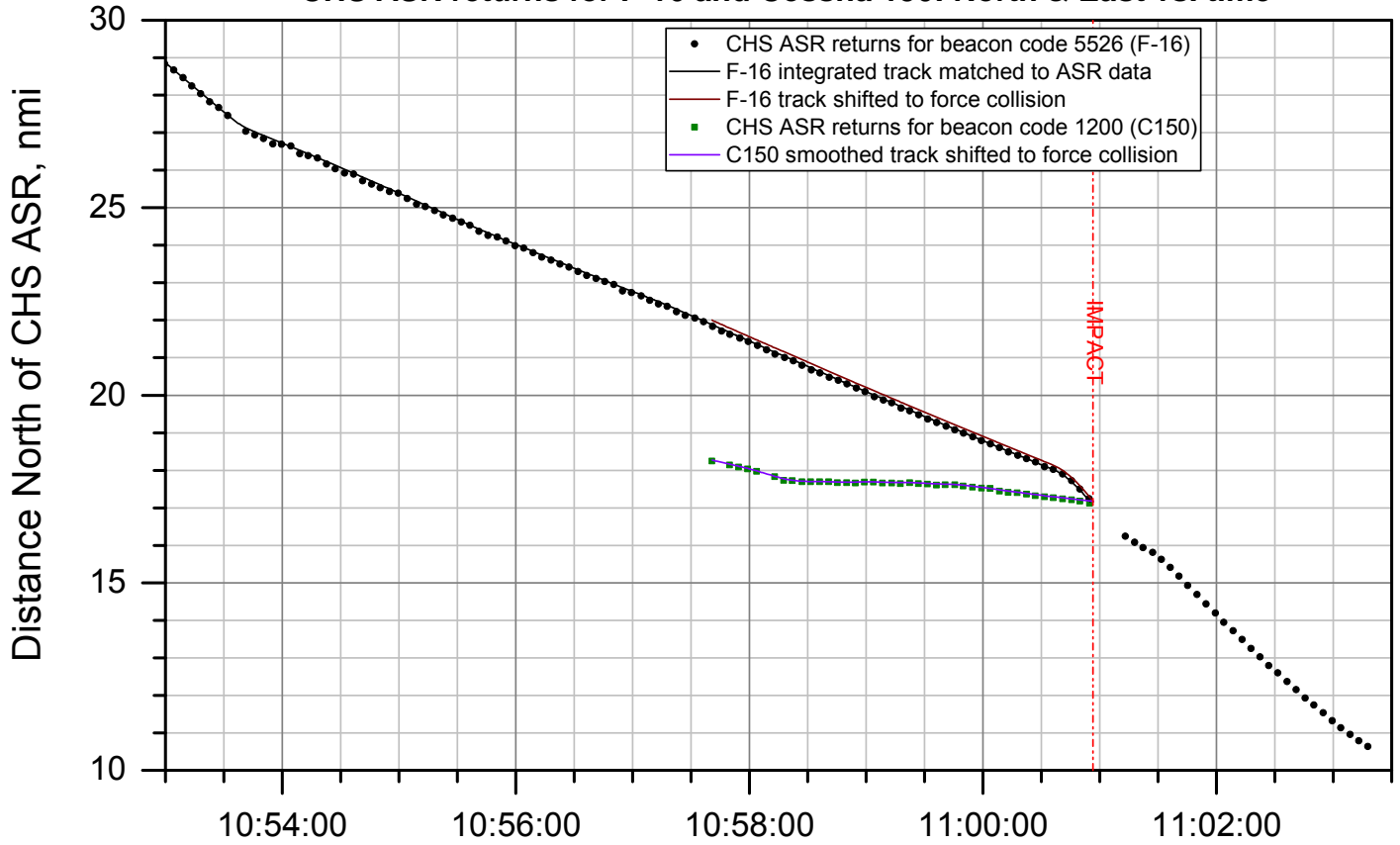


Figure 6b.

ERA15FA259AB: Midair collision, F-16 / C150, Moncks Corner, SC, 7/7/2015

CHS ASR returns for F-16 and Cessna 150: North & East vs. time



KCHS ASR time, HH:MM:SS EDT

Figure 7a.

ERA15FA259AB: Midair collision, F-16 / C150, Moncks Corner, SC, 7/7/2015

CHS ASR returns for F-16 and Cessna 150: North & East vs. time (detail)

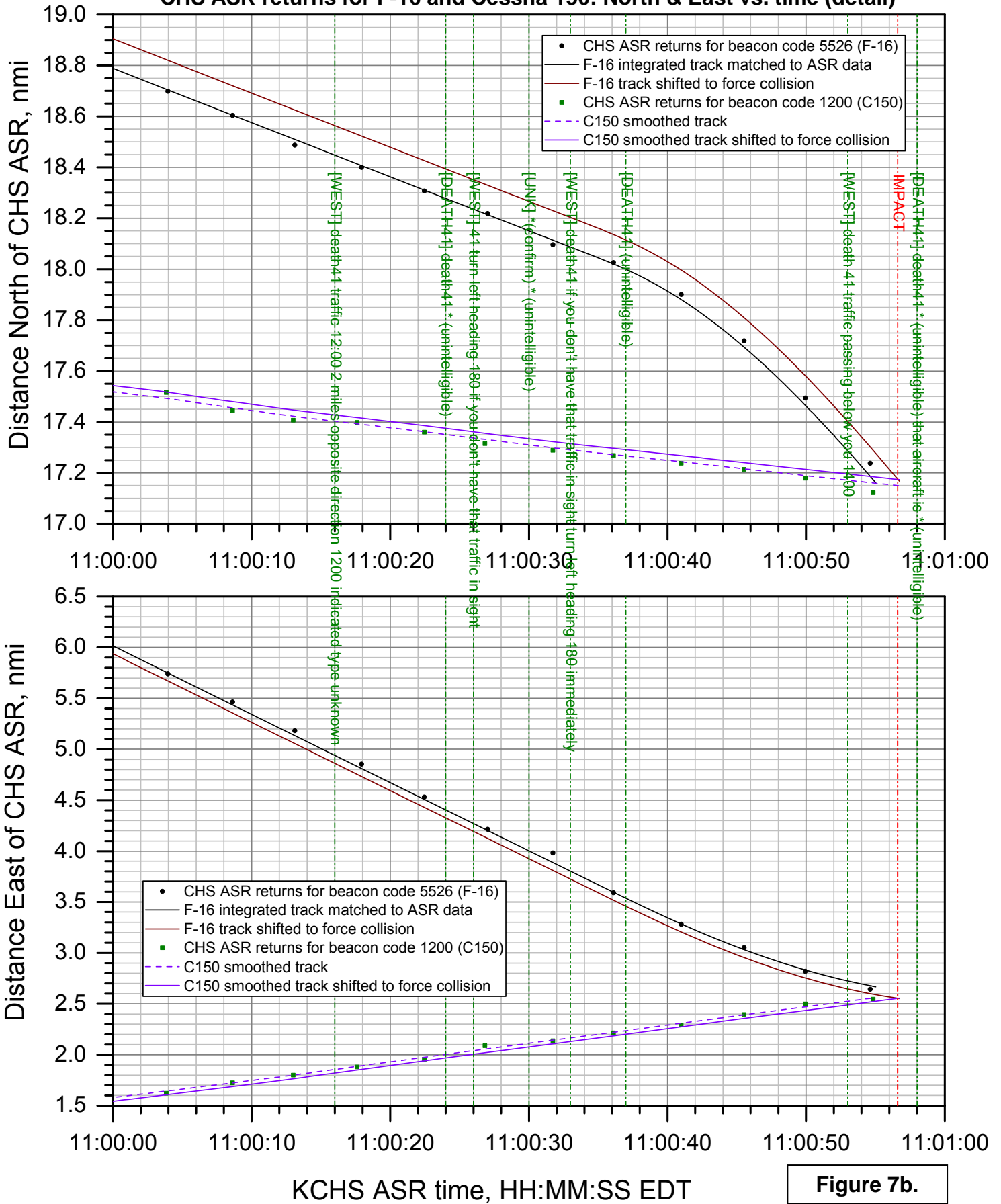
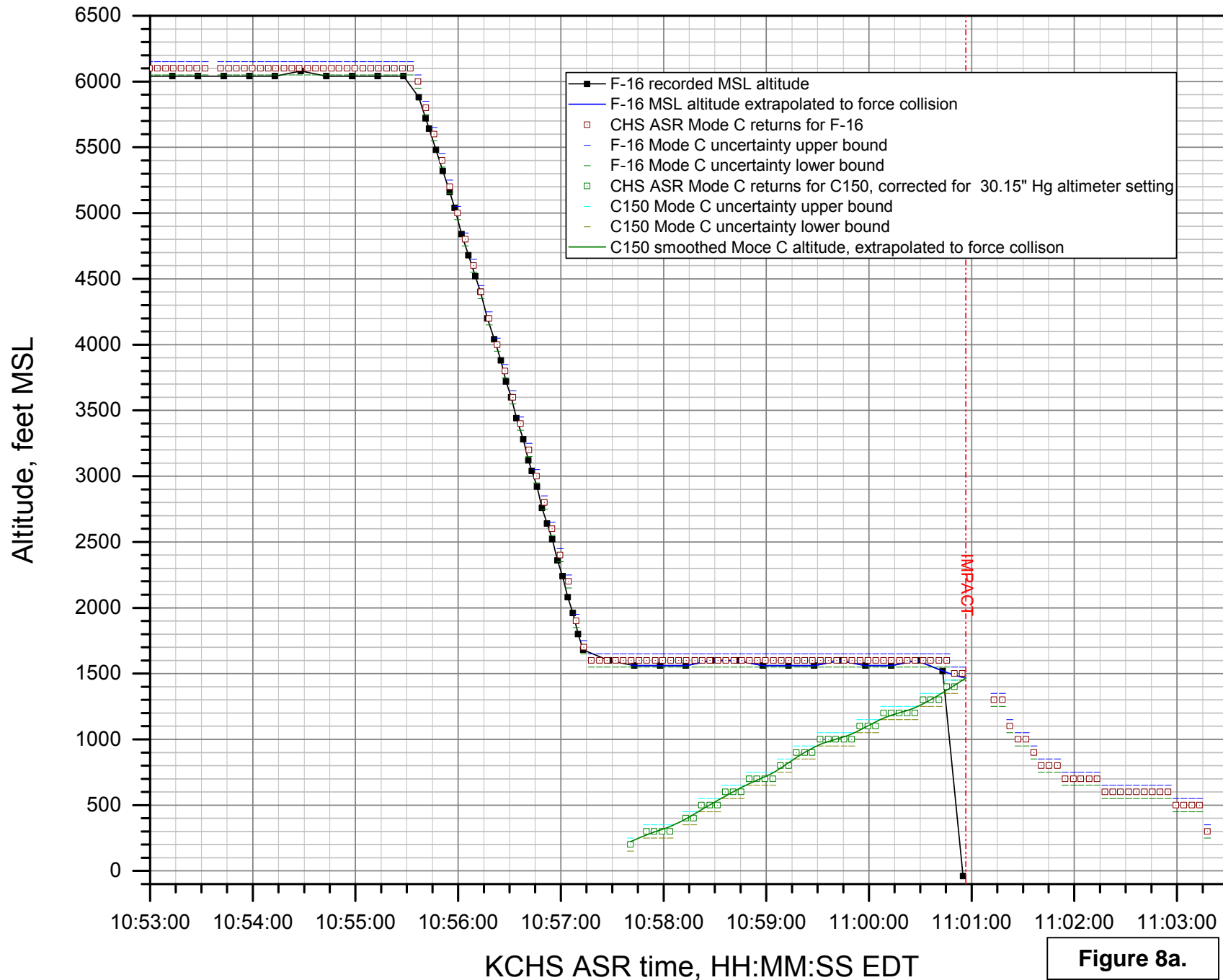


Figure 7b.

ERA15FA259AB: Midair collision, F-16 / C150, Moncks Corner, SC, 7/7/2015
F-16 and Cessna 150 altitude vs. time



ERA15FA259AB: Midair collision, F-16 / C150, Moncks Corner, SC, 7/7/2015

F-16 and Cessna 150 altitude vs. time (detail)

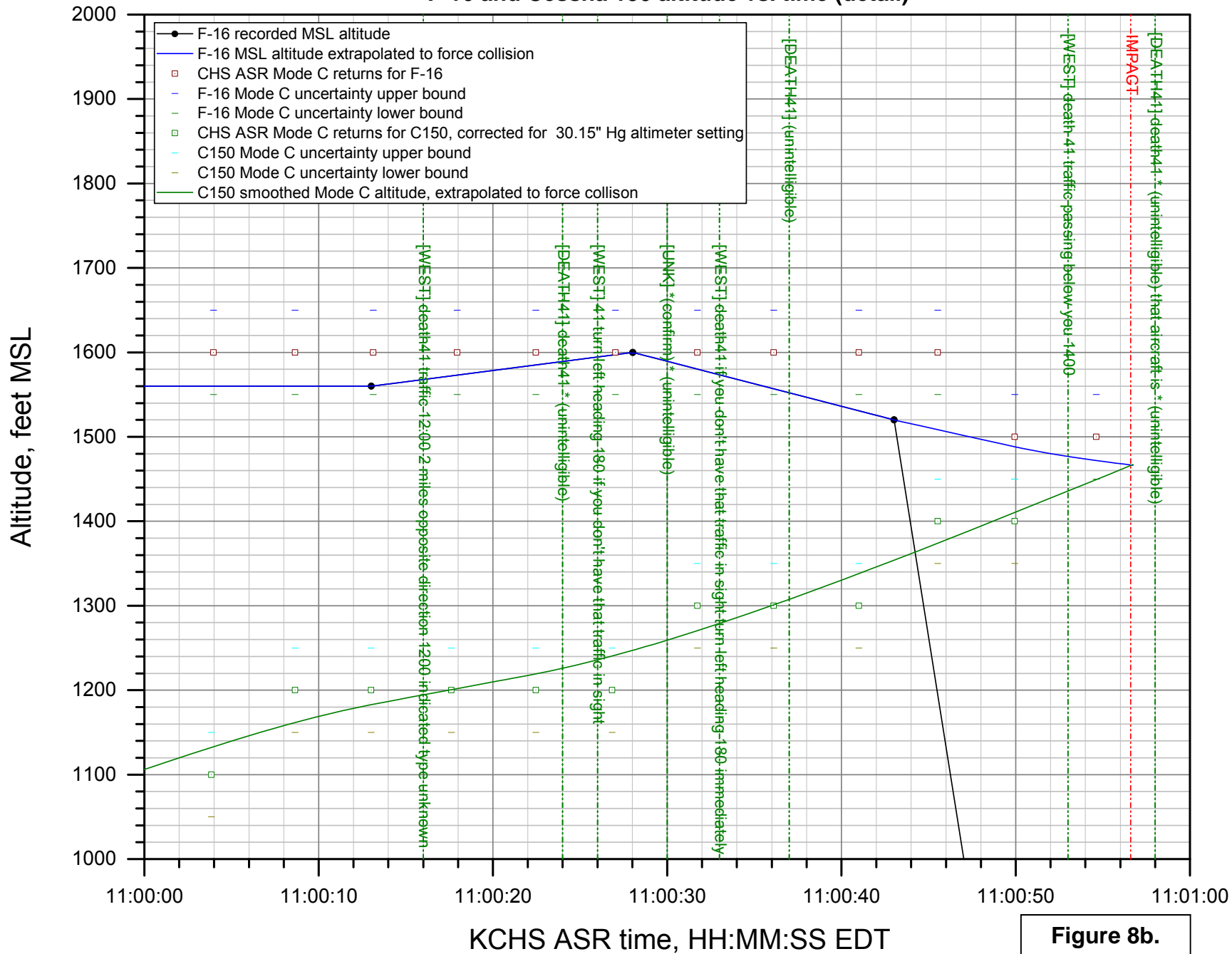
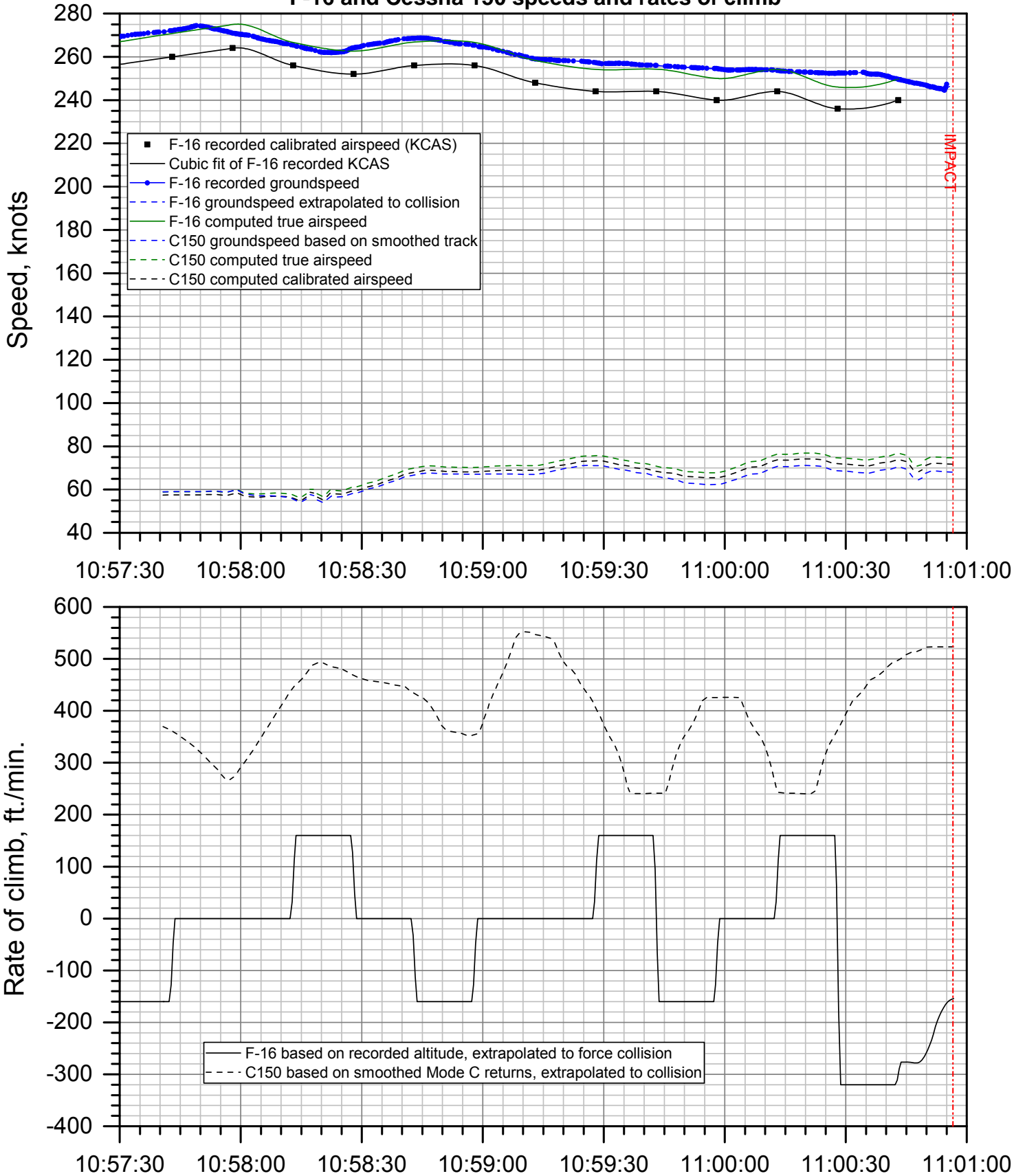


Figure 8b.

ERA15FA259AB: Midair collision, F-16 / C150, Moncks Corner, SC, 7/7/2015

F-16 and Cessna 150 speeds and rates of climb

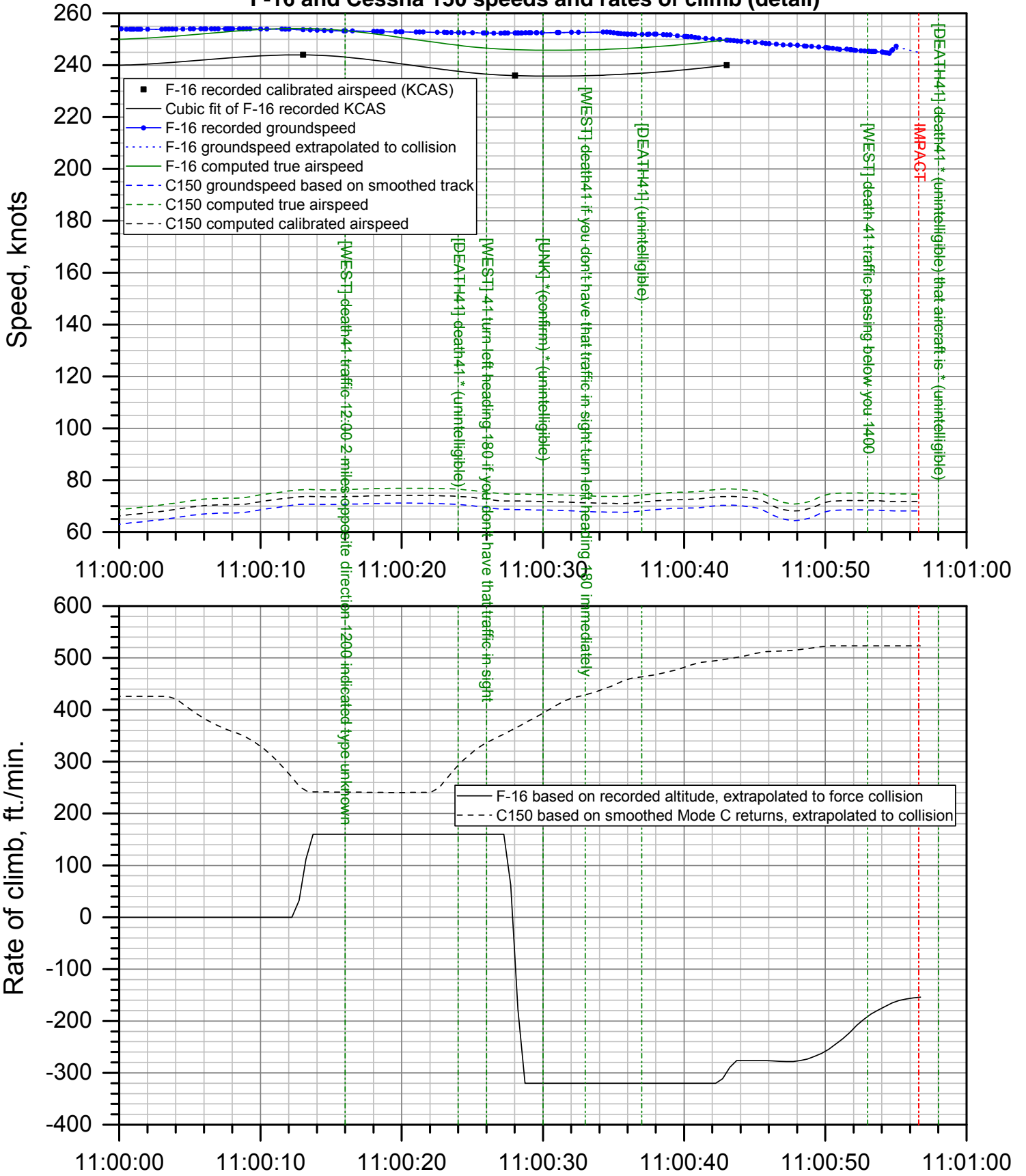


KCHS ASR time, HH:MM:SS EDT

Figure 9a.

ERA15FA259AB: Midair collision, F-16 / C150, Moncks Corner, SC, 7/7/2015

F-16 and Cessna 150 speeds and rates of climb (detail)



KCHS ASR time, HH:MM:SS EDT

Figure 9b.

ERA15FA259AB: Midair collision, F-16 / C150, Moncks Corner, SC, 7/7/2015 F-16 and Cessna 150 separation distance and closure rate

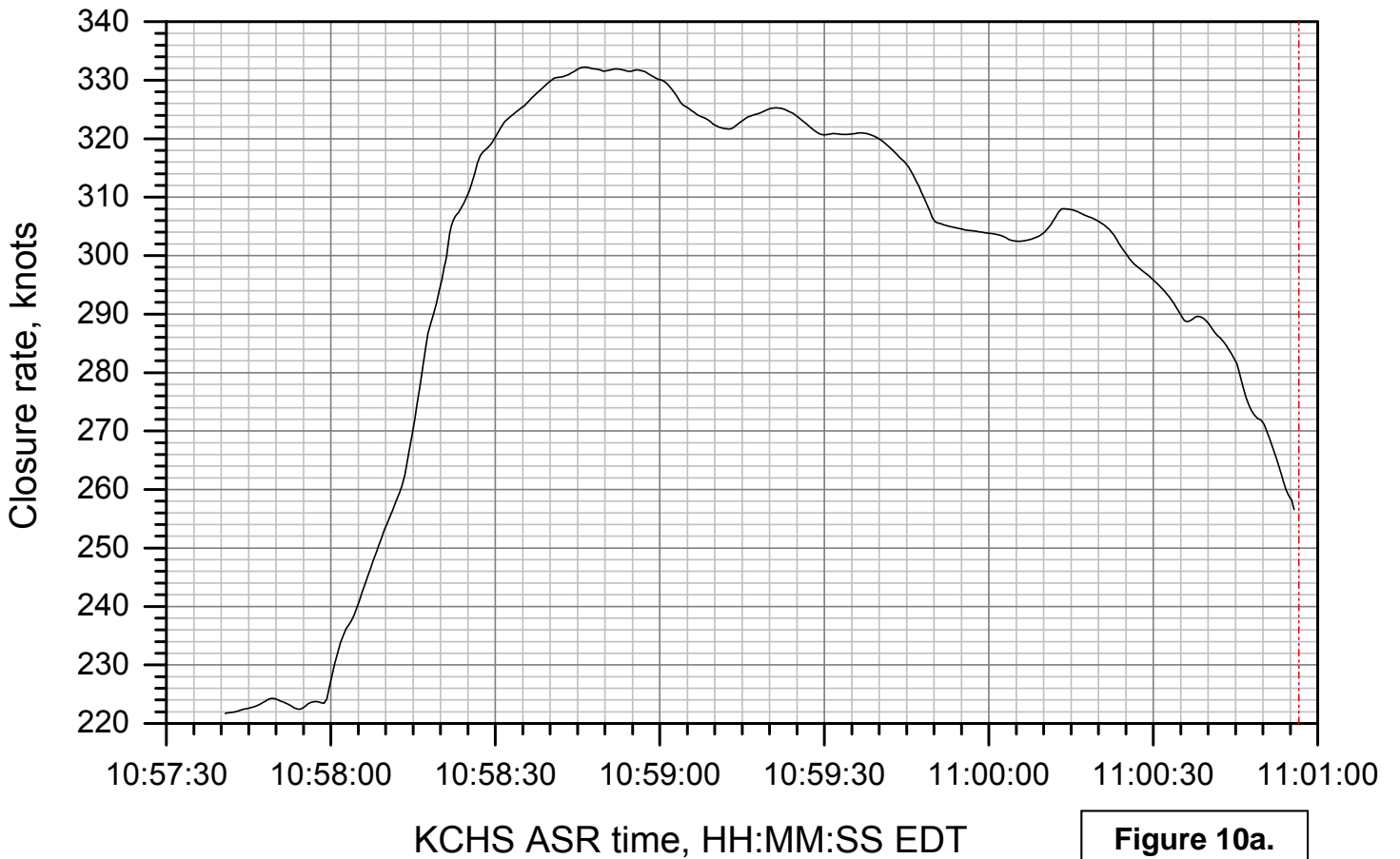
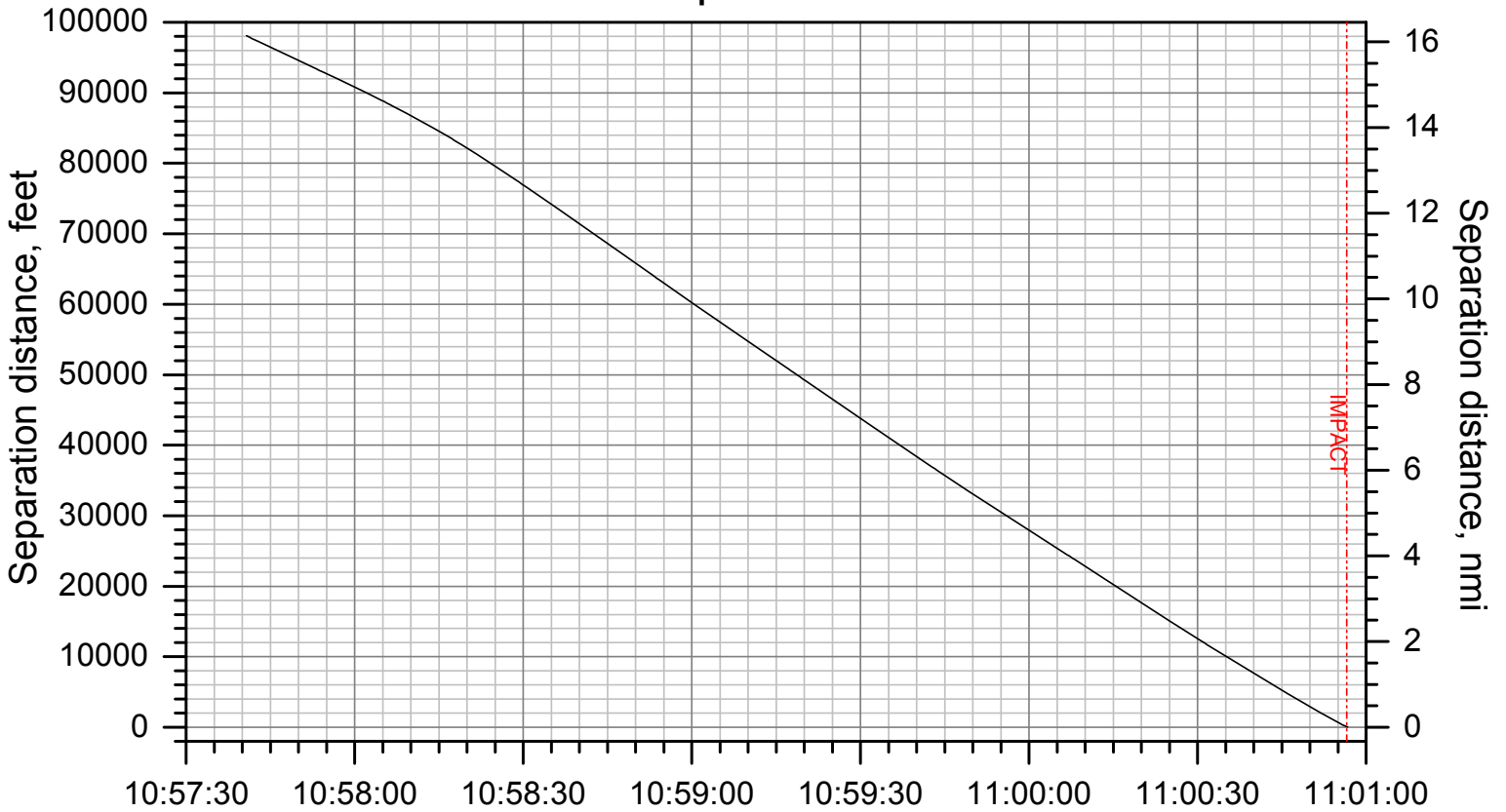


Figure 10a.

ERA15FA259AB: Midair collision, F-16 / C150, Moncks Corner, SC, 7/7/2015
F-16 and Cessna 150 separation distance and closure rate (detail)

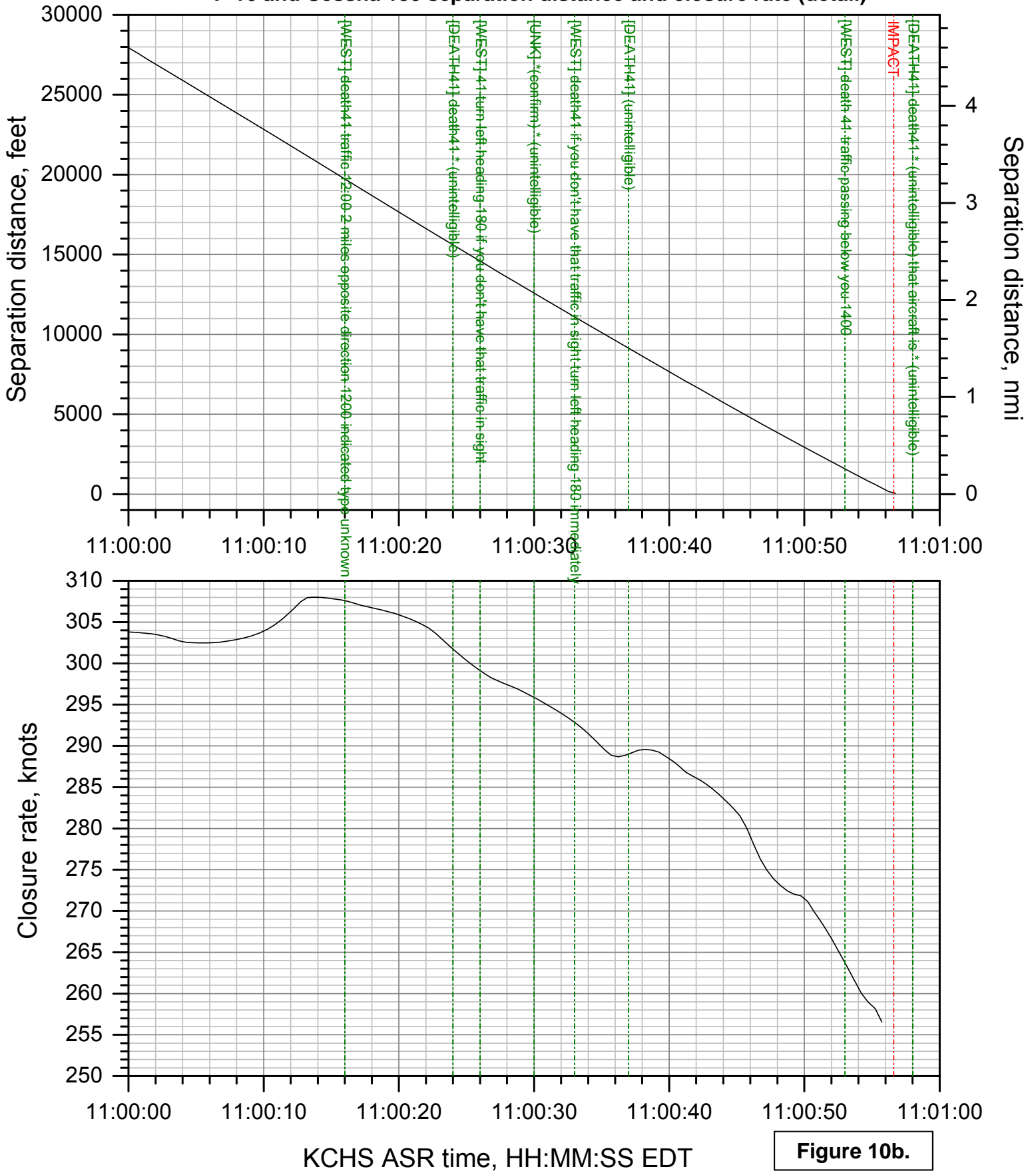


Figure 10b.

ERA15FA259AB: Midair collision, F-16 / C150, Moncks Corner, SC, 7/7/2015

F-16 and Cessna 150 Euler angles vs. time

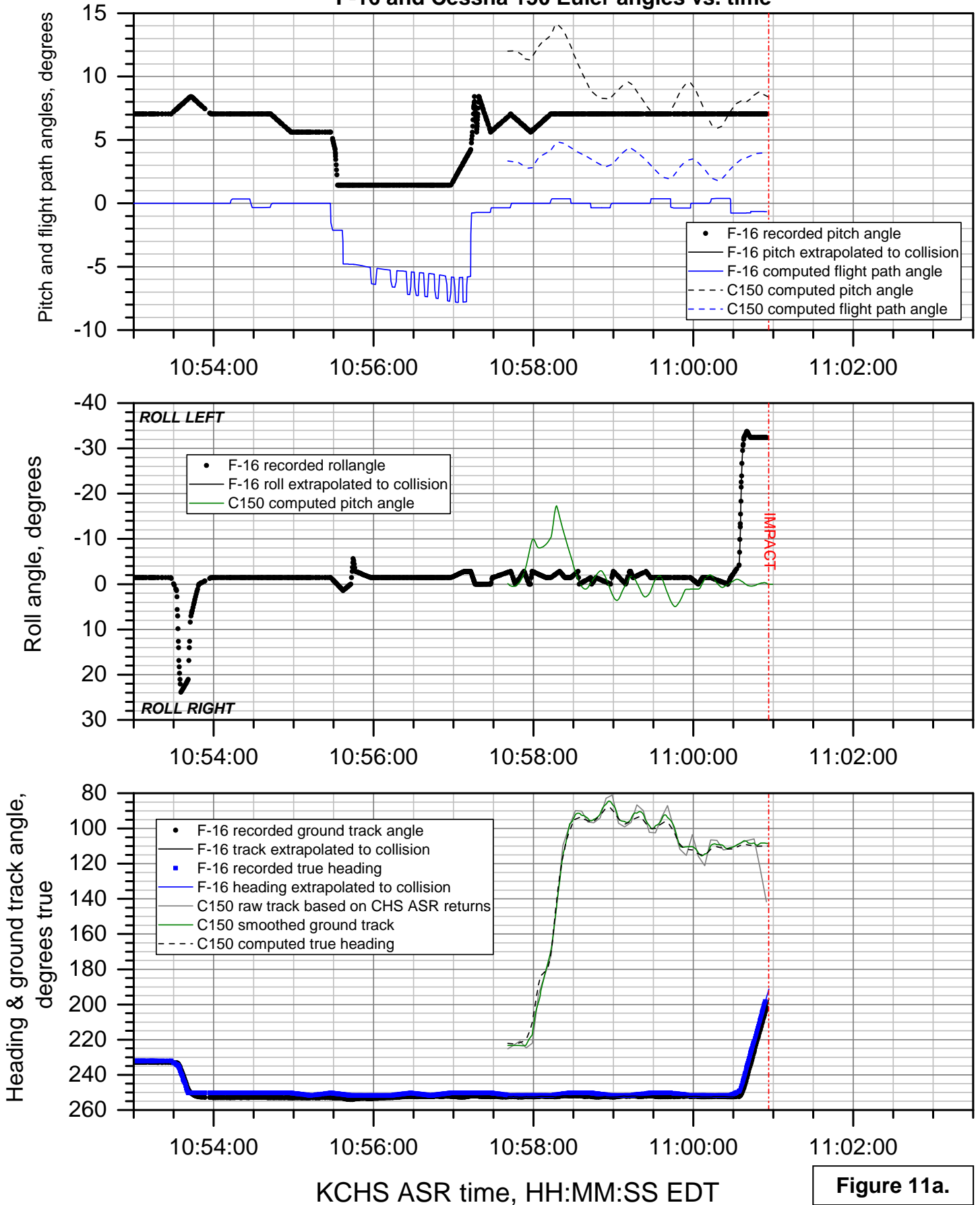


Figure 11a.

ERA15FA259AB: Midair collision, F-16 / C150, Moncks Corner, SC, 7/7/2015

F-16 and Cessna 150 Euler angles vs. time (detail)

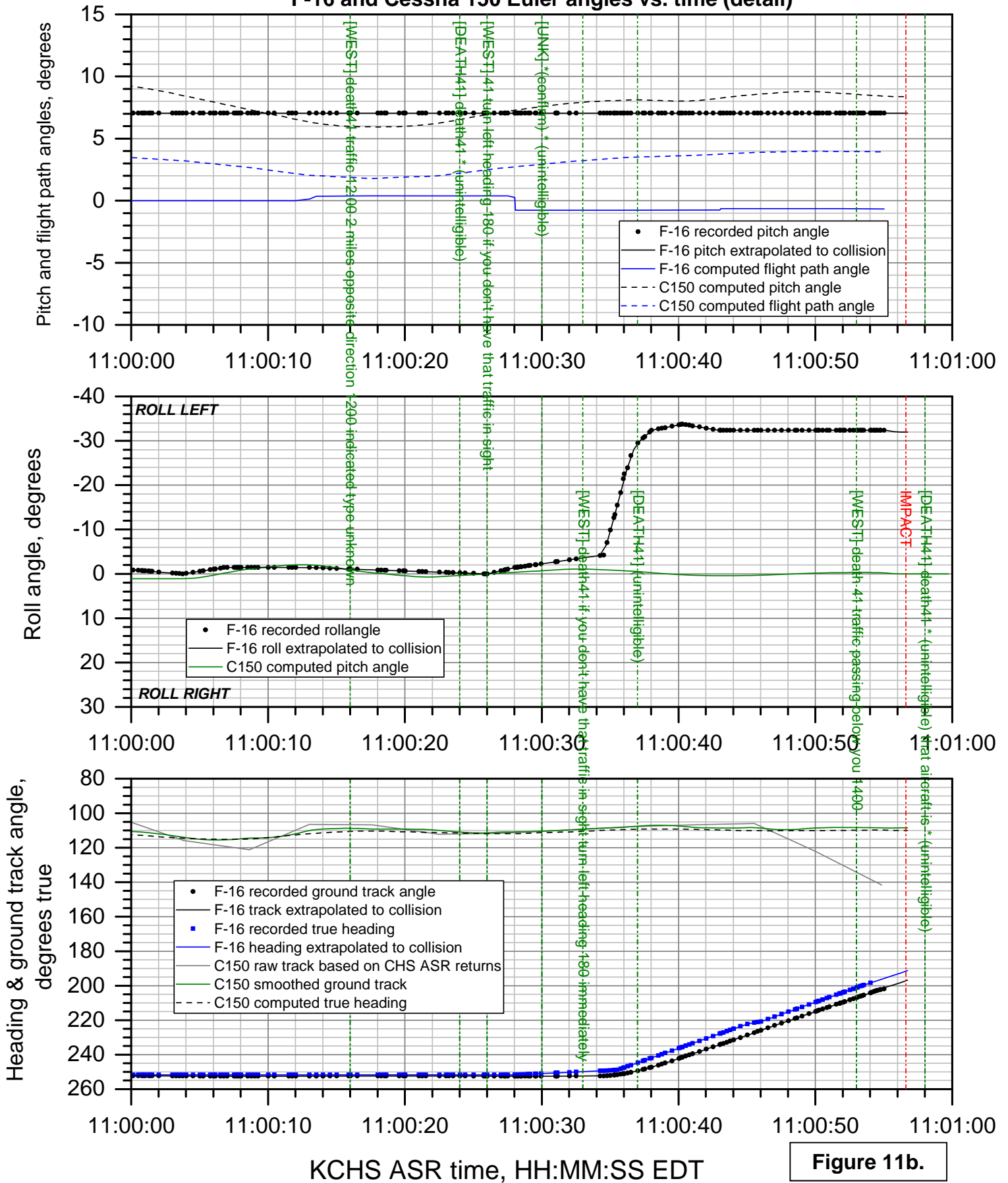
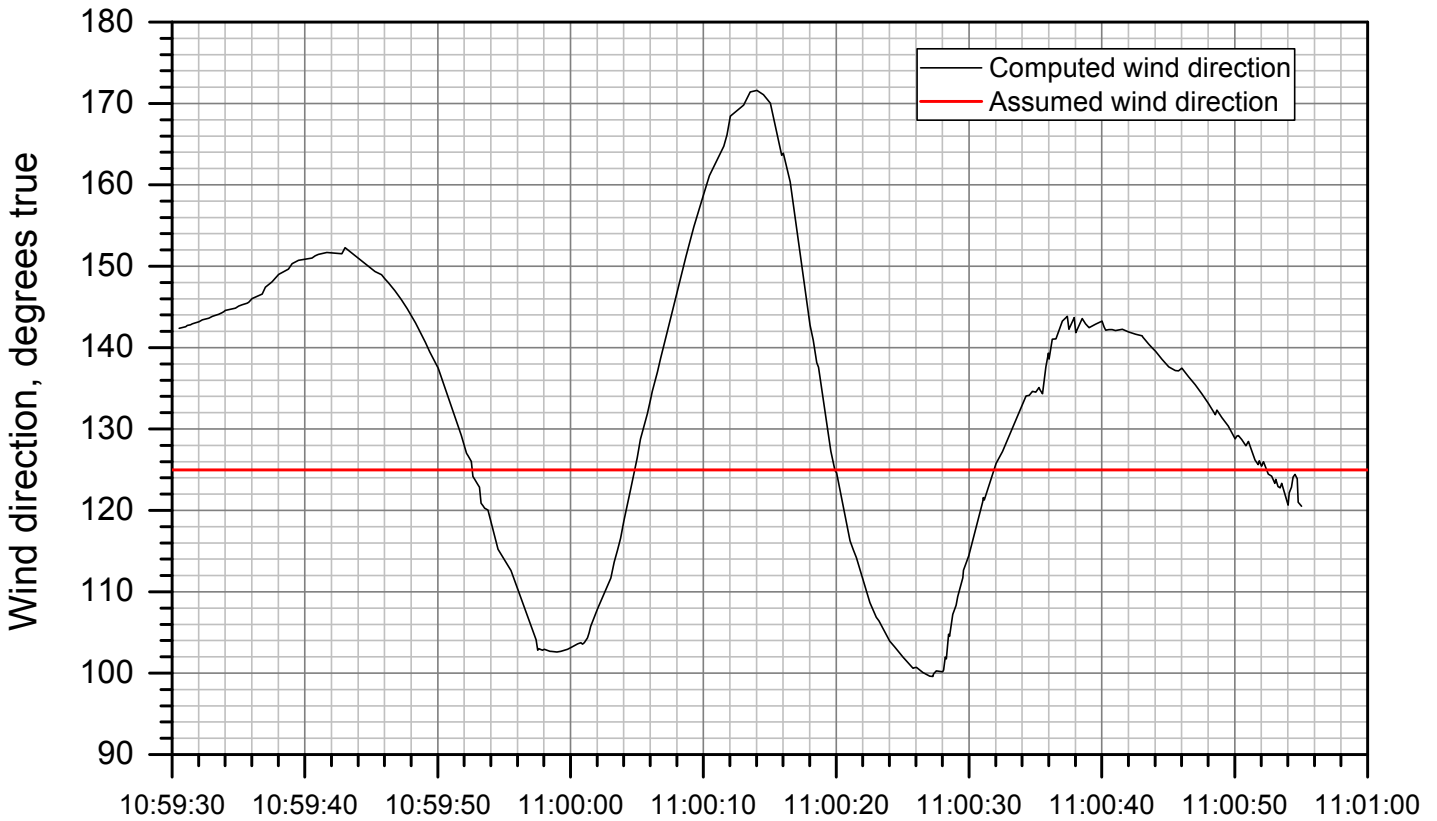
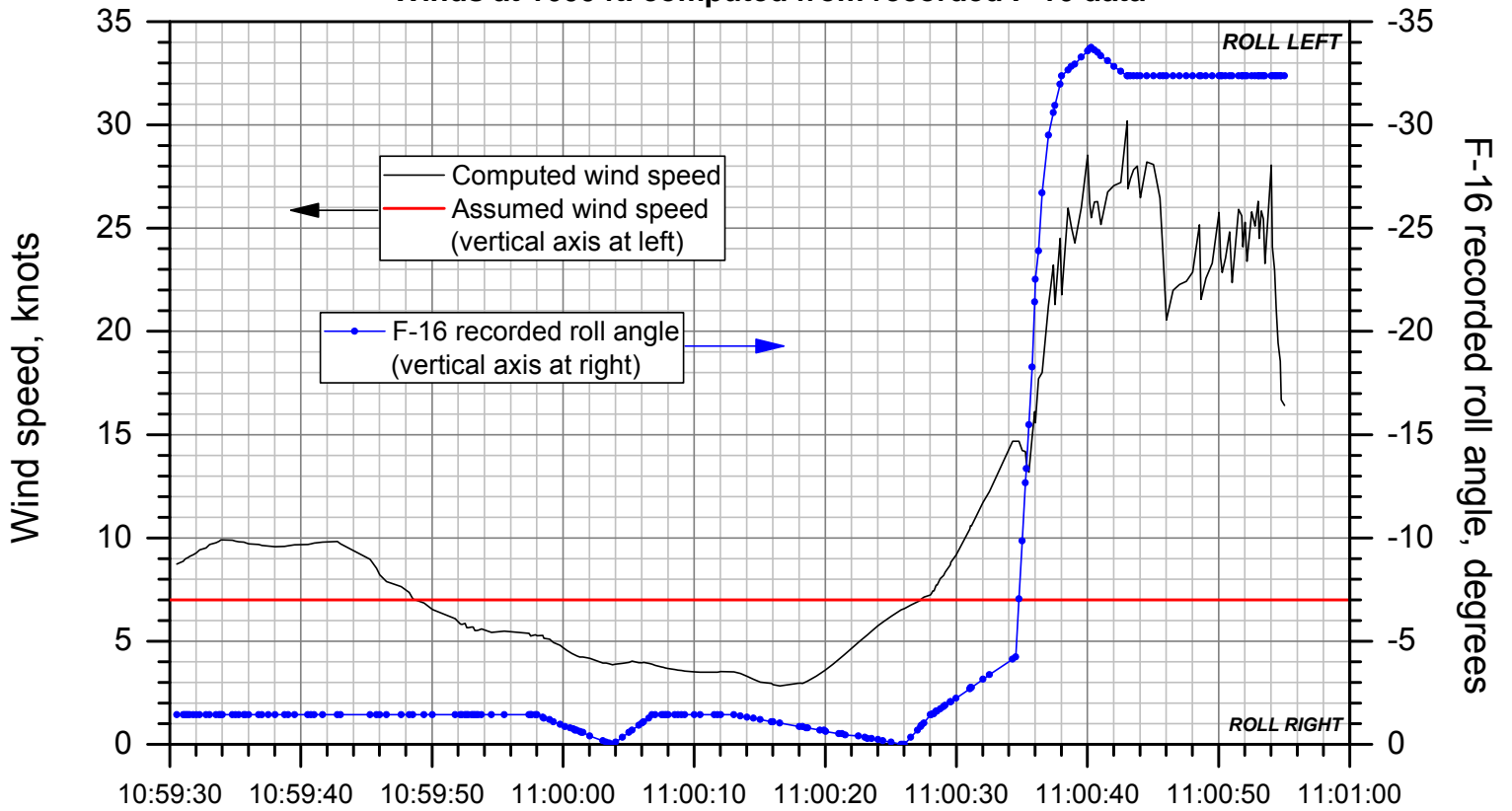


Figure 11b.

ERA15FA259AB: Midair collision, F-16 / C150, Moncks Corner, SC, 7/7/2015

Winds at 1600 ft. computed from recorded F-16 data



KCHS ASR time, HH:MM:SS EDT

Figure 12.

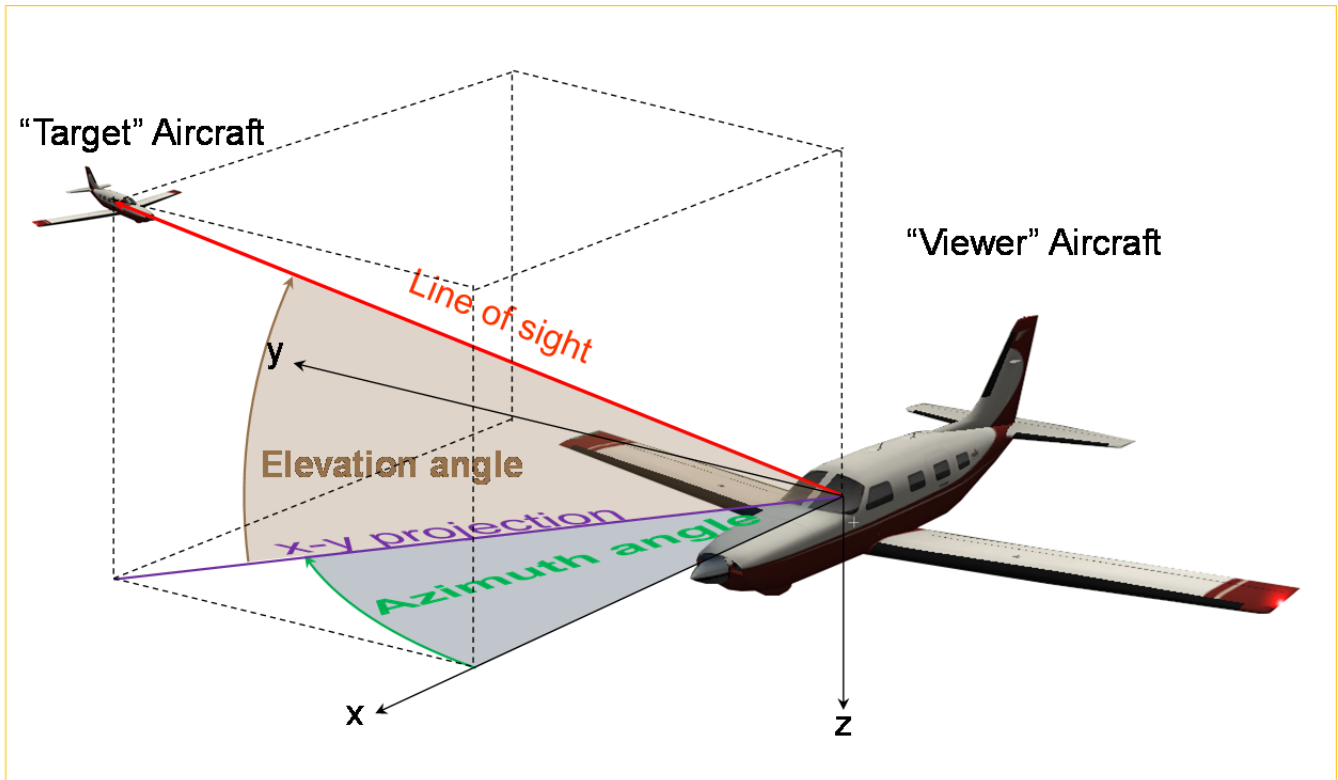
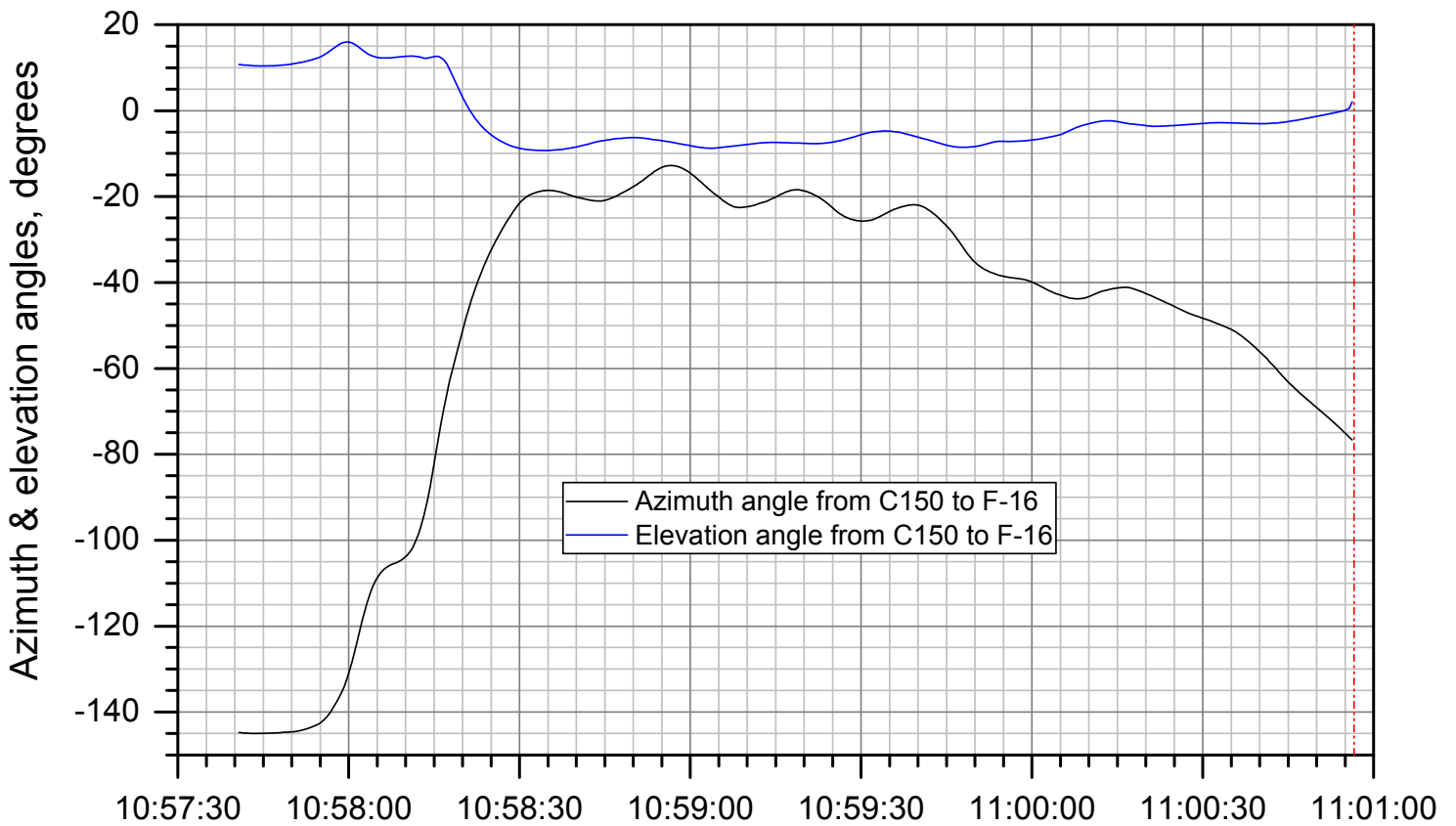
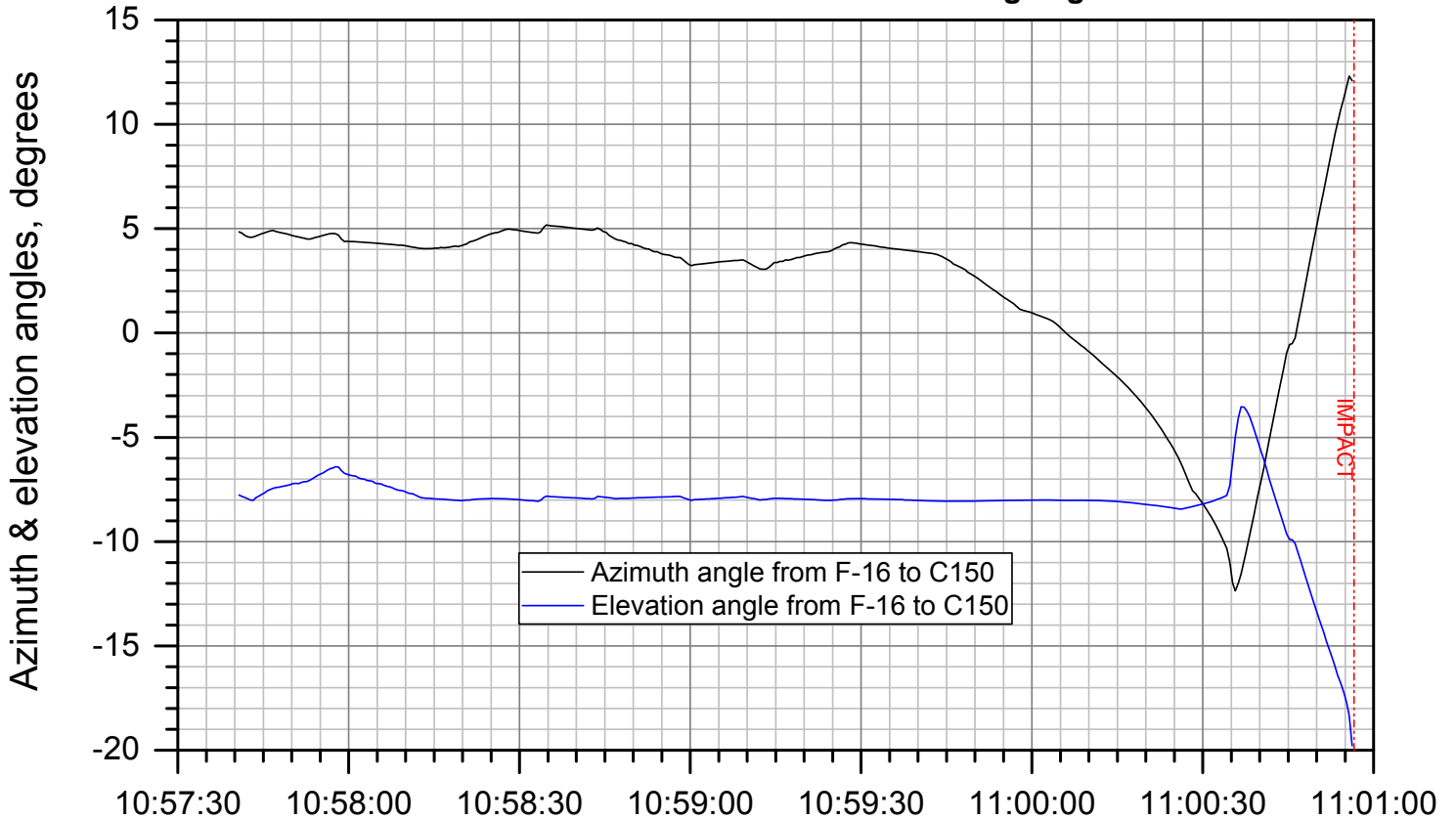


Figure 13. Azimuth and elevation angles from "viewer" airplane to "target" airplane.

ERA15FA259AB: Midair collision, F-16 / C150, Moncks Corner, SC, 7/7/2015

F-16 and Cessna 150 azimuth & elevation viewing angles vs. time



KCHS ASR time, HH:MM:SS EDT

Figure 14a.

ERA15FA259AB: Midair collision, F-16 / C150, Moncks Corner, SC, 7/7/2015

F-16 and Cessna 150 azimuth & elevation viewing angles vs. time (detail)

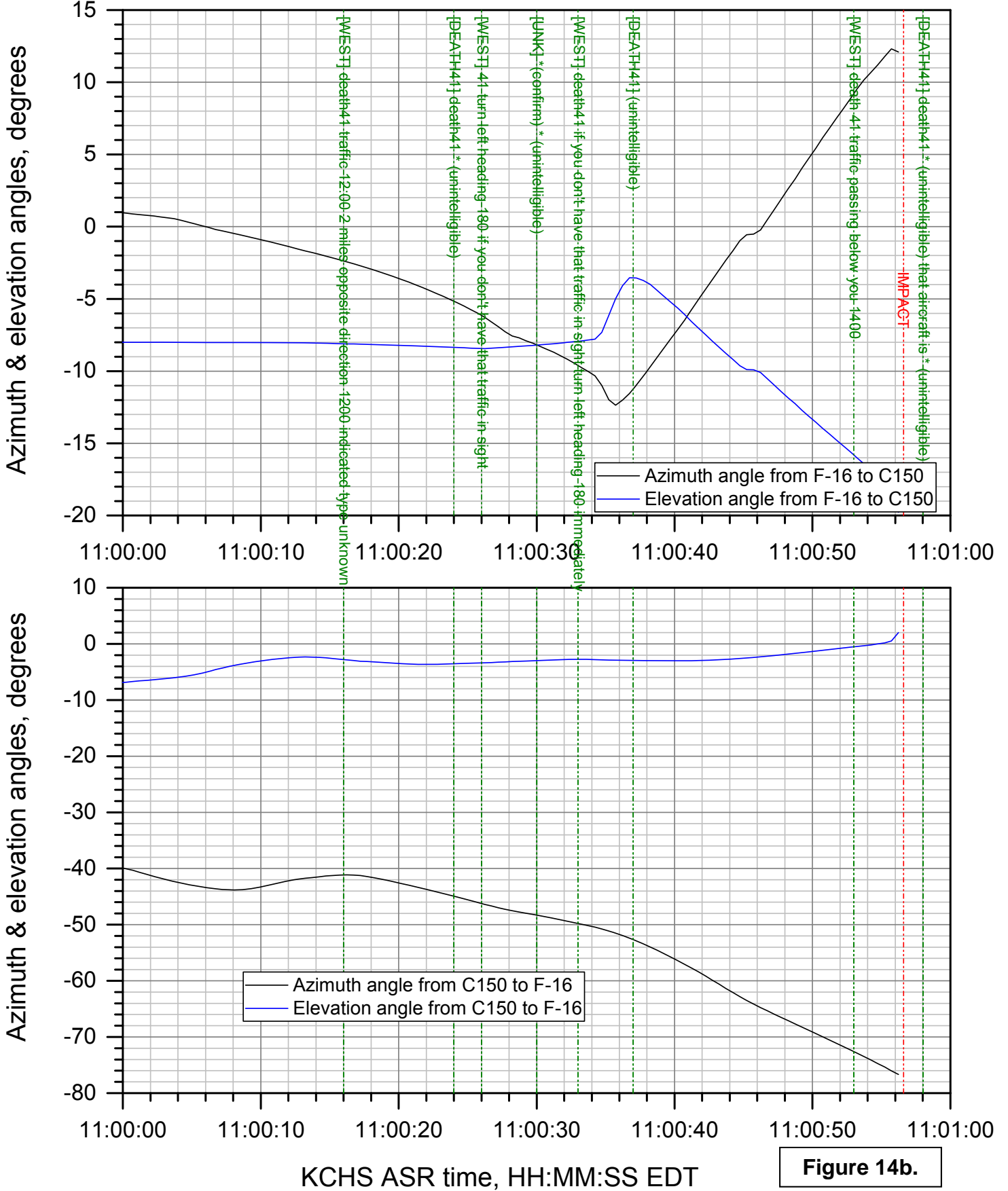


Figure 14b.

ERA15FA259AB: Midair collision, F-16 / C150, Moncks Corner, SC, 7/7/2015

F-16 and Cessna 150: azimuth & elevation viewing angles

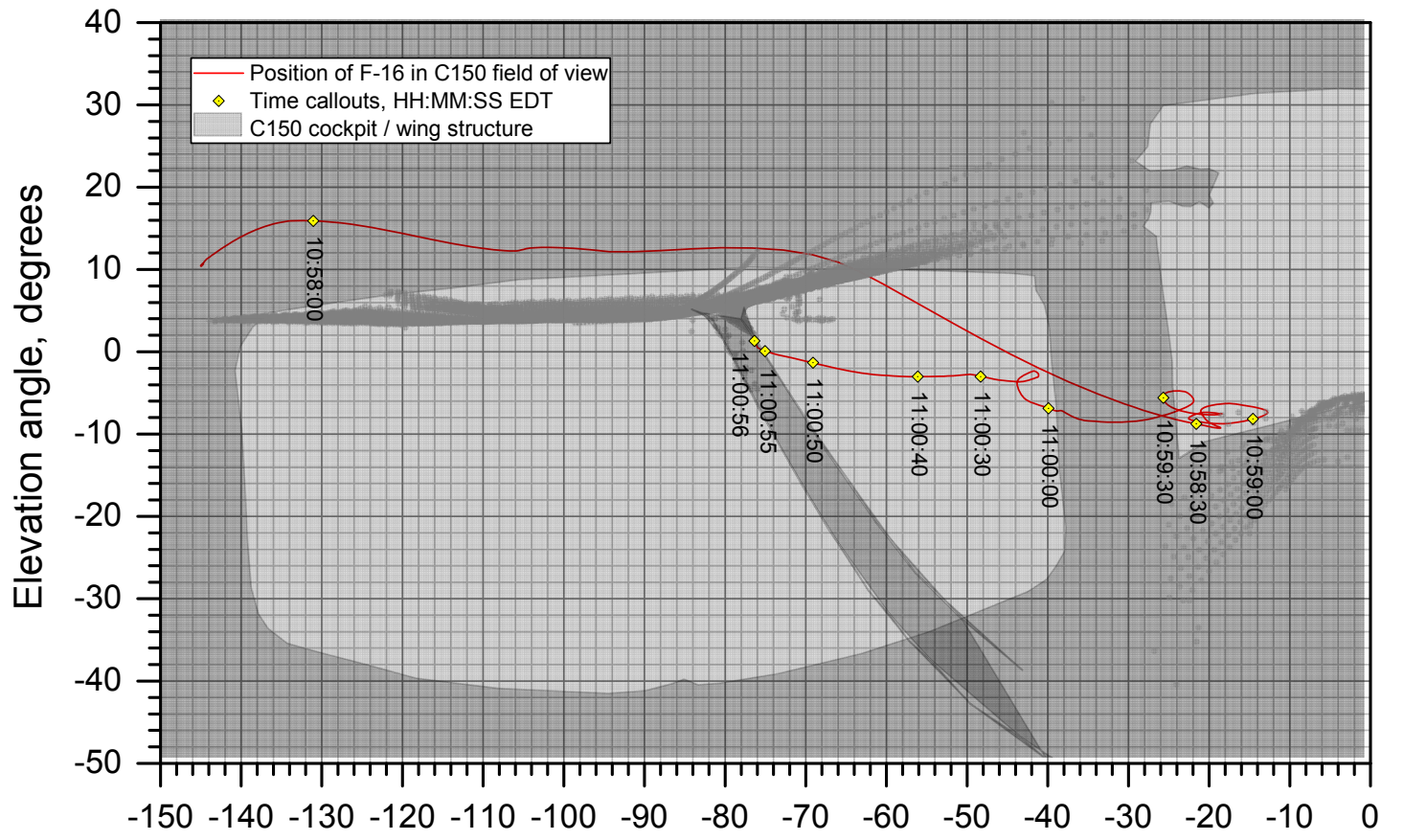
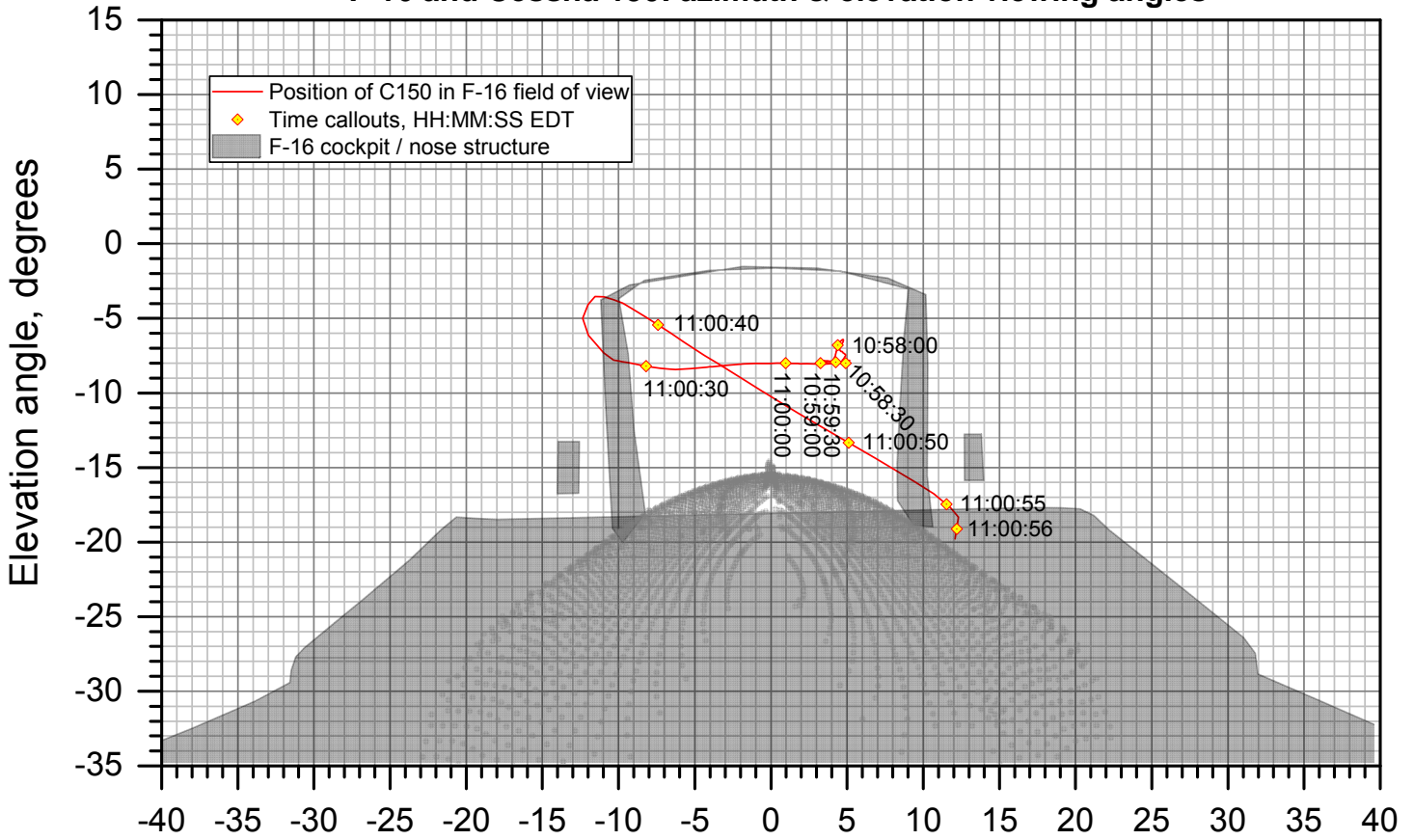


Figure 15a.

F-16 cockpit viewed from (azimuth, elevation) angles of $(0^\circ, 0^\circ)$.



C150 cockpit viewed from (azimuth, elevation) angles of $(-75^\circ, 0^\circ)$.



Figure 15b.

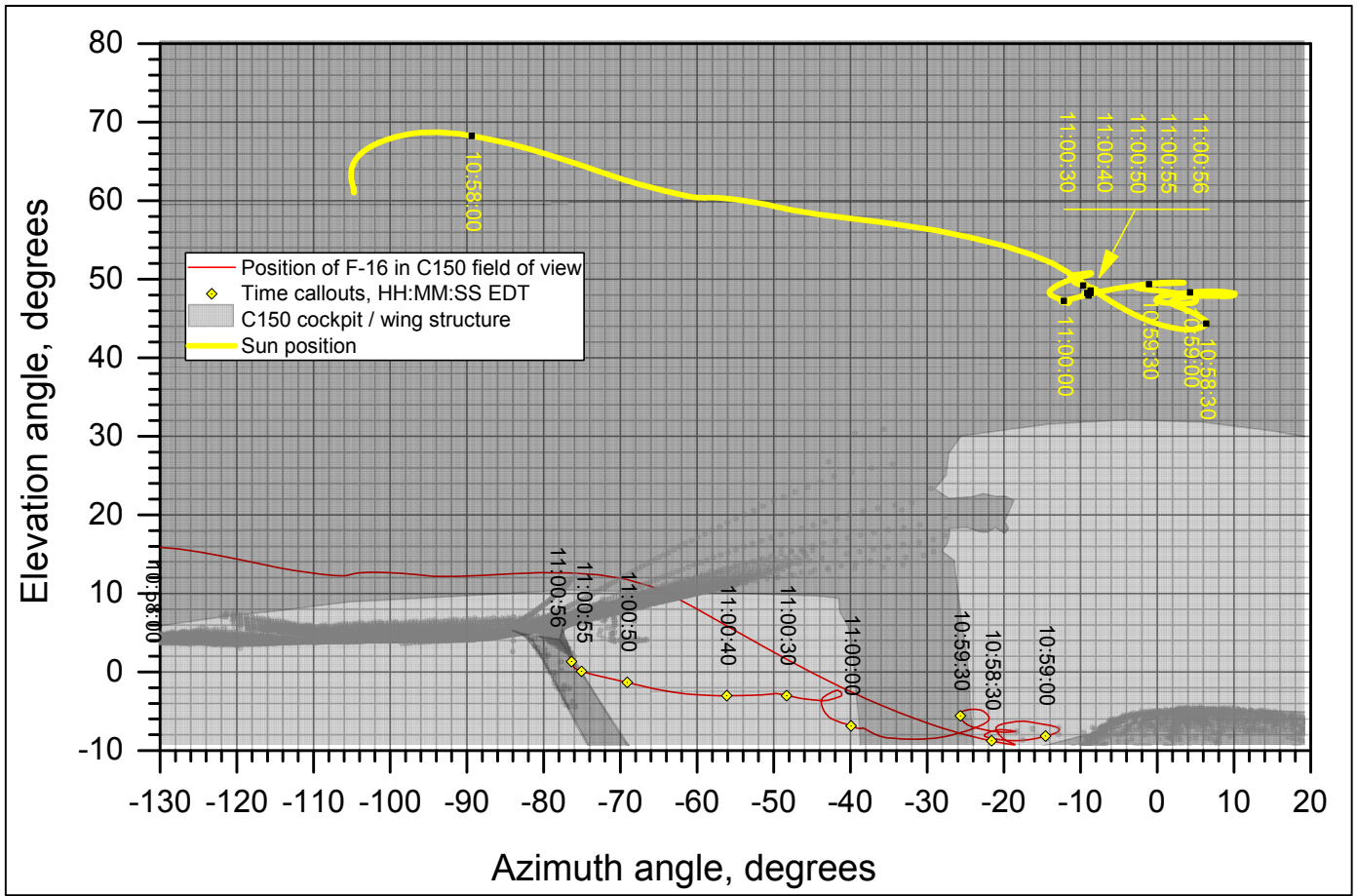


Figure 16. Azimuth and elevation angles of the sun in the C150 field of view.

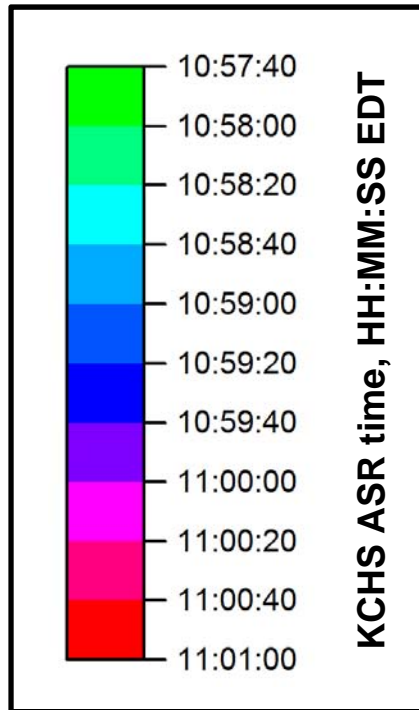


Figure 17. Color legend for "target" airplane trajectory line in Figures 18 and 19.

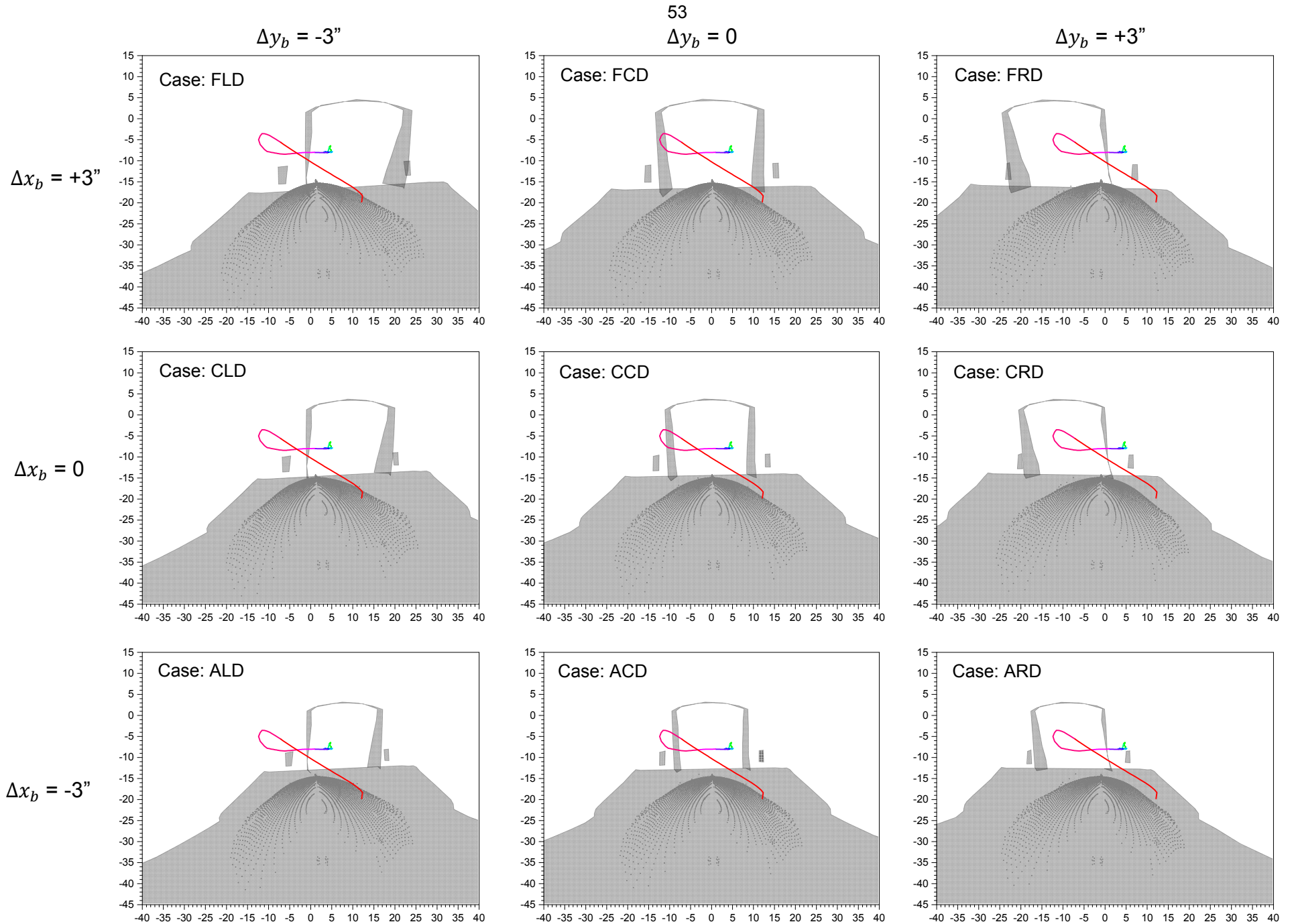


Figure 18a. Viewing angles for F-16 at $\Delta z_b = +1.5$ inches (i.e., down). Plots are elevation angle vs. azimuth angle (in degrees).

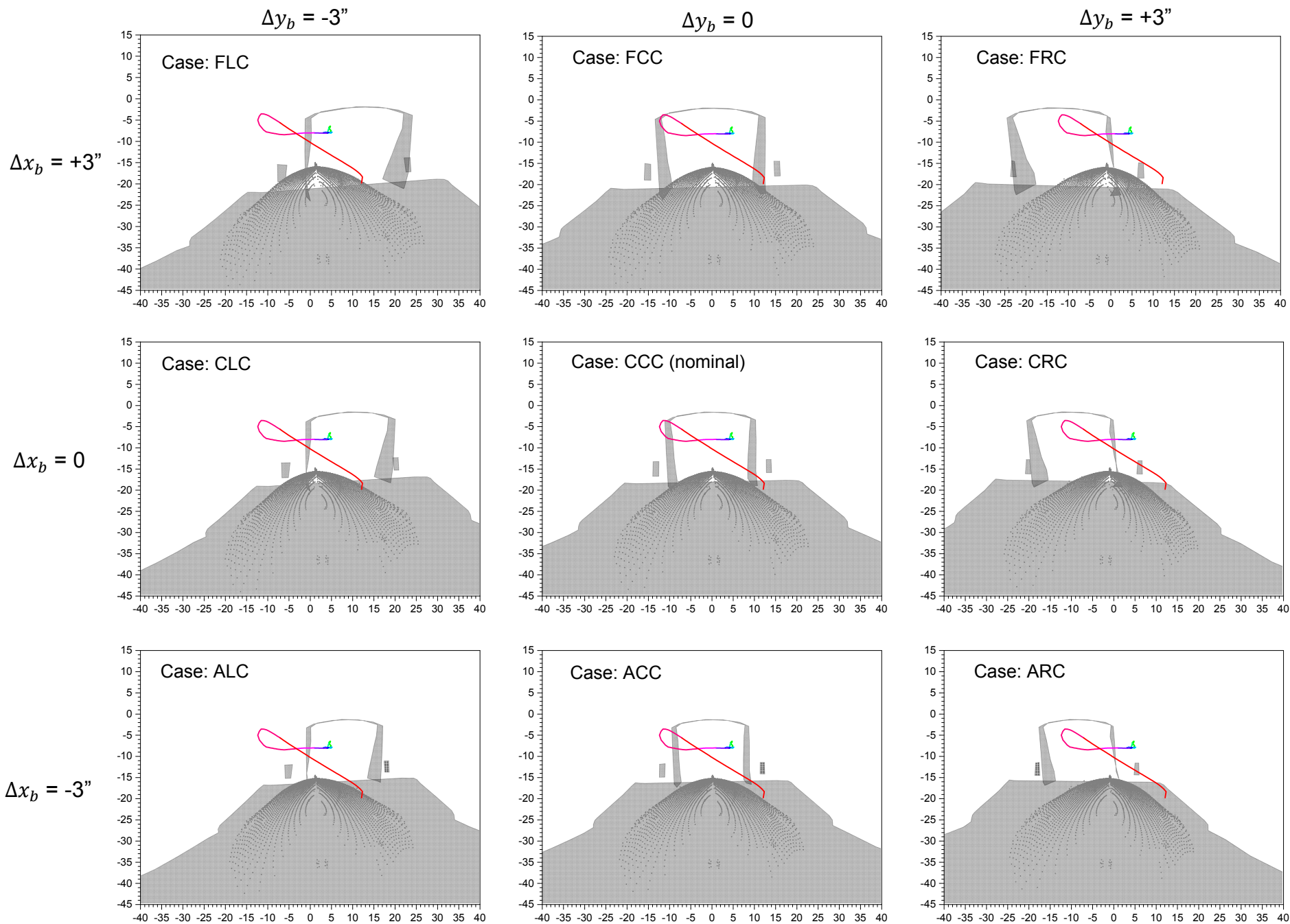


Figure 18b. Viewing angles for F-16 at $\Delta z_b = 0$. Plots are elevation angle vs. azimuth angle (in degrees).

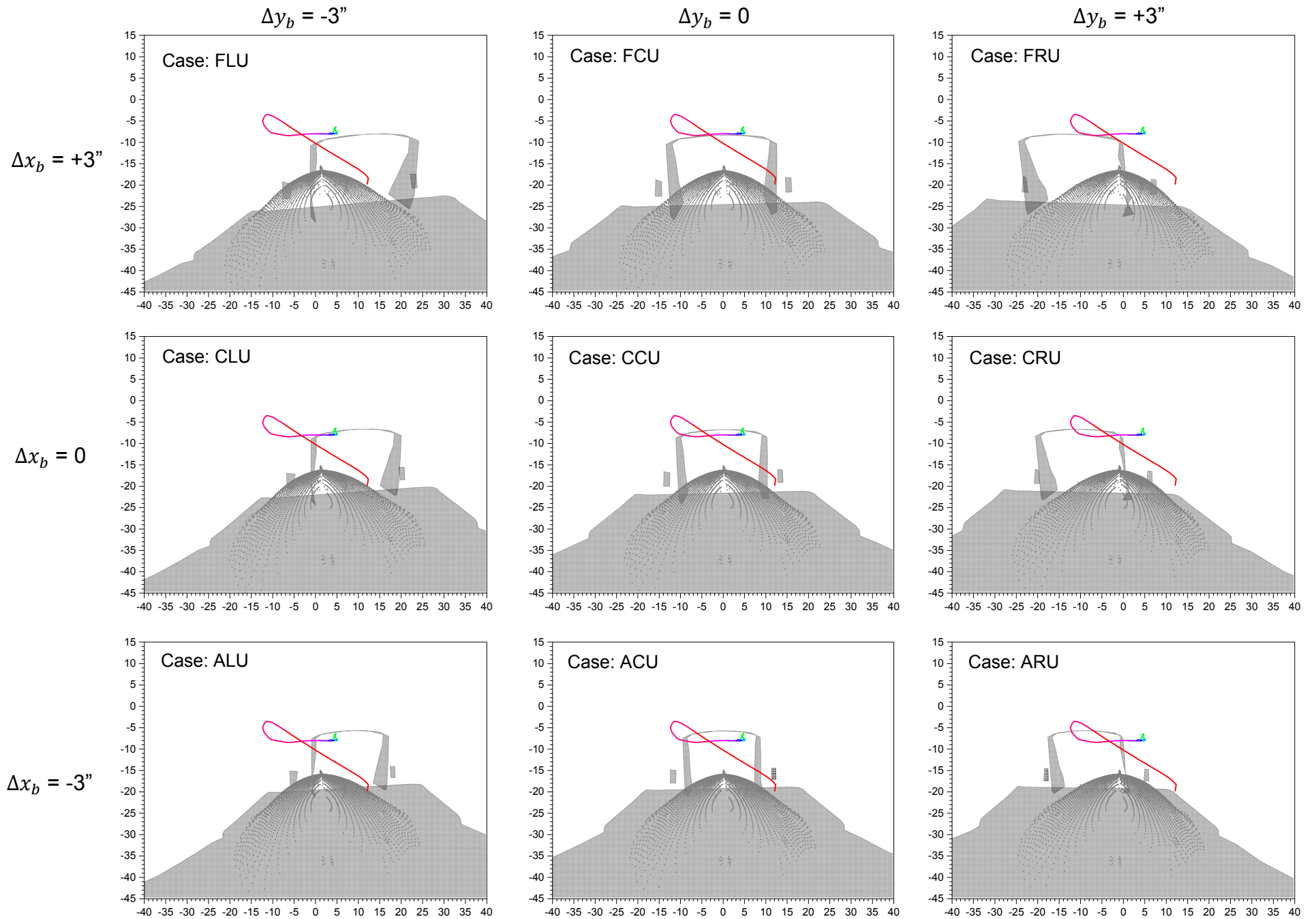


Figure 18c. Viewing angles for F-16 at $\Delta z_b = -1.5$ inches (i.e., up). Plots are elevation angle vs. azimuth angle (in degrees).

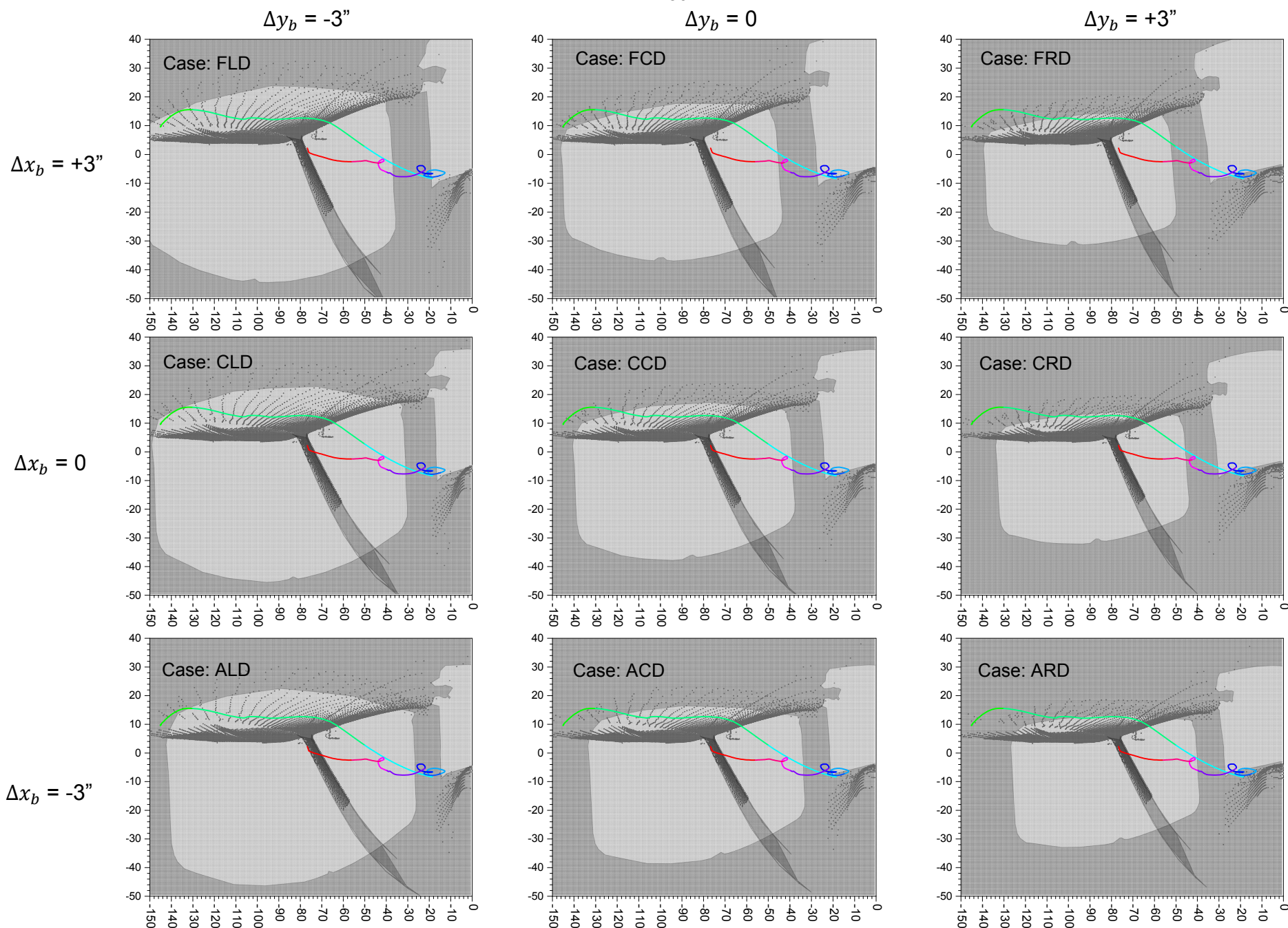


Figure 19a. Viewing angles for C150 at $\Delta z_b = +1.5$ inches (i.e., down). Plots are elevation angle vs. azimuth angle (in degrees).

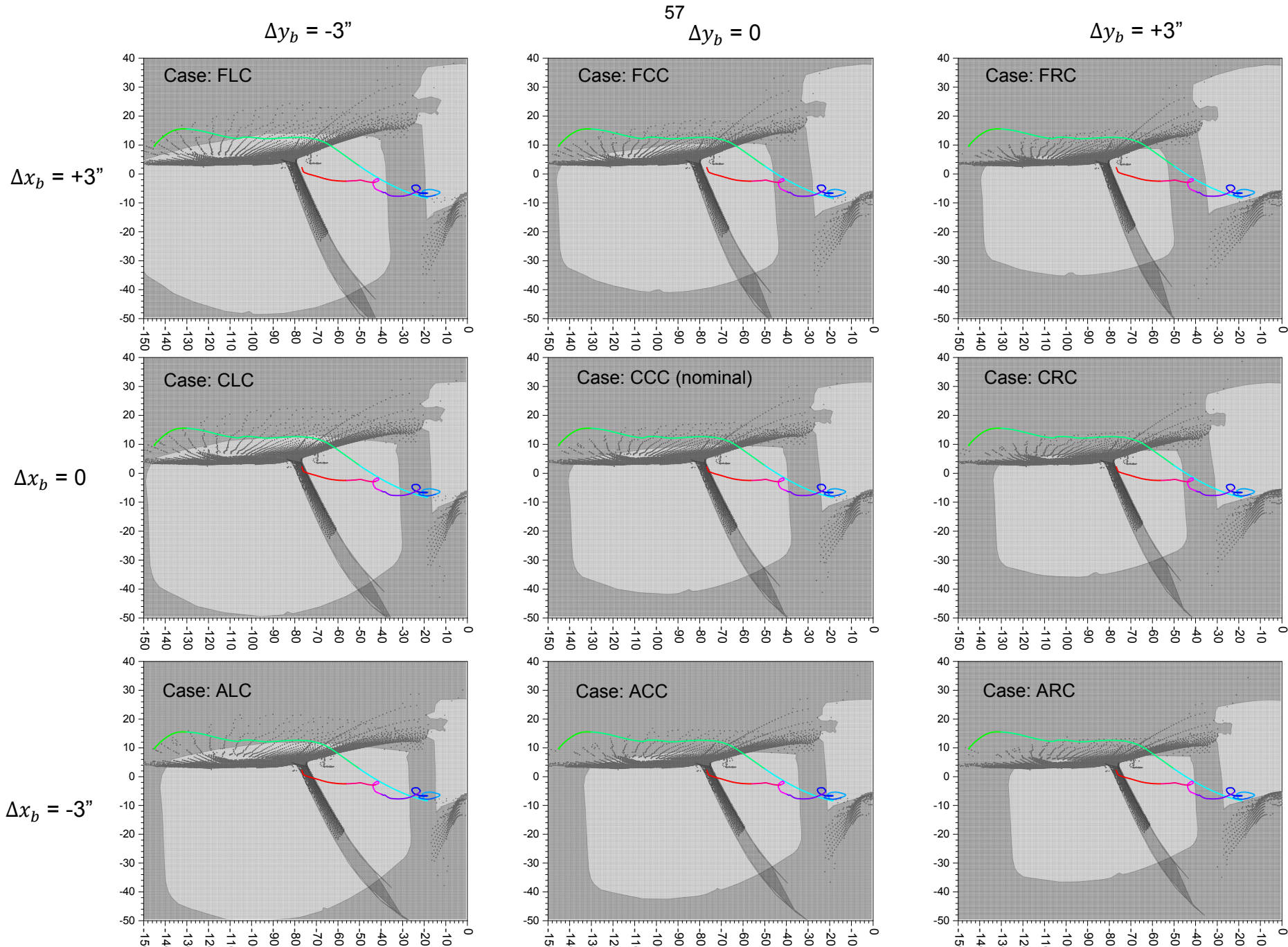


Figure 19b. Viewing angles for C150 at $\Delta z_b = 0$. Plots are elevation angle vs. azimuth angle (in degrees).

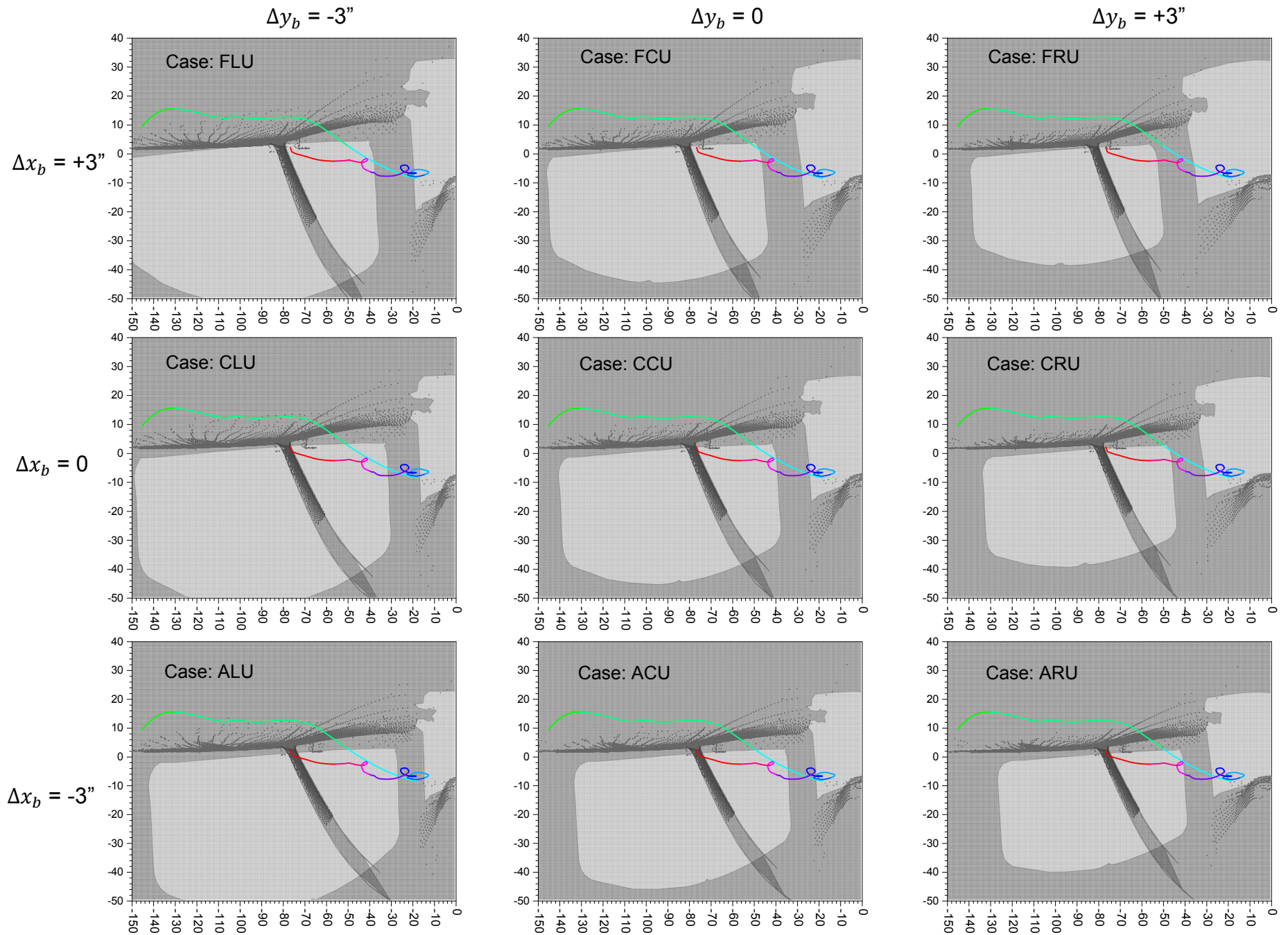
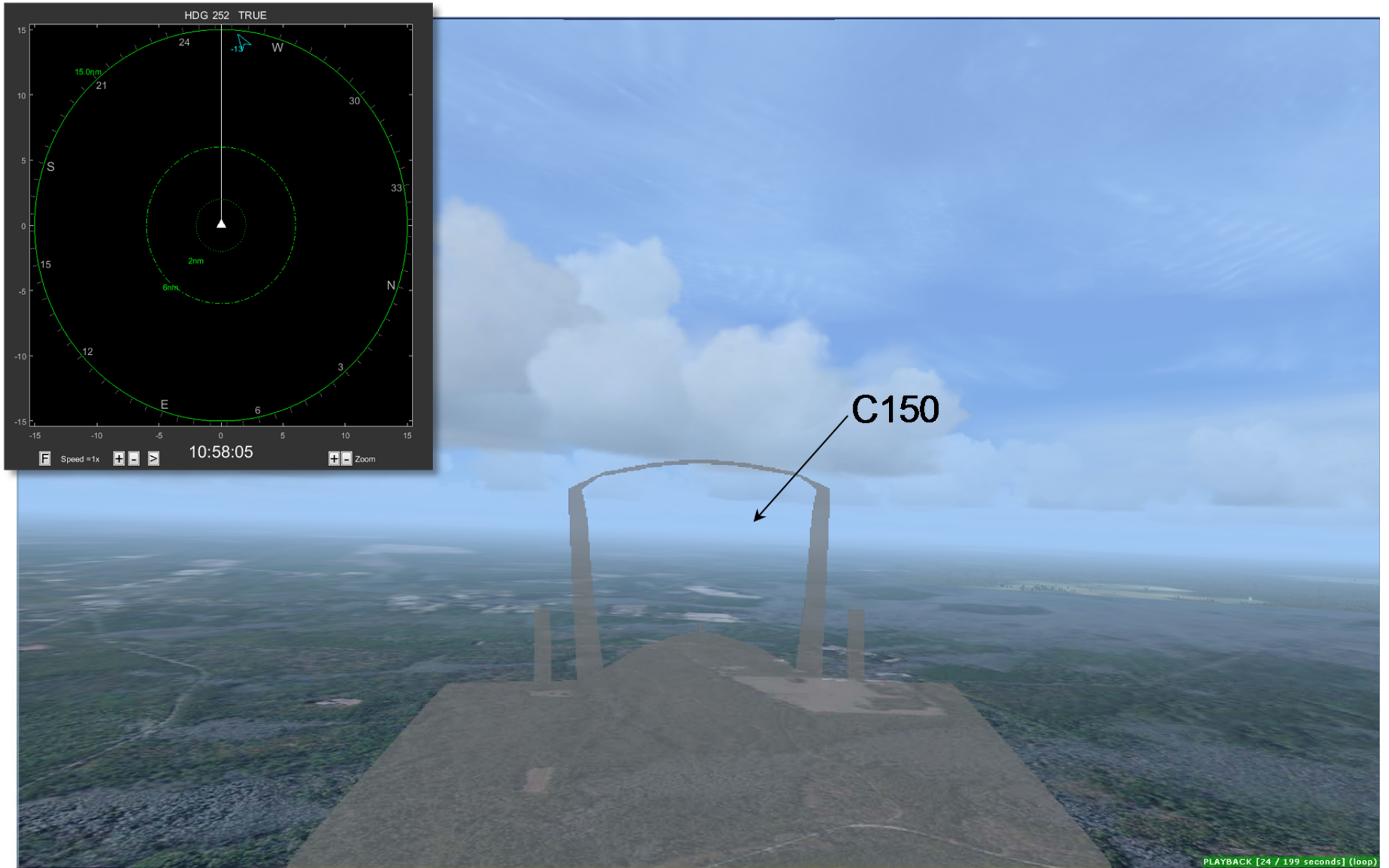
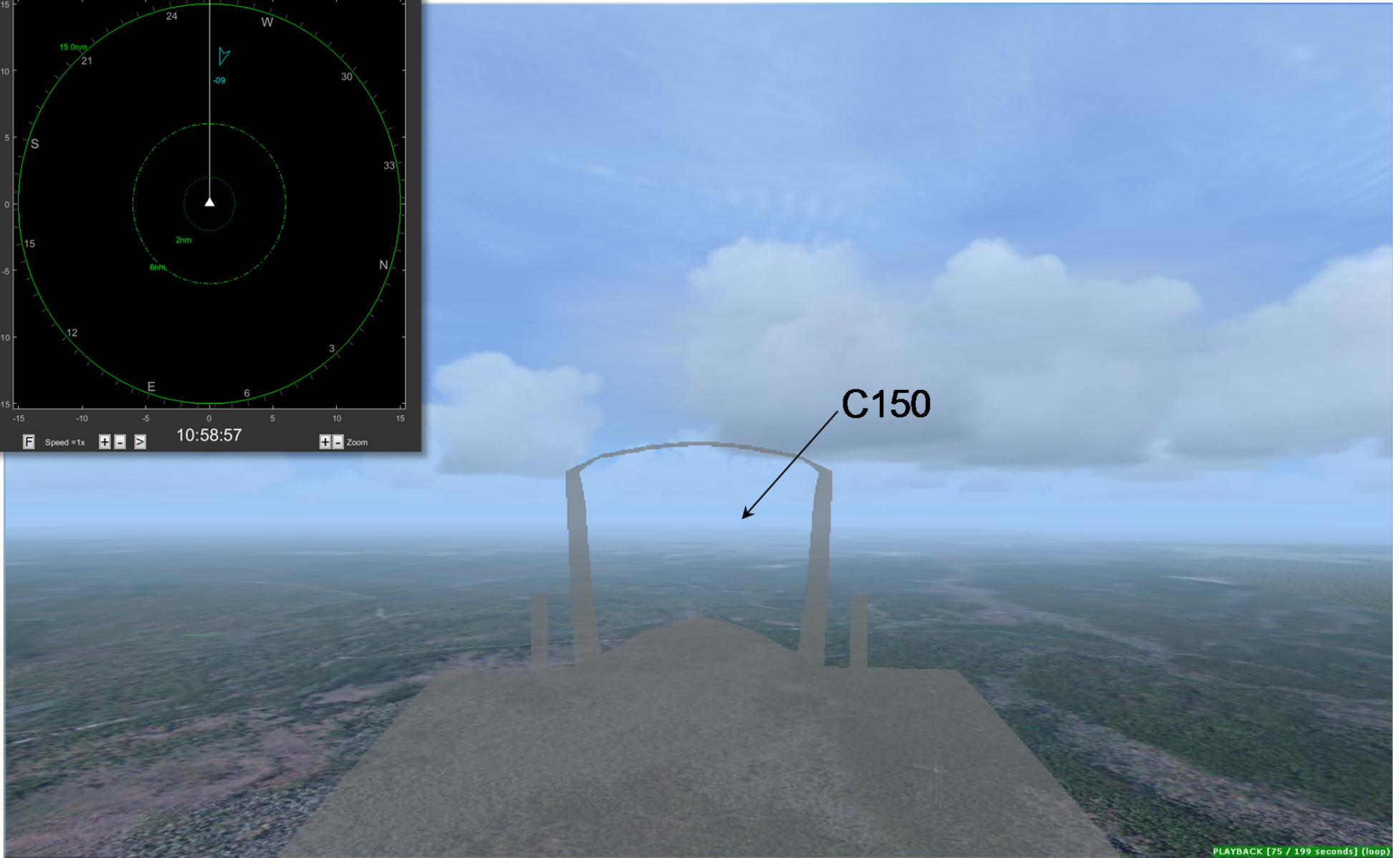
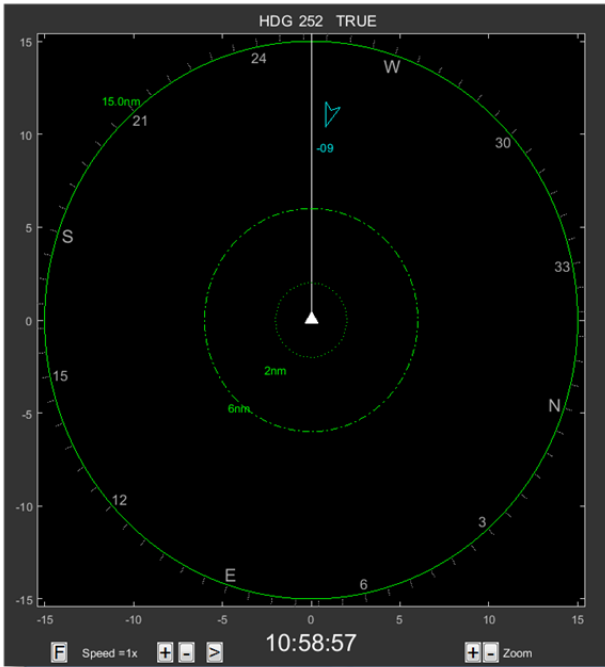


Figure 19c. Viewing angles for C150 at $\Delta z_b = -1.5$ inches (i.e., up). Plots are elevation angle vs. azimuth angle (in degrees).



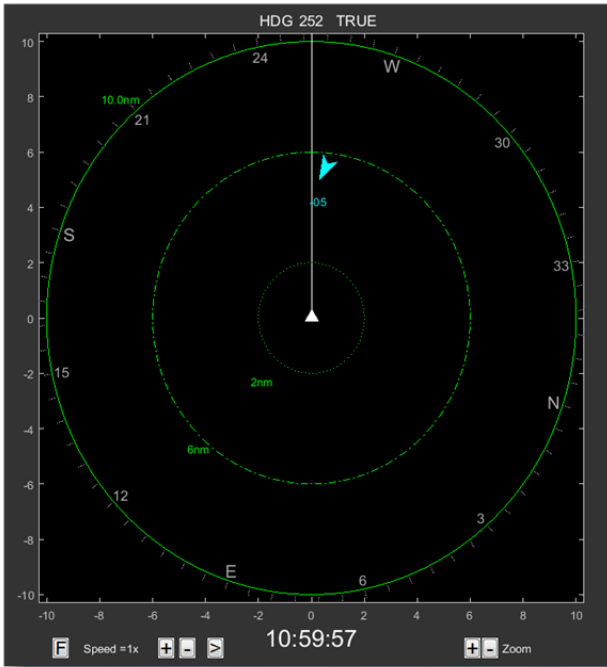
10:58:05

Figure 20a.



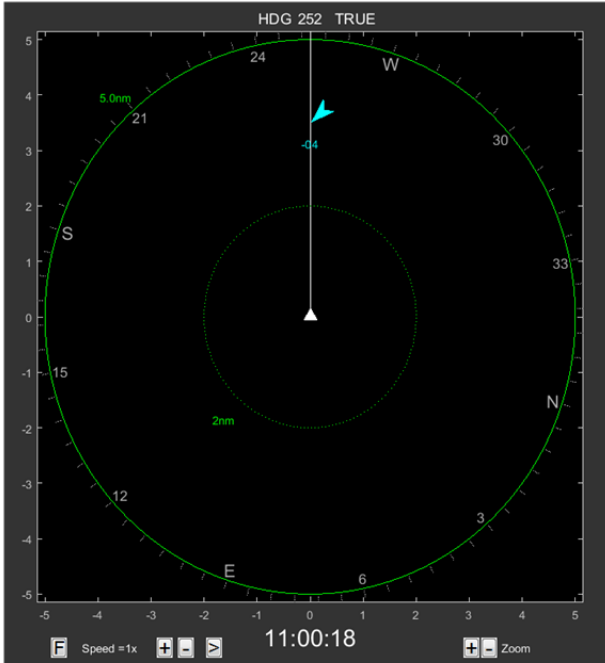
10:58:56.6

Figure 20b.

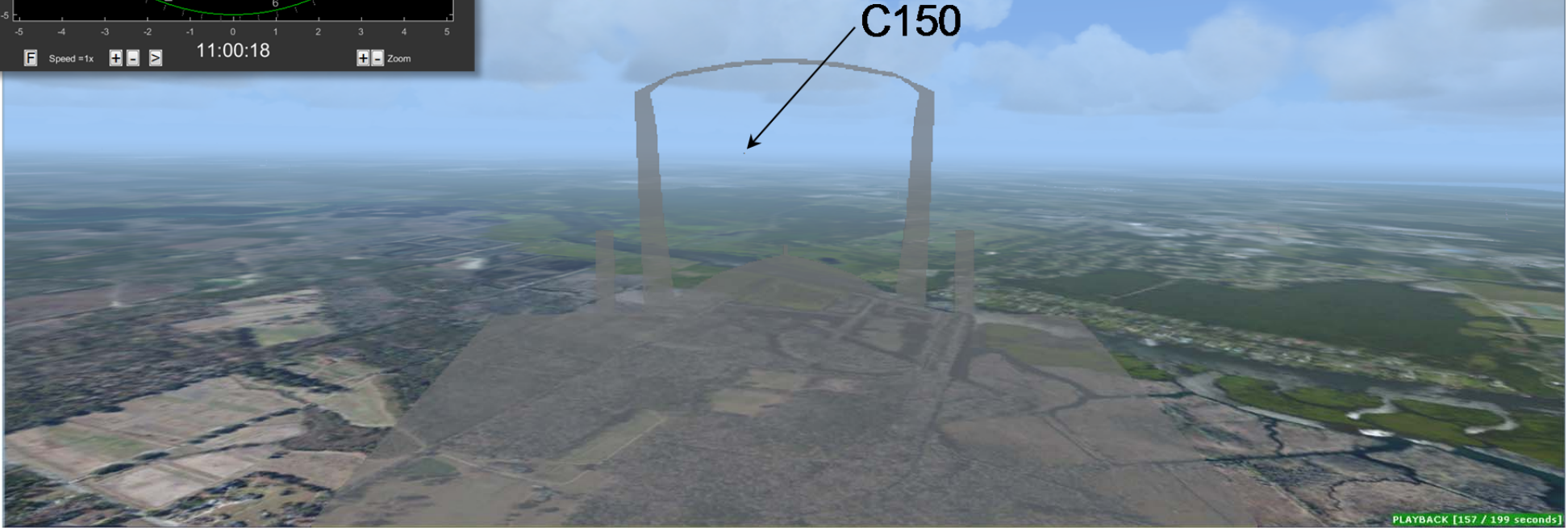


10:59:56.6

Figure 20c.

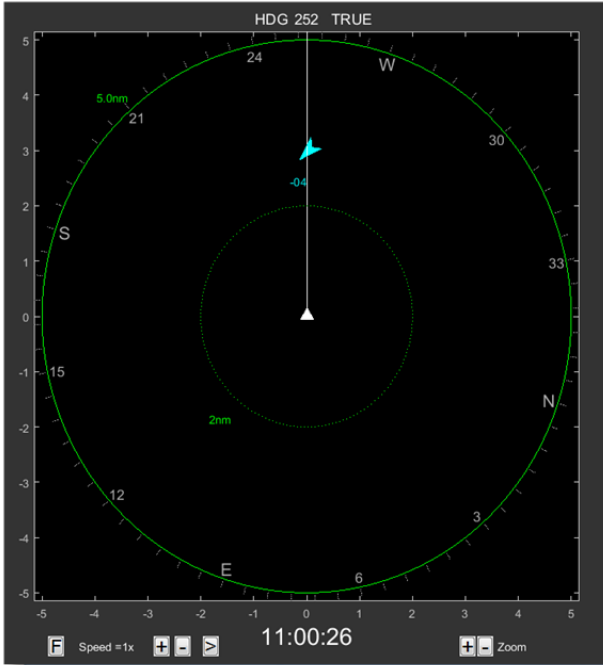


[WEST (@ 11:00:16)] death41 traffic twelve o'clock 2 miles opposite direction 1200 indicated type unknown

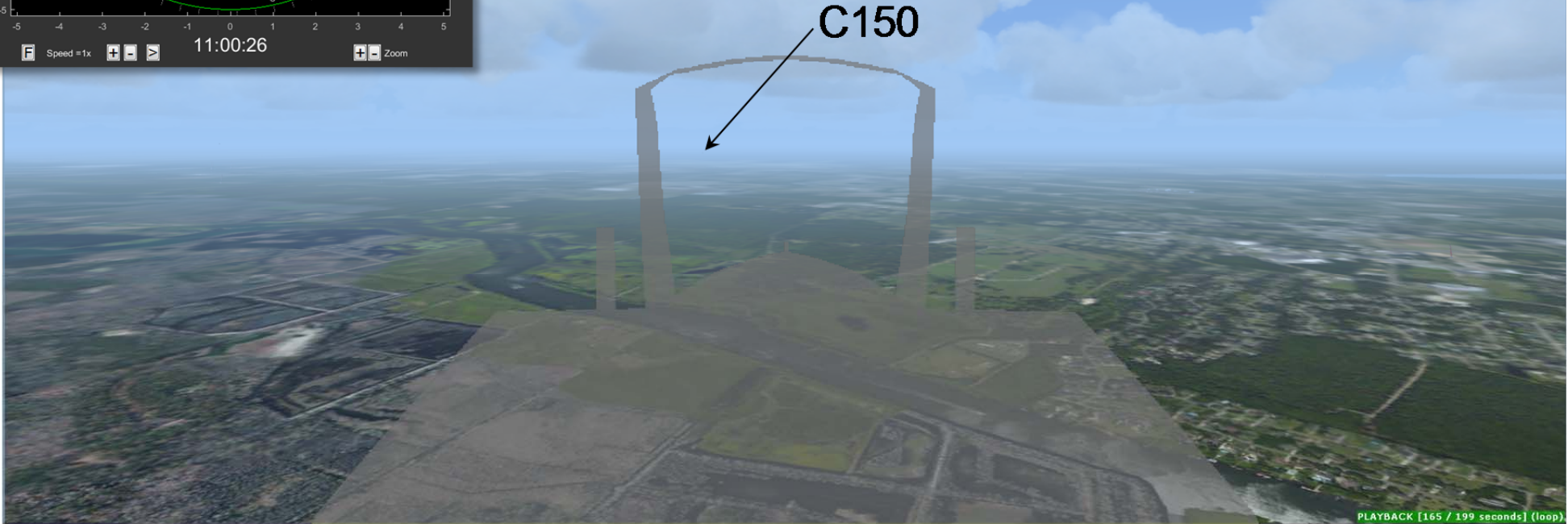


11:00:18

Figure 20d.



[WEST] 41 turn left heading 180 if you don't have that traffic in sight

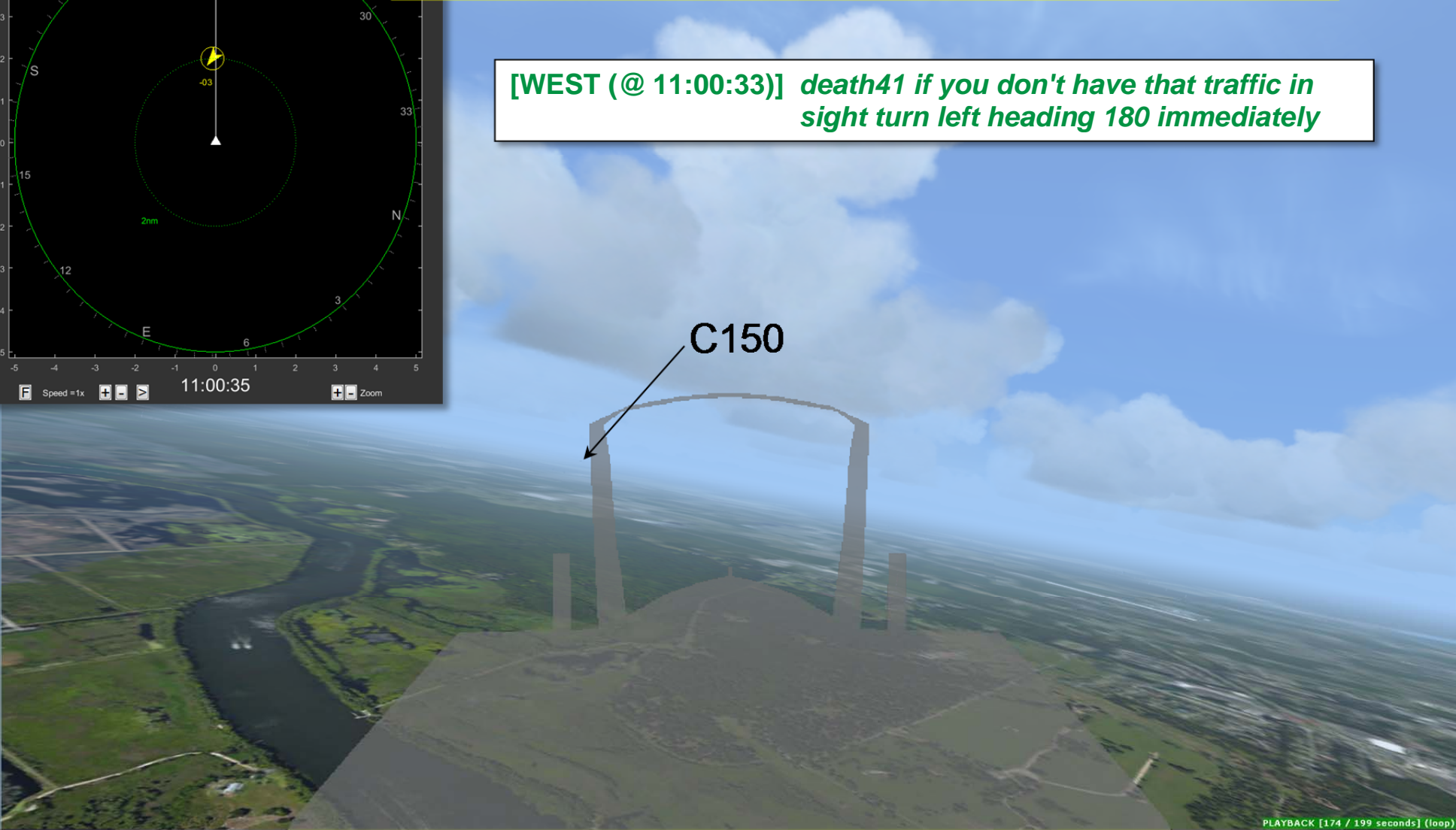
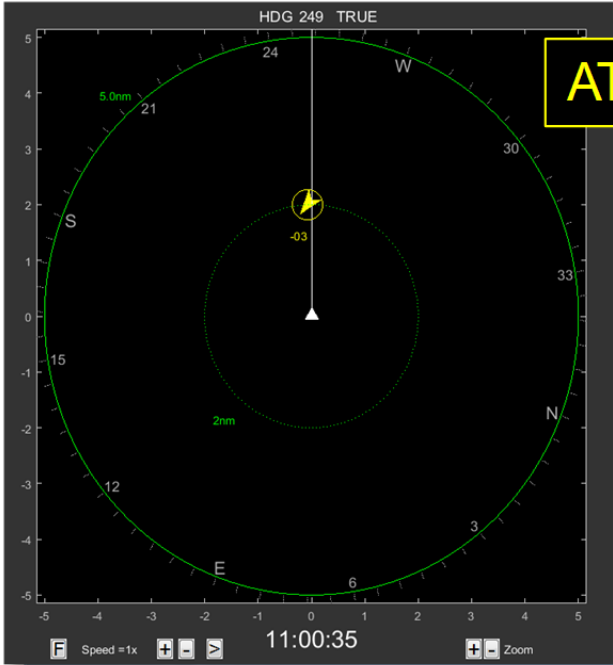


11:00:26

Figure 20e.

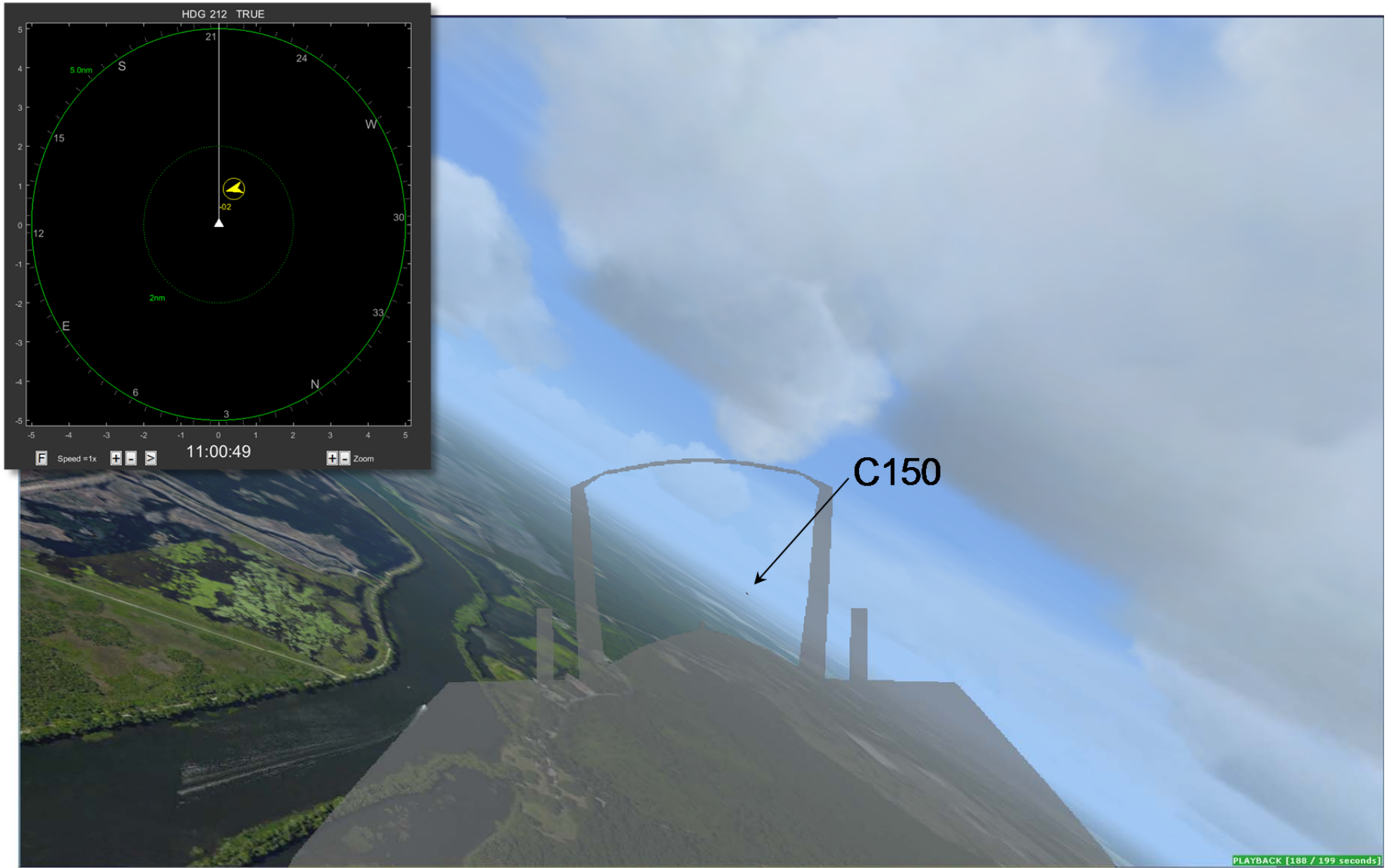
ATAS aural alert: "Traffic, 12 o'clock, low, 2 miles."

[WEST (@ 11:00:33)] death41 if you don't have that traffic in sight turn left heading 180 immediately



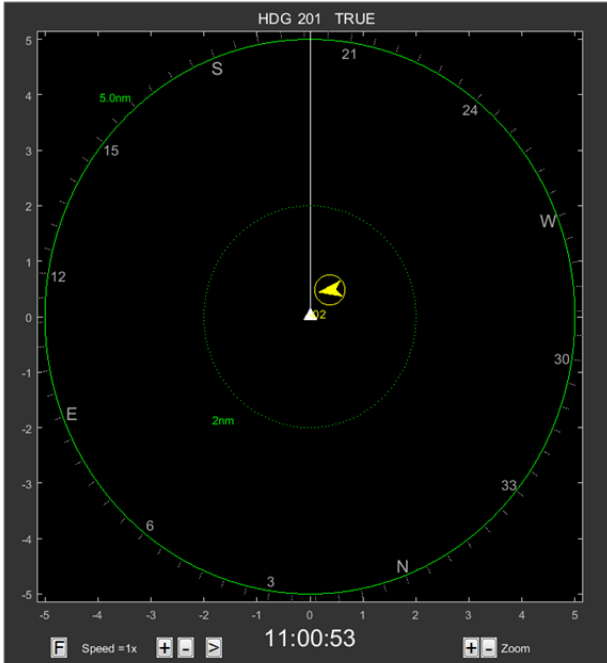
11:00:35

Figure 20f.

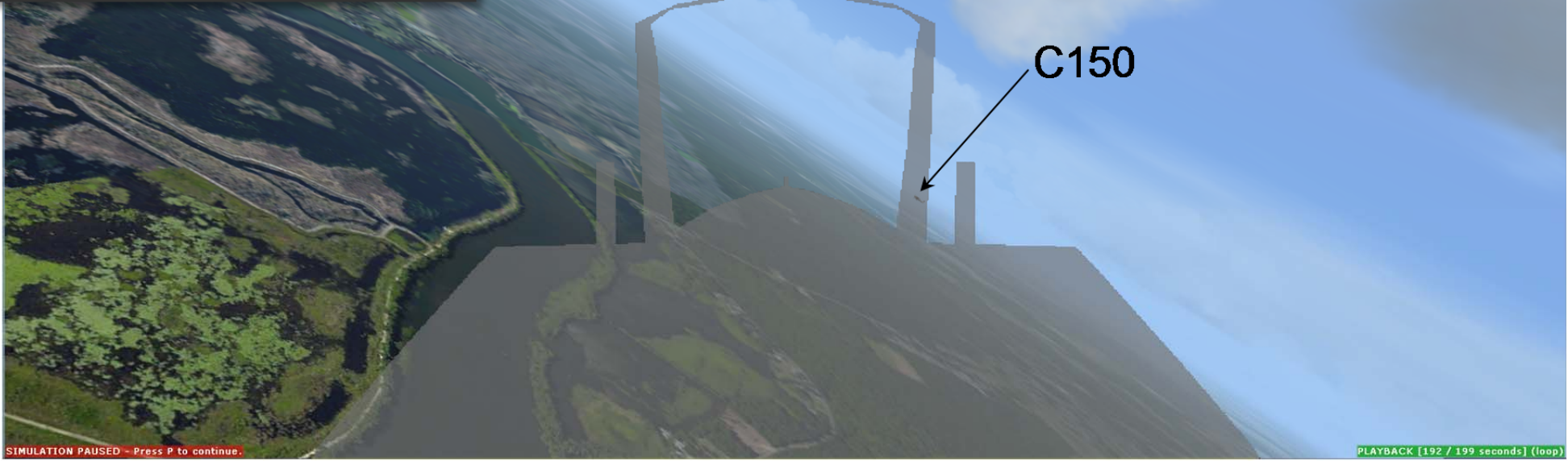


11:00:49

Figure 20g.



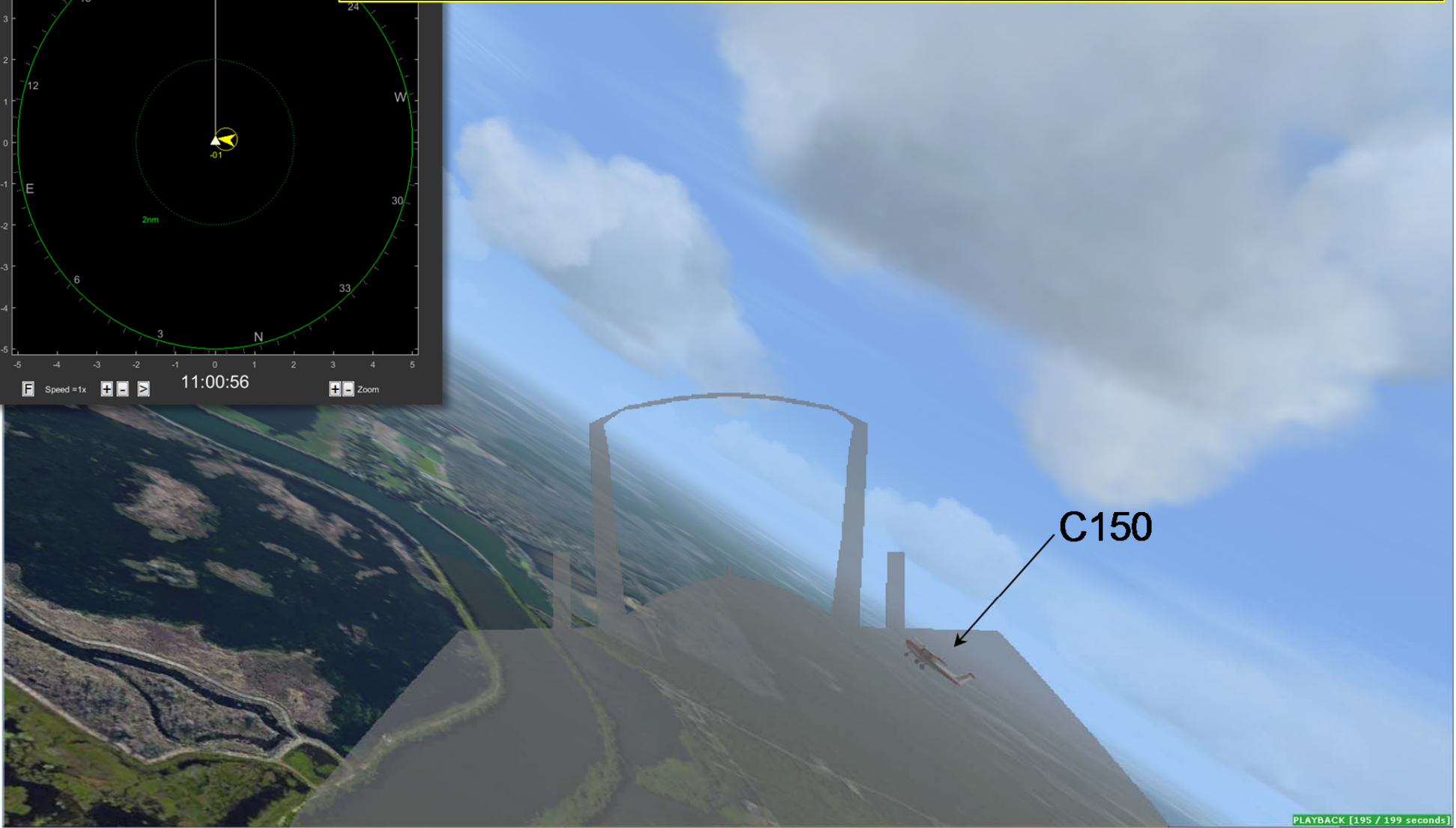
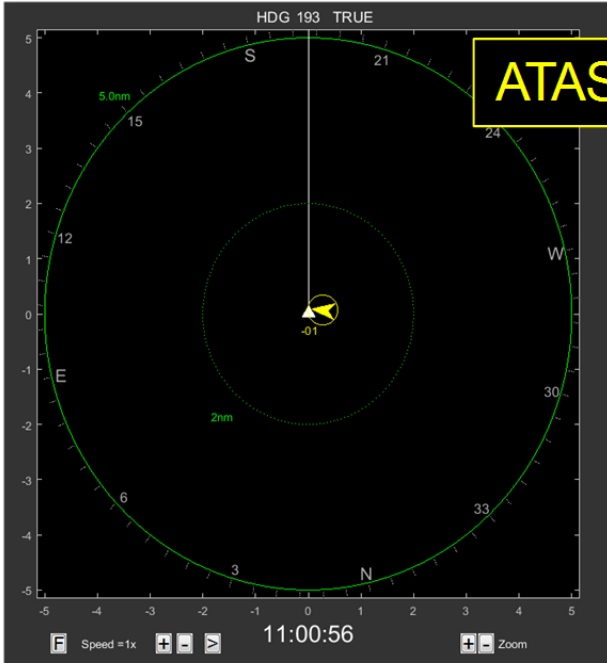
[WEST] death 41 traffic passing below you 1400



11:00:53

Figure 20h.

ATAS aural alert: "Traffic, 2 o'clock, same altitude, 0 miles."



11:00:56

Figure 20i.

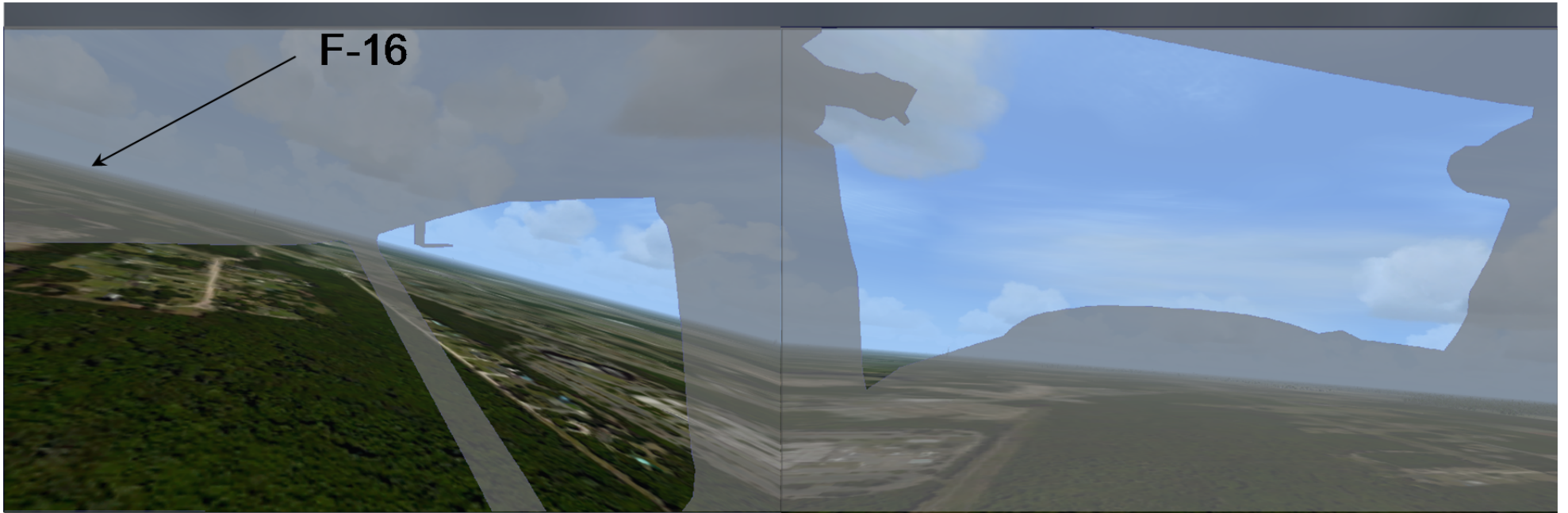


Figure 21a.

10:58:05

F-16



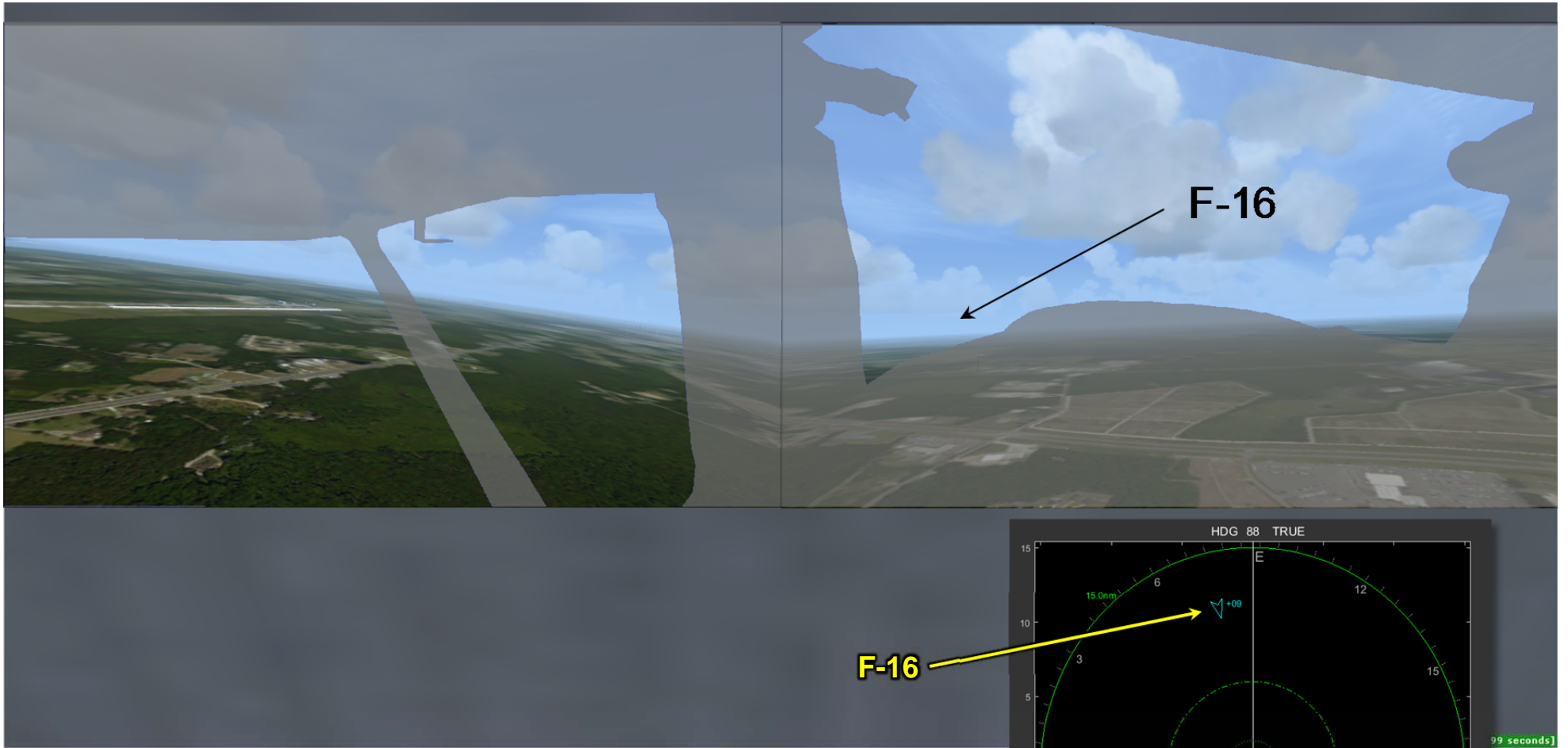
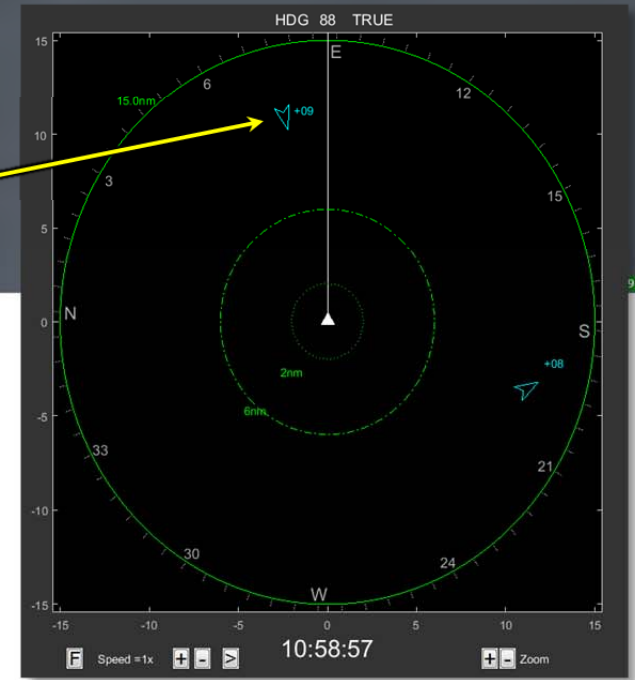


Figure 21b.

10:58:56.6

F-16



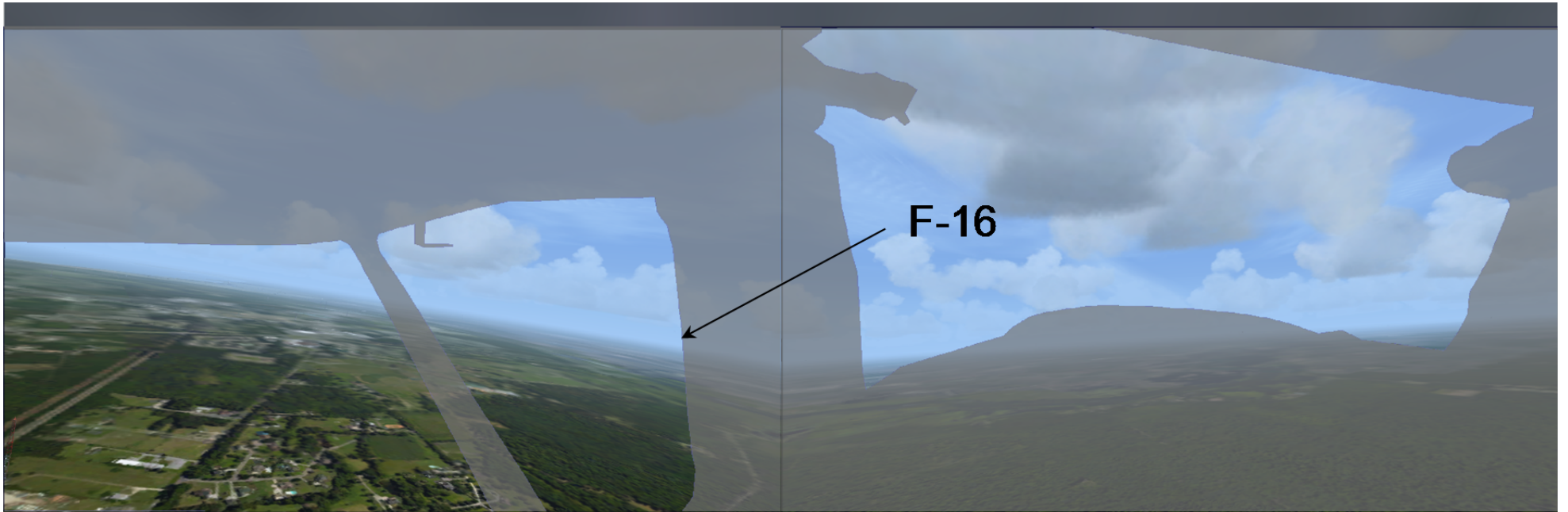
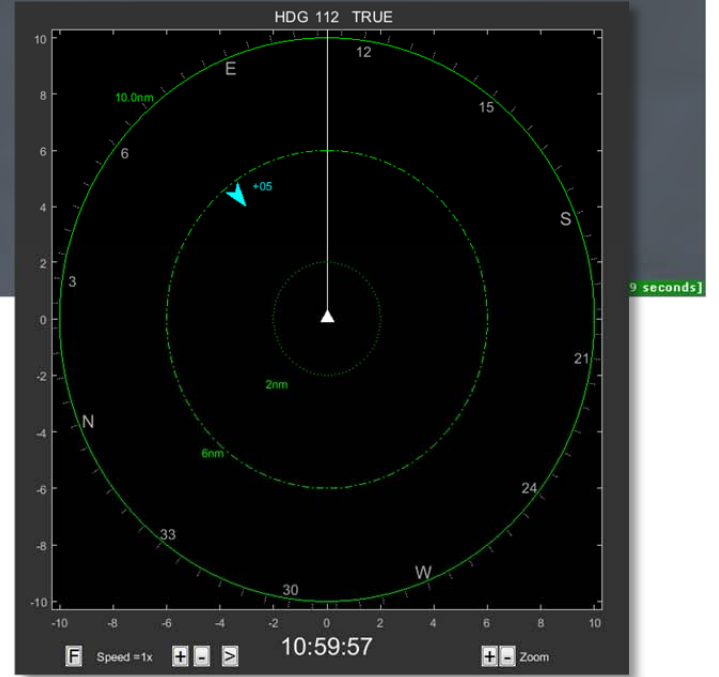


Figure 21c.

10:59:56.6



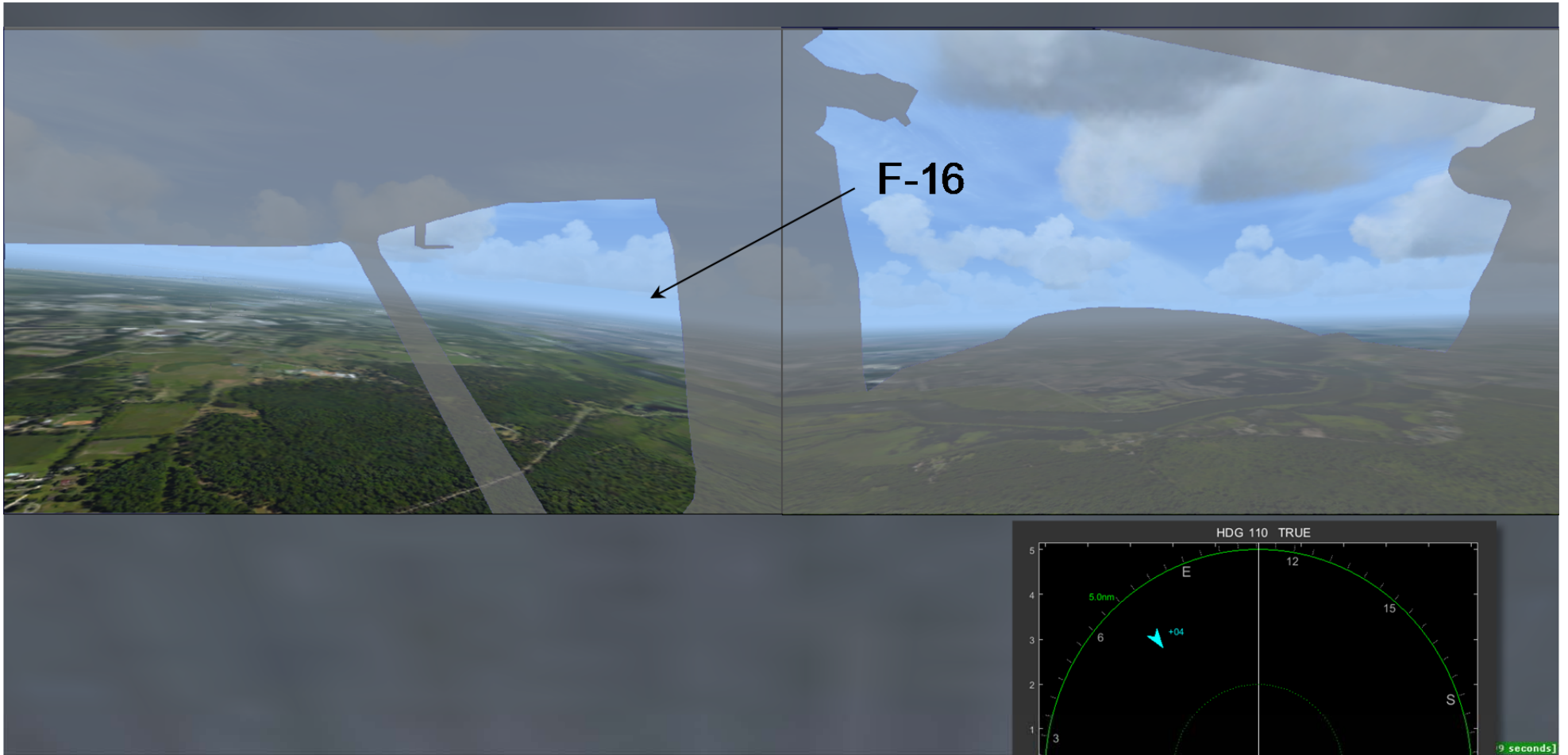


Figure 21d.

11:00:18



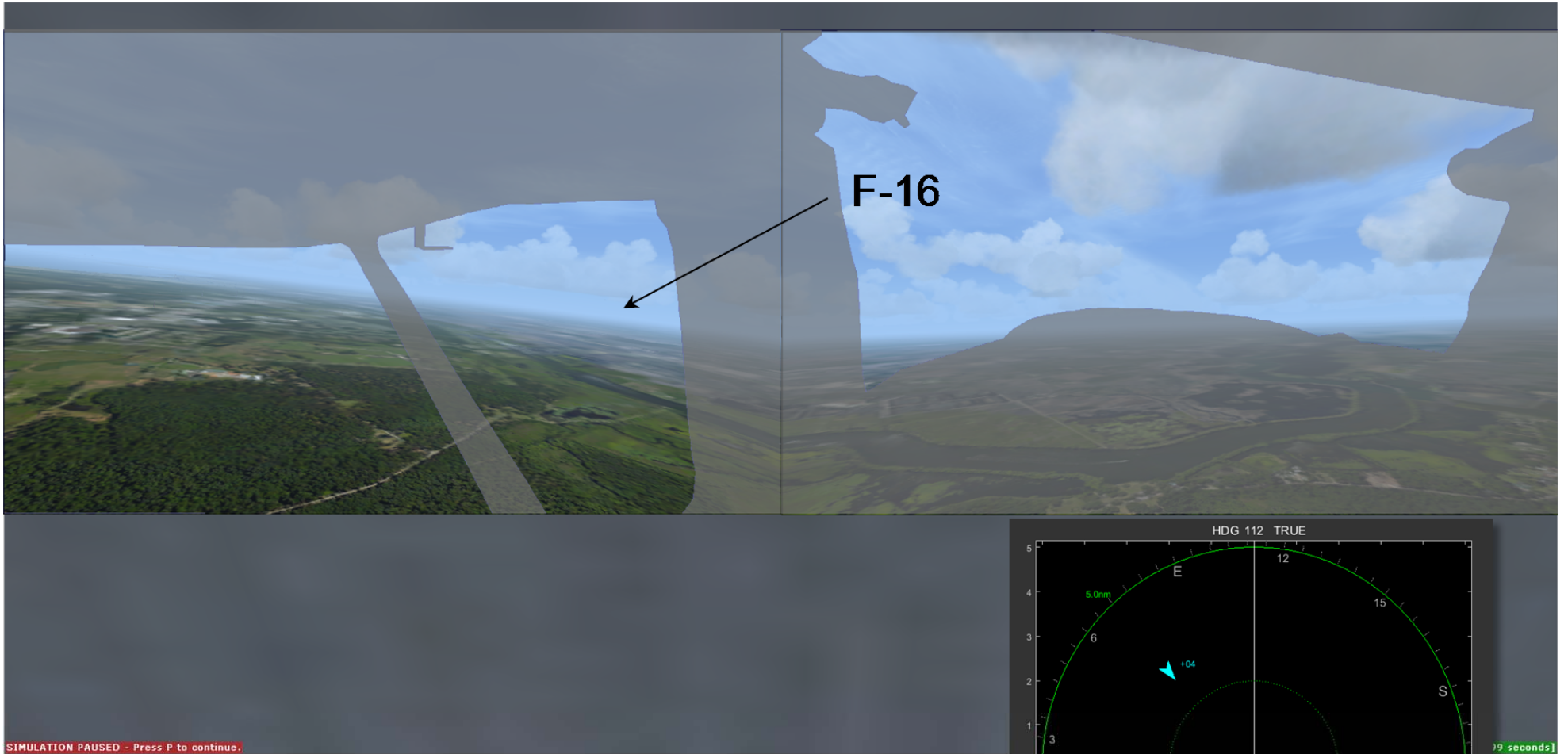
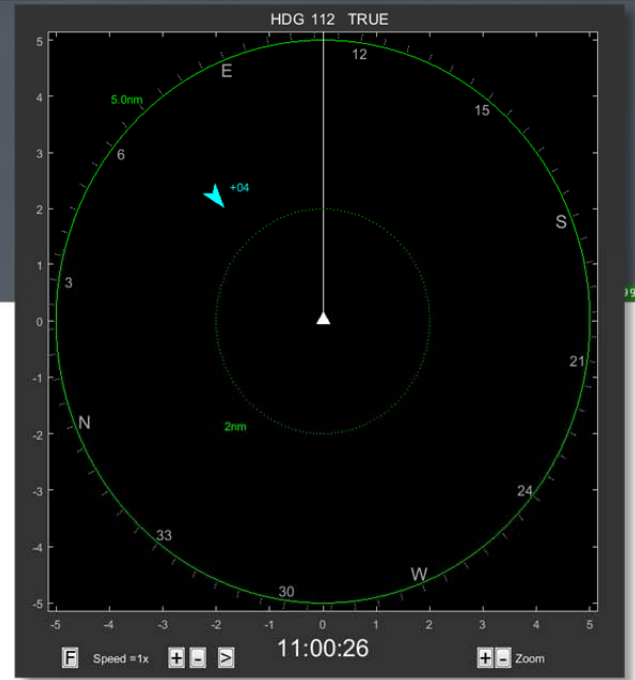
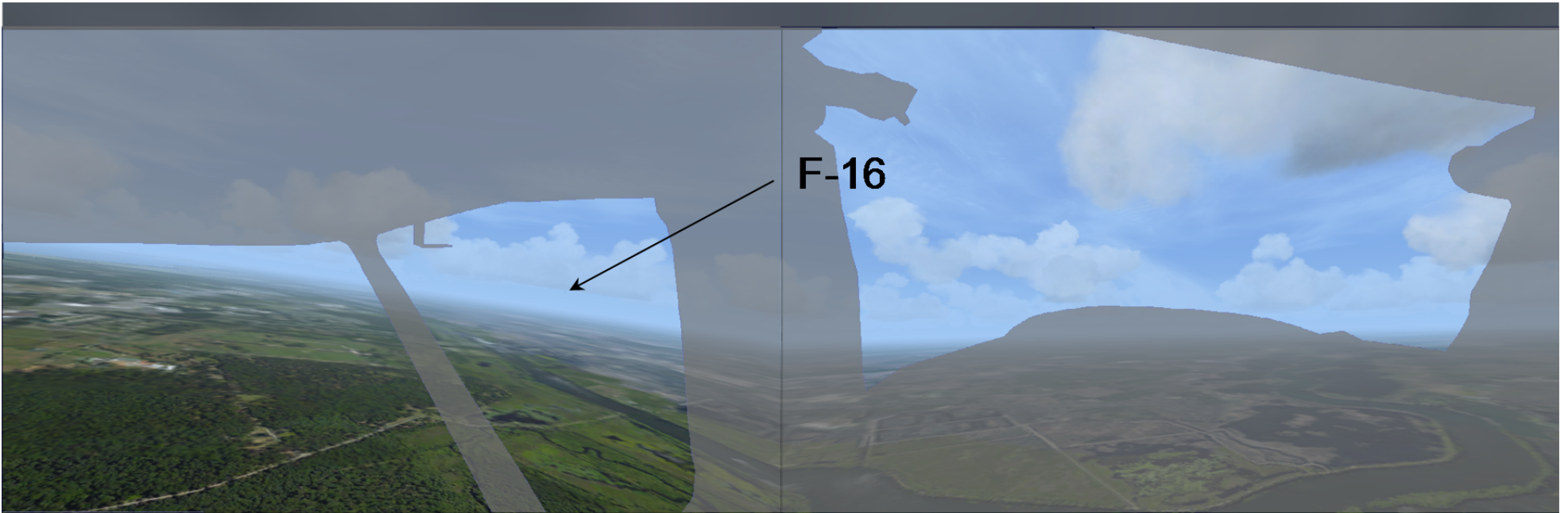


Figure 21e.

11:00:26





F-16

ATAS aural alert: "Traffic, 11 o'clock, high, 1 mile."

SIMULATION PAUSED - Press P to continue.

Figure 21f.

11:00:35



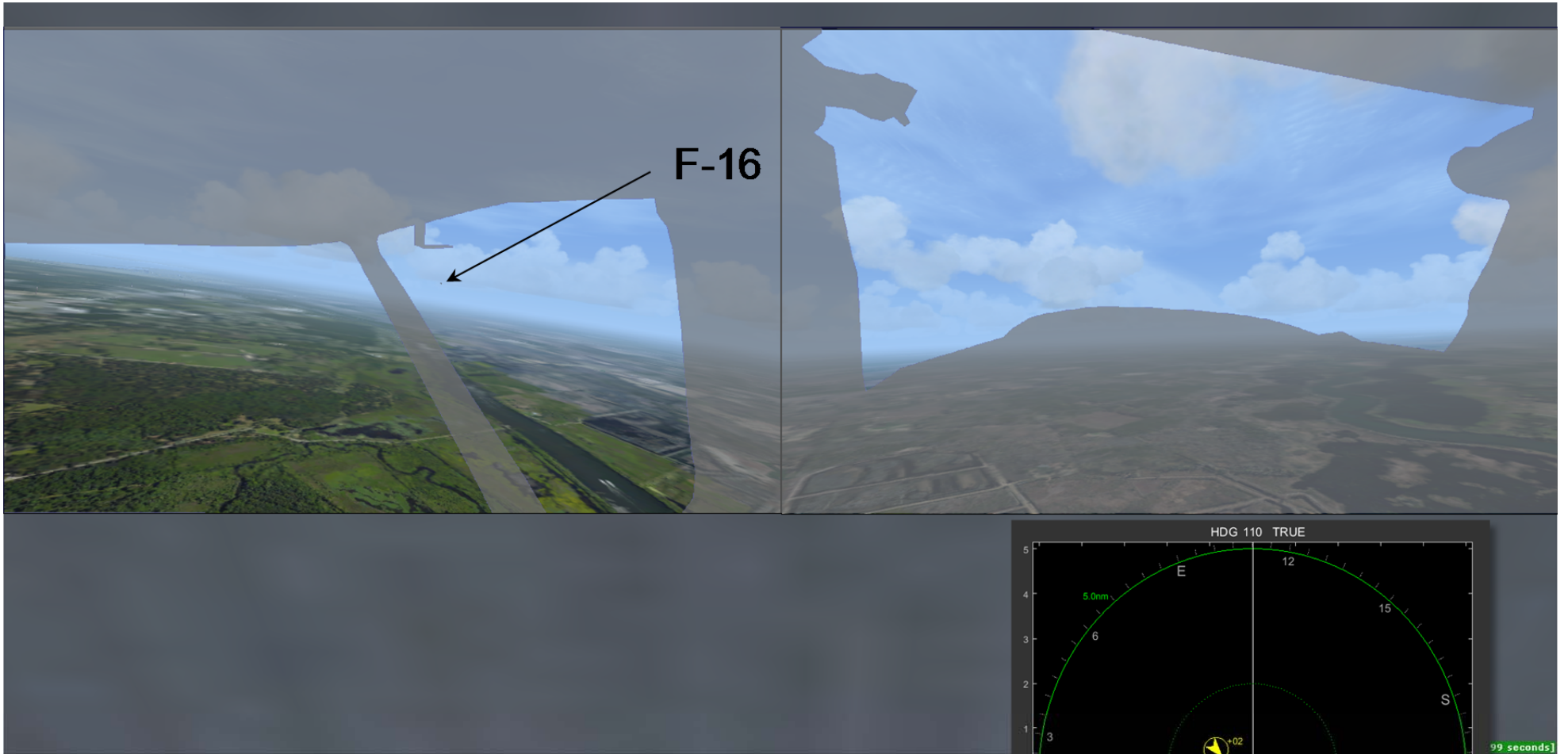


Figure 21g.

11:00:49



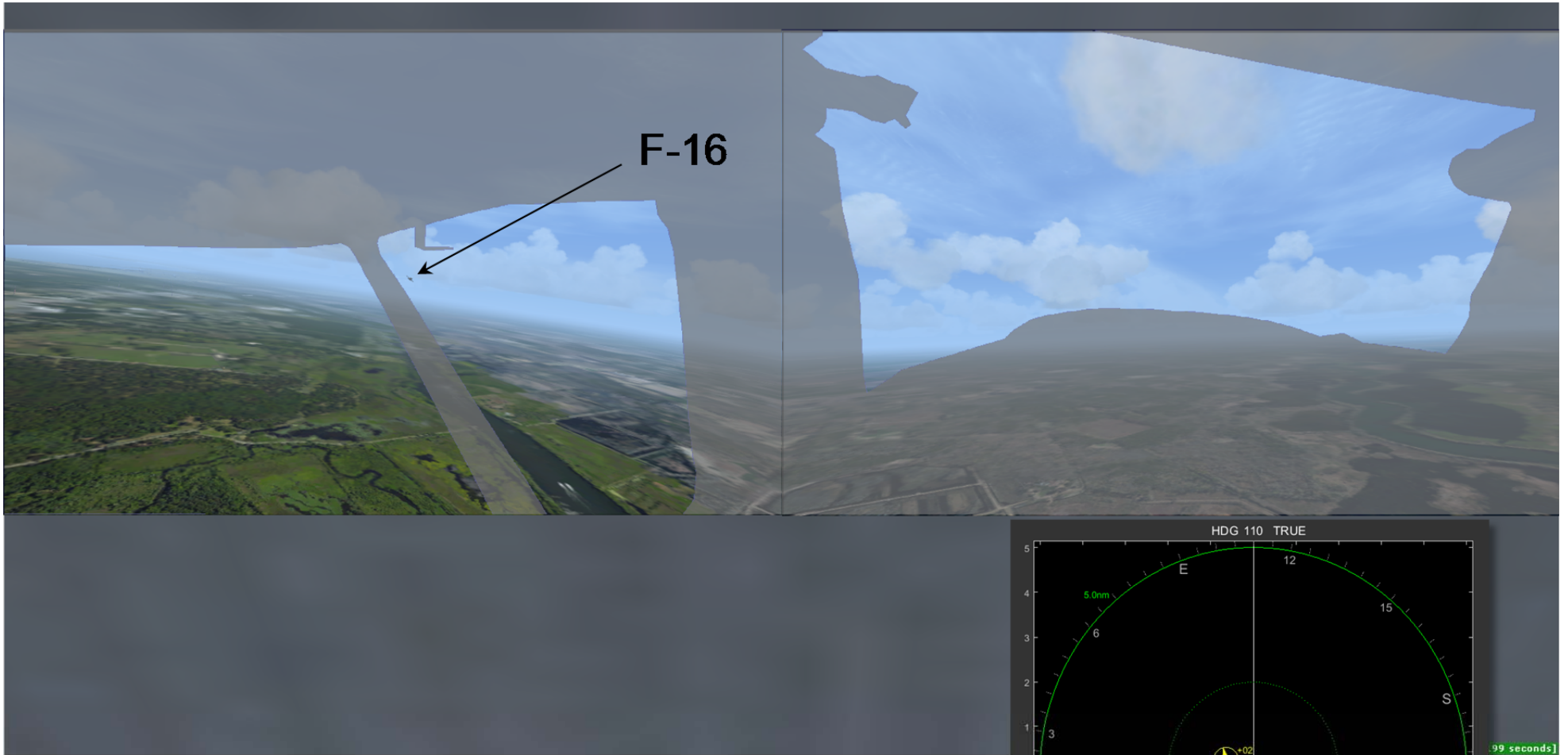


Figure 21h.

11:00:53



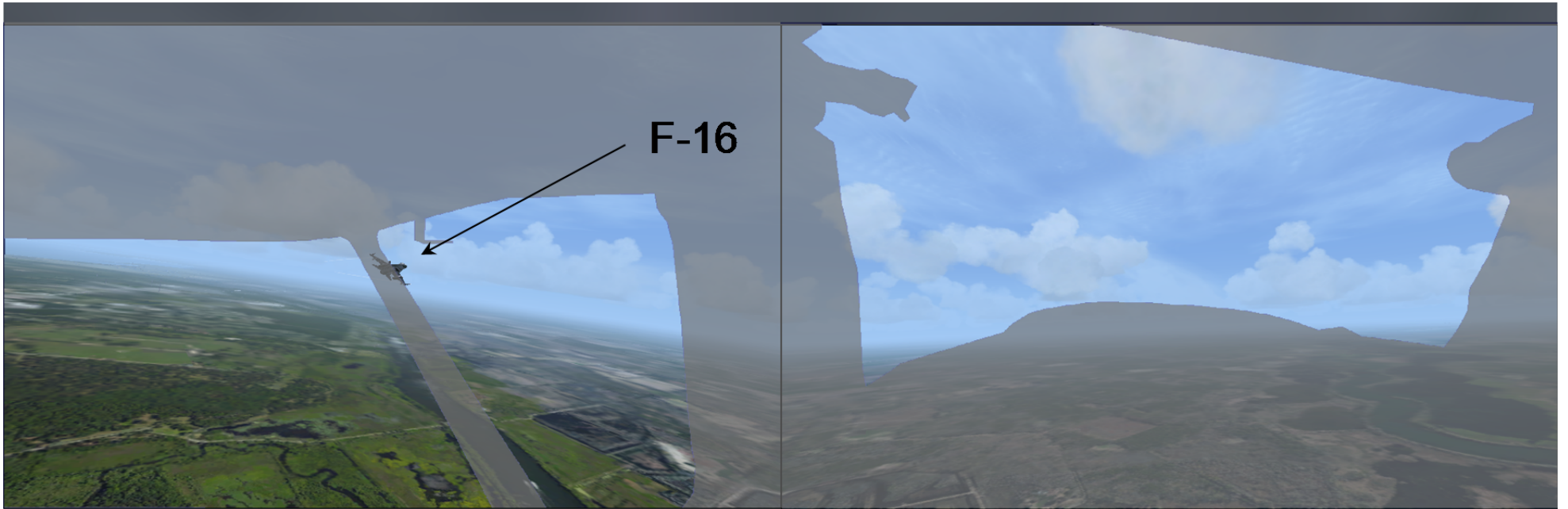


Figure 21i.

11:00:56



ERA15FA259AB: Midair collision, F-16 / C150, Moncks Corner, SC, 7/7/2015

"Target" airplane size growth vs. time

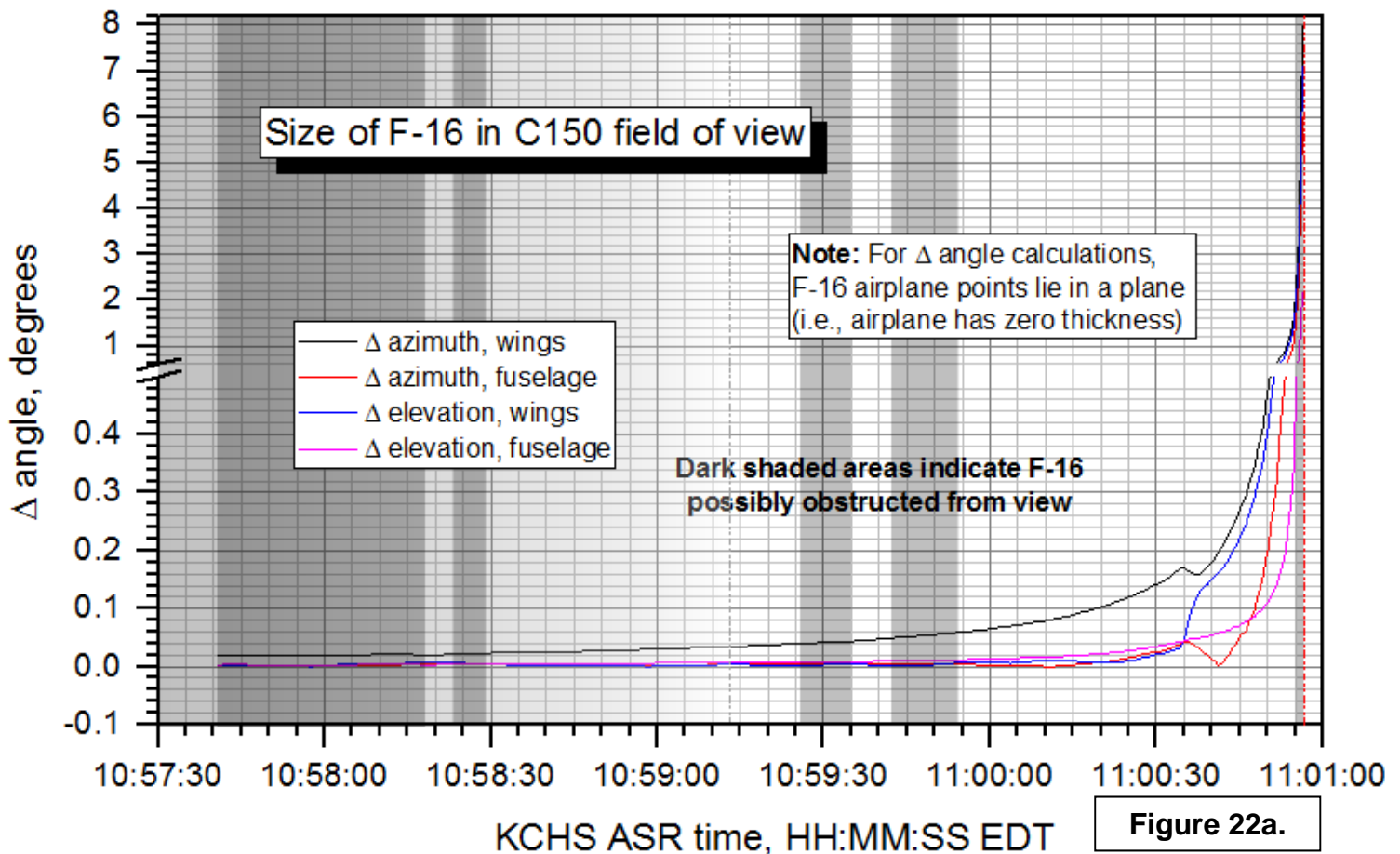
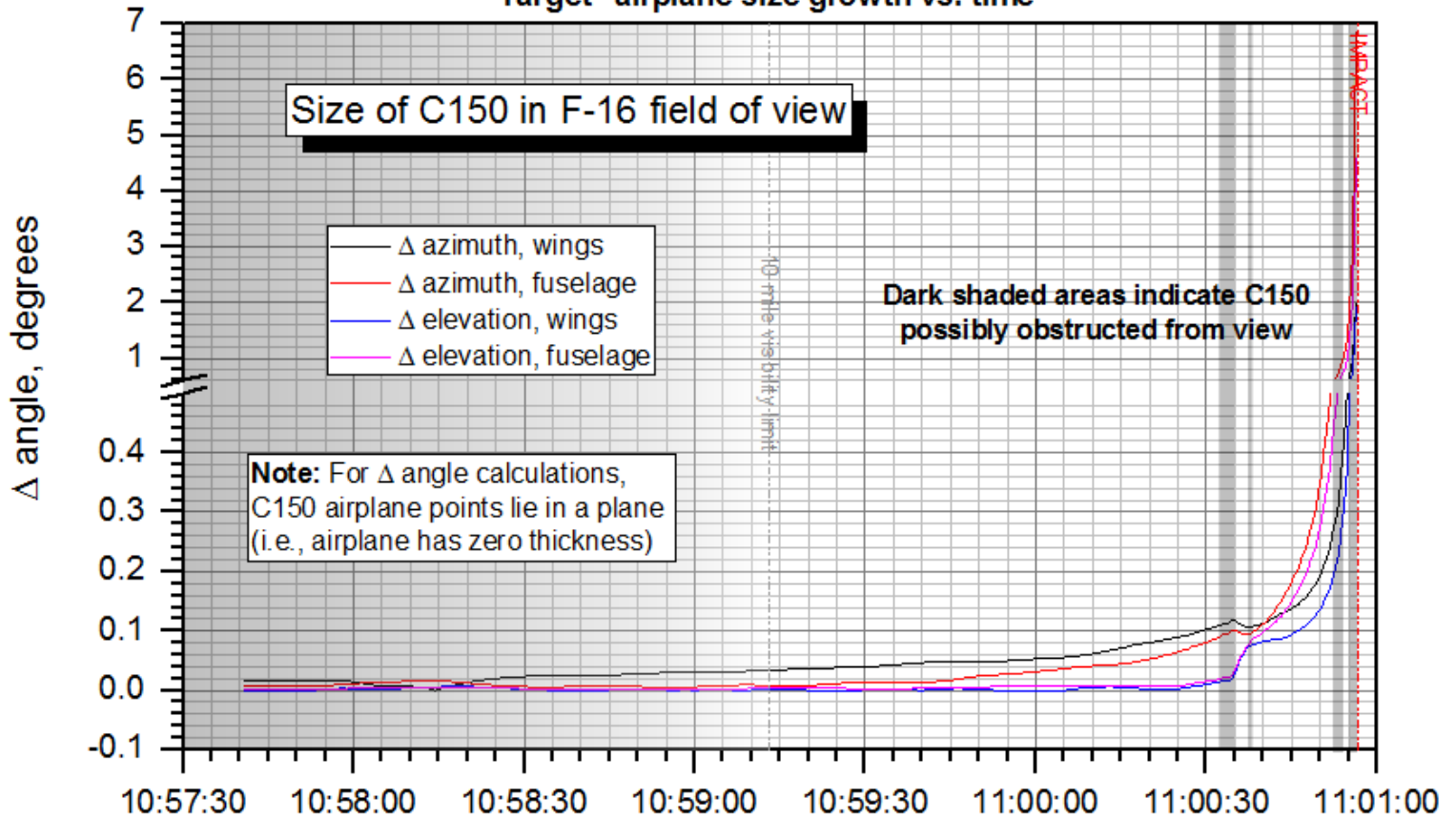
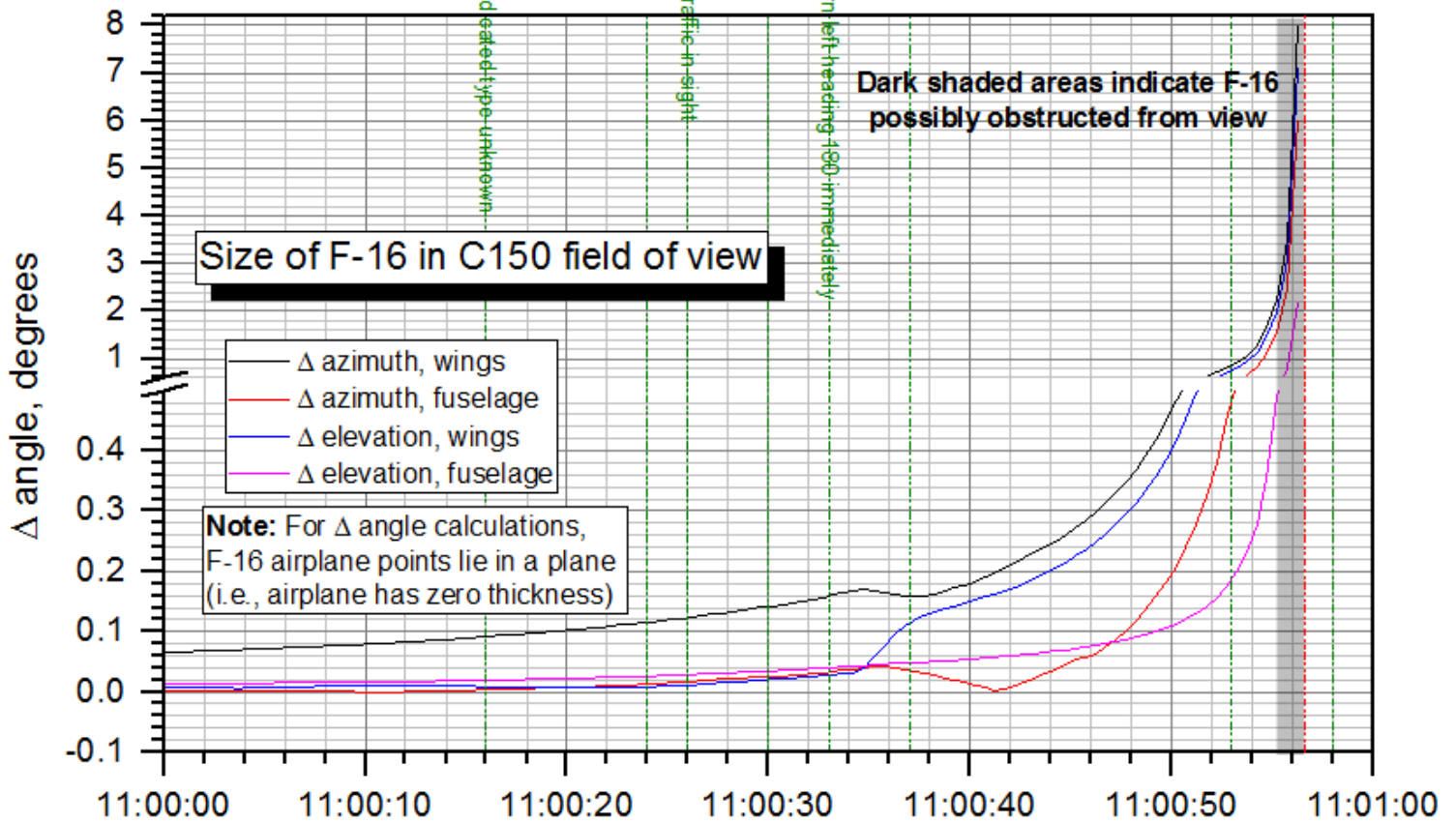
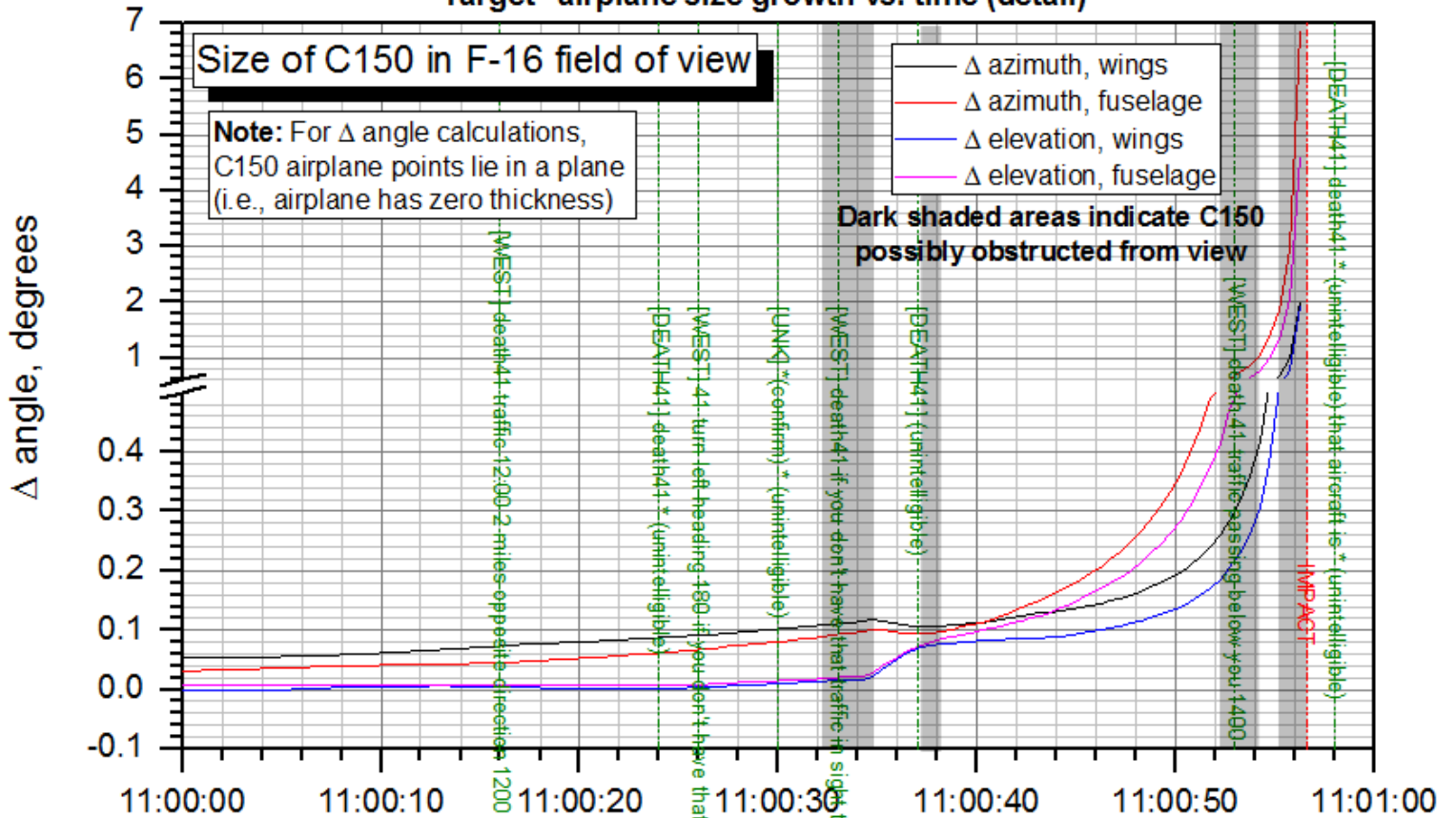


Figure 22a.

ERA15FA259AB: Midair collision, F-16 / C150, Moncks Corner, SC, 7/7/2015

"Target" airplane size growth vs. time (detail)



KCHS ASR time, HH:MM:SS EDT

Figure 22b.

APPENDIX A:

**Computing the Azimuth and Elevation Angles of
Airplane Cockpit Windows and other Structures from Laser Scans**

APPENDIX A: Computing the Azimuth and Elevation Angles of Airplane Cockpit Windows and other Structures from Laser Scans

Azimuth and elevations of “target” aircraft relative to “viewer” aircraft

The “visibility angles” from the “viewer” airplane to the “target” airplane correspond to the angular coordinates of the line of sight between the airplanes, measured in a coordinate system fixed to the viewer airplane (the viewer’s “body axis” system), and consist of the azimuth angle and elevation angle (see Figure A1). The azimuth angle is the angle between the x-axis and the projection of the line of sight onto the x-y plane. The elevation angle is the angle between the line of sight itself, and its projection onto the x-y plane. At 0° elevation, 0° azimuth is straight ahead, and positive azimuth angles are to the right. 90° azimuth would be out the right window parallel to the y axis of the airplane. At 0° azimuth, 0° elevation is straight ahead, and positive elevation angles are up. 90° elevation would be straight up parallel to the z axis. The azimuth and elevation angles depend on both the position of the viewer and target airplanes, and the orientation (yaw, pitch, and bank angles) of the viewer.

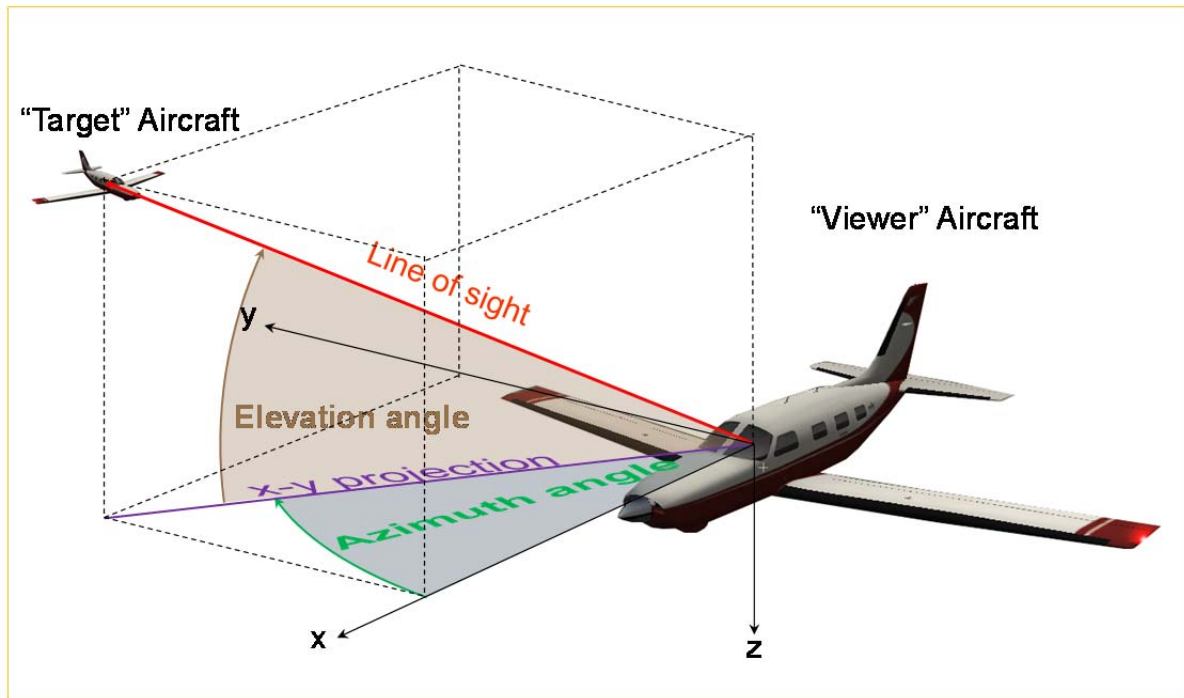


Figure A1. Azimuth and elevation angles from “viewer” airplane to “target” airplane.

The target airplane will be visible from the viewer airplane unless a non-transparent part of the viewer’s structure lies in the line of sight between the two airplanes. To determine if this is the case, the azimuth and elevation coordinates of the boundaries of the viewer’s transparent structures (windows) must be known, as well as the coordinates of the viewer’s structure visible from the cockpit (such as the wings). If the line of sight passes through a non-transparent structure (such as the instrument panel, a window post, or a wing), then the target airplane will be obscured from the viewer.

Azimuth and elevation angles of airplane structures from laser scans

The azimuth and elevation angles of the window boundaries and other structures of the airplane of interest can be determined from the interior and exterior dimensions of the airplane, as measured using a FARO laser scanner.¹ The laser scanner produces a “point cloud” generated by the reflection of laser light off of objects in the laser’s path, as the scanner sweeps through 360° of azimuth and approximately 150° of elevation. The 3-dimensional coordinates of each point in the cloud are known, and the coordinates of points from multiple scans (resulting from placing the scanner in different positions) are “merged” by the scanner software² into a common coordinate system. By placing the scanner in a sufficient number of locations so that the scanner can “see” every part of the airplane, the complete exterior and interior geometry of the airplane can be defined.

Coordinate transformations: scanner axes to body axes

The scanner software merges the point clouds from multiple scans into a single, “global” coordinate system. By default, this coordinate system is centered at the first scan location, which in general will not be coincident or aligned with the airplane body axis system. Hence, to compute azimuth and elevation angles of the scanned points relative to the pilot’s eyes, the following transformations must be accomplished:

1. Translate the scanner global coordinates to the origin of the airplane body axis system.
2. Transform the translated scanner global coordinates into the airplane body axis system using a transformation matrix defined by the three rotations required to align the scanner axis system with the body axis system.
3. Determine the location of the pilot’s eyes in the body axis system.
4. Determine the positions of the scanned points relative to the pilot’s eyes in the body axis system.
5. Compute the azimuth and elevation angles from the pilot’s eyes to the scanned points.

¹ Specifically, the FARO “Focus 3D” scanner; see <http://www.faro.com/focus/us>.

² FARO SCENE software: see <http://www.faro.com/focus/us/software>.

Note that to accomplish these steps, the following must also be known:

- The scanner global coordinates of the origin of the body axis system
- The three rotation angles between the scanner global coordinates and the body axis system

As will be shown below, these items can be determined from the scanned geometry of the airplane and the following known points:

- The scanner global coordinates at which the body x axis passes through the front and back of the airplane
- The body x coordinates of these points
- The scanner global coordinates of the left and right wingtips
- The body (x,y,z) coordinates of the wingtips

The body coordinates of the points listed above can be determined from technical or scaled drawings of the airplane.

The transformation equations and details of the steps outlined above can be derived starting from the sketch shown in Figure A2, where:

\vec{R}_{sb} = Vector from the origin of the scanner global axis system to the origin of the airplane body axis system

\vec{R}_s = Vector from the origin of the scanner global axis system to point P

\vec{R}_b = Vector from the origin of the airplane body axis system to point P

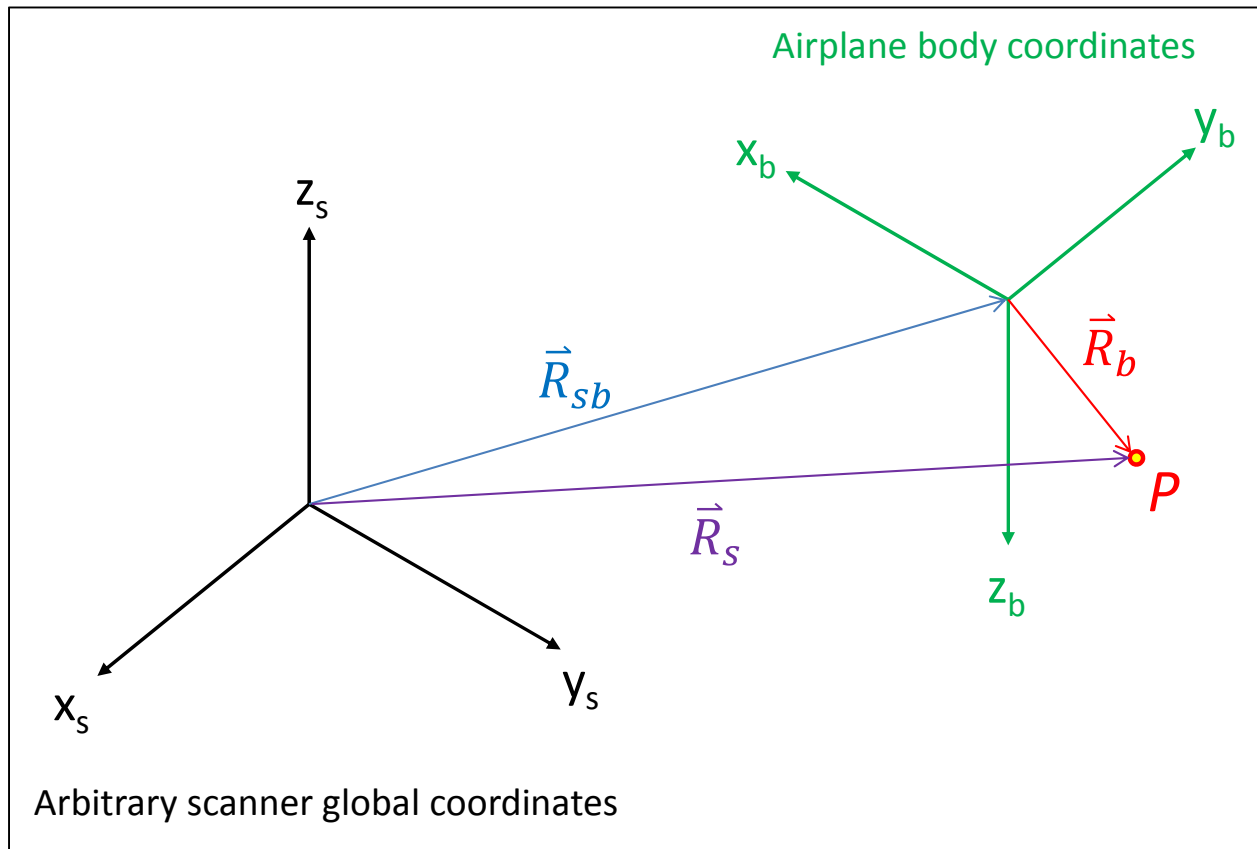


Figure A2. Vectors used to determine coordinates of point P in body axes coordinates.

The vectors \vec{R}_{sb} , \vec{R}_s , and \vec{R}_b are expressed in the scanner global coordinates. We would like to know the coordinates of point P in body axis coordinates; let \vec{r}_b be the vector from the origin of the body axis system to point P , expressed in body coordinates. Then, \vec{r}_b is simply \vec{R}_b transformed from scanner global coordinates to body axis coordinates. This transformation can be computed as follows. First, note that:

$$\vec{r}_b = \begin{Bmatrix} x \\ y \\ z \end{Bmatrix}_b = \text{coordinates of point } P \text{ from body axis origin, in body axes}$$

$$\vec{R}_b = \begin{Bmatrix} x \\ y \\ z \end{Bmatrix}_s = \text{coordinates of point } P \text{ from body axis origin, in scanner axes}$$

$$\vec{R}_s = \begin{Bmatrix} x_s \\ y_s \\ z_s \end{Bmatrix}_s = \text{coordinates of point } P \text{ from scanner axis origin, in scanner axes}$$

$\vec{R}_{sb} = \begin{Bmatrix} x_{sb} \\ y_{sb} \\ z_{sb} \end{Bmatrix}_s$ = coordinates of body axis origin from scanner axis origin, in scanner axes

From Figure A2,

$$\vec{R}_b = \vec{R}_s - \vec{R}_{sb} = \begin{Bmatrix} x_s \\ y_s \\ z_s \end{Bmatrix}_s - \begin{Bmatrix} x_{sb} \\ y_{sb} \\ z_{sb} \end{Bmatrix}_s = \begin{Bmatrix} x \\ y \\ z \end{Bmatrix}_s \quad [\text{A1}]$$

Equation [A1] translates the coordinates of point P from the origin of the scanner axis system to the origin of the body axis system, which is step 1 in the procedure outlined above. The coordinates are transformed into the body axis system (step 2 in the procedure) using a transformation matrix:

$$\vec{r}_b = [T_{sb}] \vec{R}_b \quad [\text{A2a}]$$

Or, equivalently,

$$\begin{Bmatrix} x \\ y \\ z \end{Bmatrix}_b = [T_{sb}] \begin{Bmatrix} x \\ y \\ z \end{Bmatrix}_s \quad [\text{A2b}]$$

Where $[T_{sb}]$ is the transformation matrix from the scanner axis system to the body axis system. This transformation matrix is defined by a series of three rotations of the scanner axis system, in the following order:

1. A rotation about the z_s axis through the angle ψ , yielding axes $(x'_s, y'_s, z'_s = z_s)$.
2. A rotation about the y'_s axis through the angle θ , yielding axes $(x''_s, y''_s = y'_s, z''_s)$.
3. A rotation about the x''_s axis through the angle ϕ , yielding axes $(x_b = x''_s, y_b, z_b)$.

There is a transformation matrix associated with each of these rotations; the elements of the matrices are sines or cosines of the rotation angles involved. Combining these transformations through matrix multiplication yields the final transformation matrix $[T_{sb}]$:

$$[T_{sb}] = \begin{bmatrix} \cos \theta \cos \psi & \cos \theta \sin \psi & -\sin \theta \\ \sin \phi \sin \theta \cos \psi - \cos \phi \sin \psi & \sin \phi \sin \theta \sin \psi + \cos \phi \cos \psi & \sin \phi \cos \theta \\ \cos \phi \sin \theta \cos \psi + \sin \phi \sin \psi & \cos \phi \sin \theta \sin \psi - \sin \phi \cos \psi & \cos \phi \cos \theta \end{bmatrix} \quad [\text{A3}]$$

The details of these operations can be found in textbooks about airplane dynamics (or other subjects associated with rigid body dynamics and coordinate transformations).³

³ See, for example, Roskam, Jan: Airplane Flight Dynamics and Automatic Flight Controls, Part I (Roskam Aviation and Engineering Corporation, 1979), pp. 24-27.

The reverse transformation (from airplane body axes to scanner axes) follows from Equations [2a] and [2b]:

$$\vec{R}_b = [T_{sb}]^{-1}\vec{r}_b = [T_{sb}]^T\vec{r}_b \quad [A4a]$$

$$\begin{Bmatrix} x \\ y \\ z \end{Bmatrix}_s = [T_{sb}]^{-1} \begin{Bmatrix} x \\ y \\ z \end{Bmatrix}_b = [T_{sb}]^T \begin{Bmatrix} x \\ y \\ z \end{Bmatrix}_b \quad [A4b]$$

Because the transformation matrix $[T_{sb}]$ is orthogonal, its inverse is equal to its transpose.

Note that Equations [A1], [A2b] and [A3] involve the coordinates of the origin of the body axis system in scanner axes $\{x_{sb}, y_{sb}, z_{sb}\}_s$, and the three rotation angles ψ , θ , and ϕ , which are all unknown and must be determined.

The coordinates $\{x_{sb}, y_{sb}, z_{sb}\}_s$ can be determined from the body axis coordinates of the points where the body x axis intersects the front and back of the airplane. It is assumed that these points are known from technical drawings of the airplane. It is also assumed that the location of these points can also be identified in the scanned point cloud by comparing the scan results to the technical drawings of the airplane, and that therefore the scanner coordinates $\{x_s, y_s, z_s\}_s$ of the points, measured from the scanner axis origin, can be determined using the scanner software.

Let $\{x_{sn}, y_{sn}, z_{sn}\}_s$ be the coordinates of the intersection of the body x axis with the front (nose) of the airplane, measured from the scanner axis origin, in scanner axes, as determined from the examination of the scanned point cloud using the scanner software.

Let $\{x_{st}, y_{st}, z_{st}\}_s$ be the coordinates of the intersection of the body x axis with the back (tail) of the airplane, measured from the scanner axis origin, in scanner axes, as determined from the examination of the scanned point cloud using the scanner software.

The distance along the body x axis from nose to tail is then

$$l_{nt} = \sqrt{(x_{sn} - x_{st})_s^2 + (y_{sn} - y_{st})_s^2 + (z_{sn} - z_{st})_s^2} \quad [A5]$$

Since the ratio of the distance between the body axis origin and the nose (i.e., $(x_n)_b$) to l_{nt} is the same in both the scanner and body axis coordinate systems, the scanner coordinates of the body axis origin, measured from the scanner axis origin, are given by

$$\begin{Bmatrix} x_{sb} \\ y_{sb} \\ z_{sb} \end{Bmatrix}_s = \begin{Bmatrix} x_{sn} \\ y_{sn} \\ z_{sn} \end{Bmatrix}_s + \left[\begin{Bmatrix} x_{st} \\ y_{st} \\ z_{st} \end{Bmatrix}_s - \begin{Bmatrix} x_{sn} \\ y_{sn} \\ z_{sn} \end{Bmatrix}_s \right] \frac{(x_n)_b}{l_{nt}} \quad [A6]$$

There remains to determine the rotation angles ψ , θ , and ϕ . From Equation [4b],

$$\begin{Bmatrix} x_n \\ y_n \\ z_n \end{Bmatrix}_s = \begin{Bmatrix} x_{sn} \\ y_{sn} \\ z_{sn} \end{Bmatrix}_s - \begin{Bmatrix} x_{sb} \\ y_{sb} \\ z_{sb} \end{Bmatrix}_s = [T_{sb}]^T \begin{Bmatrix} x_n \\ y_n \\ z_n \end{Bmatrix}_b \quad [A7]$$

Where $\{x_n, y_n, z_n\}_s$ are the scanner coordinates of the nose measured from the scanner origin, and $\{x_n, y_n, z_n\}_b$ are the body coordinates of the nose measured from the body origin. From Equations [A7] and [A3],

$$\{z_{sn} - z_{sb}\}_s = (-\sin \theta)\{x_n\}_b + (\sin \phi \cos \theta)\{y_n\}_b + (\cos \phi \cos \theta)\{z_n\}_b \quad [A8]$$

Since by definition the “nose” lies on the x body axis, $(y_n)_b = (z_n)_b = 0$, and Equation [A8] gives

$$\theta = \sin^{-1} \left(\frac{-\{x_n\}_b}{\{z_{sn} - z_{sb}\}_s} \right) \quad [A9]$$

Similarly, Equations [A7] and [A3] with $(y_n)_b = (z_n)_b = 0$ give

$$\{x_{sn} - x_{sb}\}_s = (\cos \theta \cos \psi)\{x_n\}_b \quad [A10]$$

$$\{y_{sn} - y_{sb}\}_s = (\cos \theta \sin \psi)\{x_n\}_b \quad [A11]$$

And therefore

$$\psi = \cos^{-1} \left(\frac{\{x_{sn} - x_{sb}\}_s}{\{x_n\}_b \cos \theta} \right) \quad [A12]$$

$$\psi = \sin^{-1} \left(\frac{\{y_{sn} - y_{sb}\}_s}{\{x_n\}_b \cos \theta} \right) \quad [A13]$$

These two equations for ψ allow the proper quadrant for ψ to be determined.

To solve for the remaining rotation angle (ϕ), the coordinates of the wingtips can be used. Let $\{x_{sl}, y_{sl}, z_{sl}\}_s$ be the coordinates of the left wingtip, measured from the scanner axis origin, in scanner axes, as determined from the examination of the scanned point

cloud using the scanner software. Similarly, let $\{x_{sr}, y_{sr}, z_{sr}\}_s$ be the corresponding coordinates for the right wing. The coordinates of the wingtips in body coordinates, measured from the body axis origin, are

$$\begin{Bmatrix} x_r \\ y_r \\ z_r \end{Bmatrix}_b = \begin{Bmatrix} x_w \\ y_w \\ z_w \end{Bmatrix}_b \text{ for the right wing, and}$$

$$\begin{Bmatrix} x_l \\ y_l \\ z_l \end{Bmatrix}_b = \begin{Bmatrix} x_w \\ -y_w \\ z_w \end{Bmatrix}_b \text{ for the left wing.}$$

From Equation [A4b],

$$\begin{Bmatrix} x_r \\ y_r \\ z_r \end{Bmatrix}_s = \begin{Bmatrix} x_{sr} \\ y_{sr} \\ z_{sr} \end{Bmatrix}_s - \begin{Bmatrix} x_{sb} \\ y_{sb} \\ z_{sb} \end{Bmatrix}_s = [T_{sb}]^T \begin{Bmatrix} x_w \\ y_w \\ z_w \end{Bmatrix}_b \quad [\text{A14}]$$

$$\begin{Bmatrix} x_l \\ y_l \\ z_l \end{Bmatrix}_s = \begin{Bmatrix} x_{sl} \\ y_{sl} \\ z_{sl} \end{Bmatrix}_s - \begin{Bmatrix} x_{sb} \\ y_{sb} \\ z_{sb} \end{Bmatrix}_s = [T_{sb}]^T \begin{Bmatrix} x_w \\ -y_w \\ z_w \end{Bmatrix}_b \quad [\text{A15}]$$

Then, from Equations [A14], [A15], and [A3],

$$\{z_{sr} - z_{sb}\}_s = (-\sin \theta)\{x_w\}_b + (\sin \phi \cos \theta)\{y_w\}_b + (\cos \phi \cos \theta)\{z_w\}_b \quad [\text{A16}]$$

$$\{z_{sl} - z_{sb}\}_s = (-\sin \theta)\{x_w\}_b + (\sin \phi \cos \theta)\{-y_w\}_b + (\cos \phi \cos \theta)\{z_w\}_b \quad [\text{A17}]$$

Solving Equations [A16] and [A17] for $\cos \phi$ gives

$$\cos \phi = \frac{\{z_{sl} - z_{sb}\}_s + \{z_{sr} - z_{sb}\}_s + 2(\sin \theta)\{x_w\}_b}{2(\cos \theta)\{z_w\}_b} \quad [\text{A18}]$$

Combining Equations [A16] and [A18] and solving for $\sin \phi$ gives

$$\sin \phi = \frac{\{z_{sr} - z_{sb}\}_s + (\sin \theta)\{x_w\}_b - (\cos \phi \cos \theta)\{z_w\}_b}{(\cos \theta)\{y_w\}_b} \quad [\text{A19}]$$

$\cos \phi$ and $\sin \phi$ then define the proper quadrant for ϕ , and ϕ itself. Now, Equations [A1], [A2b] and [A3] can be used to compute the body axis coordinates of any scanned point, starting from the scanner coordinates of that point.

Azimuth and elevation angles from body axis coordinates

Once the coordinates of the scanned points are available in the body axis system, the azimuth and elevation angles of these points relative to the pilot's eye position can be computed. In keeping with the previous notation, let $\{x_e, y_e, z_e\}_b$ be the body-axis coordinates of one of the pilot's eyes,⁴ and $\{x_p, y_p, z_p\}_b$ be the body-axis coordinates of a point P . Then the distance from the eye to point P is

$$l_{eP} = \sqrt{(x_p - x_e)_b^2 + (y_p - y_e)_b^2 + (z_p - z_e)_b^2} \quad [\text{A20}]$$

The azimuth angle from the eye to the point P is

$$\Psi = \tan^{-1} \left[\frac{(y_p - y_e)_b}{(x_p - x_e)_b} \right] \quad [\text{A21}]$$

The elevation angle from the eye to the point P is

$$\Theta = -\sin^{-1} \left[\frac{(z_p - z_e)_b}{l_{eP}} \right] \quad [\text{A22}]$$

⁴ Note that the pilot's left and right eyes are in slightly different positions, so these calculations should be made for each eye.

APPENDIX B:

**Creating Geometrically Correct Cockpit Window “Masks”
in Microsoft Flight Simulator X (FSX)**

APPENDIX B: Creating Geometrically Correct Cockpit Window “Masks” in Microsoft Flight Simulator X (FSX)

Field of view vs. FSX screen display coordinates

The geometry of an airplane’s cockpit windows and other structures can be defined in terms of their azimuth and elevation angles (Ψ and Θ , respectively) from the pilot’s eyes. The visual systems of flight simulation programs, such as *FSX*, include a “cockpit view” that similarly displays the cockpit and other airplane structures from the “pilot’s point of view.” The *FSX* “virtual cockpit,” in particular, depicts a 3-dimensional model of the airplane interior from the pilot’s seat (or any other point at which a “camera” is placed). The 3D model can be explored by rotating and / or translating the camera from the pilot’s eye position.

While many airplane models for *FSX* include “virtual cockpits” that are very convincing and satisfactory for gaming or flight training purposes, the geometrical accuracy of these models is unknown, and so they are not suitable for determining whether outside objects would be visible or obscured in the real airplane in any particular scenario. *FSX* also includes a simple “2D cockpit” view, which presents a forward-looking scene of the outside world, overlaid with an instrument panel that is a compromise between realism, and the desire to have all the necessary flight instruments (and a sufficiently large out-the-window view) visible to the user at the same time, given limited screen real estate. These “2D cockpits” are necessarily less representative of the real airplane than the “virtual cockpits.” However, the default 2D cockpit instrument panel can be substituted with a user-created “panel” that correctly represents the pilot’s view of the cockpit and airplane structures in the real airplane, as determined from the airplane geometry measured with a laser scanner (see Appendix A). This “geometrically correct” panel can be used to determine whether an object outside the airplane is obstructed from the pilot’s view.

The custom panel created by the user is a whole-screen instrument panel that contains transparent and non-transparent areas. The transparent areas correspond to areas of the windows that offer unobstructed views of the outside world; the non-transparent areas correspond to everything else (cockpit structure, and exterior structure visible from the cockpit that obstructs the outside view). The “panel” is simply a 1024 x 768 bitmap image file, in which transparent areas are defined by assigning pixels a particular color (e.g., black) that *FSX* interprets as “transparent.” Hence, the coordinates and color of the pixels in the bitmap file define the shapes of the panel transparent and non-transparent areas.

However, while the scope of the scene of the outside world displayed on the screen is defined in terms of angular and vertical “fields of view,” the screen coordinates of objects “seen” by the camera (including the cockpit windows) are not simply proportional to the angular Ψ and Θ coordinates of those objects from the camera position. Instead, the screen coordinates of an object correspond to the points where the line of sight from the camera to the object intercepts a flat surface (the screen) placed some distance R between the camera and the object, as shown in Figure B1 (this Figure, and the discussion below, is adapted from Reference B1).

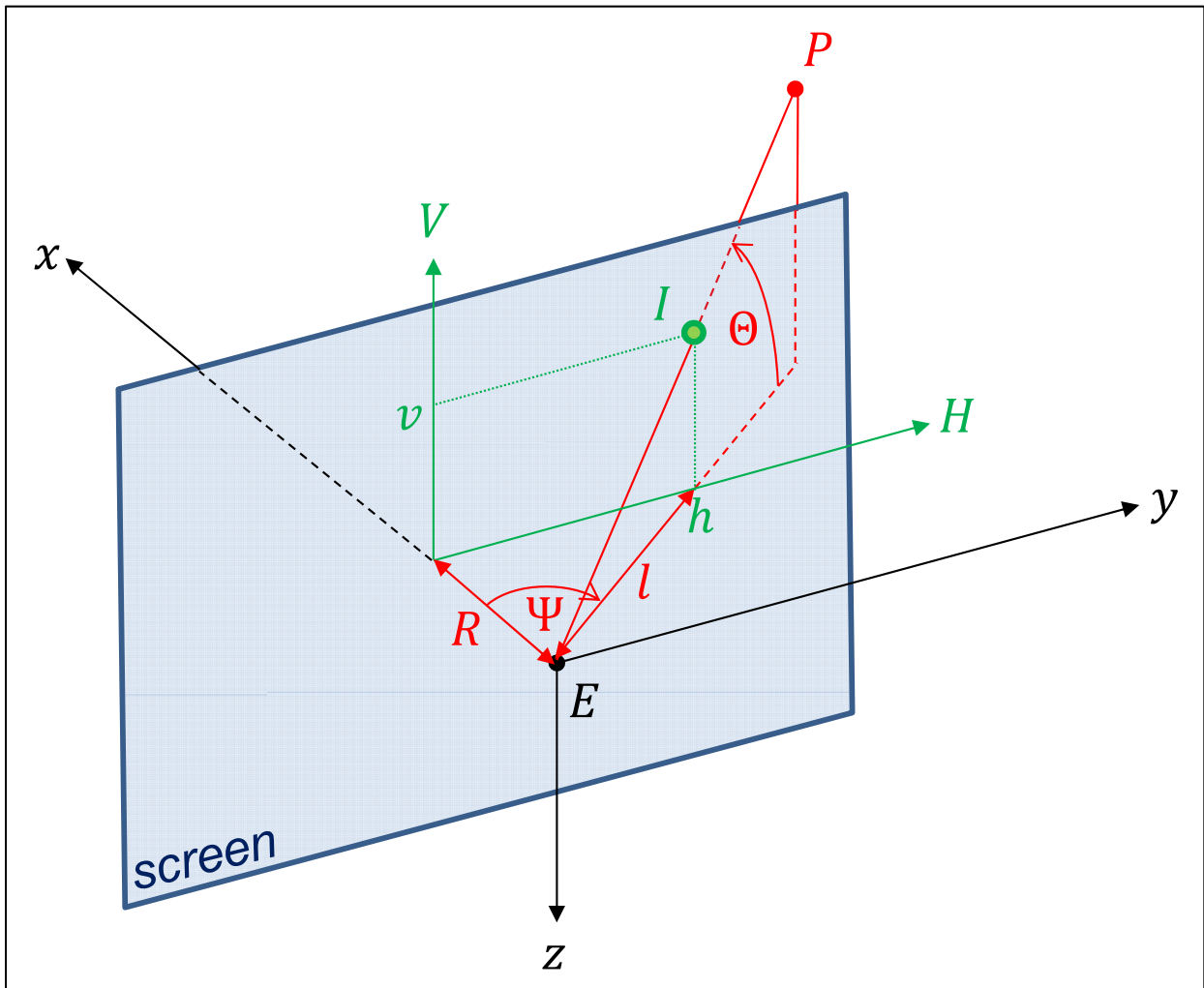


Figure B1. Relationships between the (Ψ, Θ) viewing angles of the line of sight from E to P (EP), and the (h, v) screen coordinates of the point I , where EP intersects the screen.

In Figure B1,

E = location of viewer's eye point (i.e., the camera location in *FSX*);

(x, y, z) = airplane body axis system with origin at E ;

P = location of point or object to be drawn on the screen;

EP = line of sight from E to P ;

Ψ = azimuth angle of EP ;

Θ = elevation angle of EP ;

I = point where EP intersects a flat screen placed in the yz plane between E and P ;

R = x coordinate of I (i.e., the distance from E to the screen along x axis);

(H, V) = screen horizontal and vertical axis coordinate system, originating where the x body axis intersects the screen;

(h, v) = screen coordinates of I ;

l = distance from E to the point defined by screen coordinates $(h, 0)$.

We seek to find the screen coordinates (h, v) at which a point P should be drawn, given the viewing angles (Ψ, Θ) from E to P .

From the geometry of Figure B1,

$$h = R \tan \Psi \quad [\text{B1}]$$

$$l = \sqrt{R^2 + h^2} = \sqrt{R^2 + R^2 \tan^2 \Psi} = R\sqrt{1 + \tan^2 \Psi} \quad [\text{B2}]$$

$$v = l \tan \Theta = R \tan \Theta \sqrt{1 + \tan^2 \Psi} \quad [\text{B3}]$$

Consequently, (h, v) can be computed from (Ψ, Θ) once the distance R is known. R can be determined in *FSX* if the angular range of the horizontal field of view (*HFOV*) and the width of the screen in pixels (w) are known. For example, at the right edge of the screen, $h = w/2$, and $\Psi = \text{HFOV}/2$. Then, from Equation [B1],

$$R = \frac{(w/2)}{\tan(\text{HFOV}/2)} \quad [\text{B4}]$$

Unfortunately, determining the exact *HFOV* in *FSX* is not straightforward. *HFOV* is modified by the *FSX* "zoom" level (smaller zoom yields greater *HFOV*), but the quantitative relationship between the zoom and *HFOV* is not specified in any *FSX* documentation. However, both the *HFOV* and vertical *VFOV* in *FSX* can be determined by experiment, using a method presented in Reference 2 and described below.

Determining the field of view in FSX

Reference 2 describes how to modify *FSX* .FLT files to customize the geometry (size, shape, and screen location) of *FSX* windows (in which visual scenes are displayed), and to control the cameras used to view the world in each window. Significantly, the camera position, orientation, and zoom level can be defined in the .FLT files.

The field of view of a window of a given shape and zoom level can be determined by creating a second window of similar shape and zoom level adjacent to the first. The camera in the second window is then rotated until the scene at the edge where the two windows meet match. The rotation of the camera required to accomplish this is known. Furthermore, the azimuth angle from the second camera to the common edge is half of the *HFOV*, and since the two windows are the same size, it is also half of the camera rotation angle. Hence, the *HFOV* is simply the rotation angle of the camera required to match the scene at the window edges (see Figure B2). This method can also be used to determine the *VFOV*.

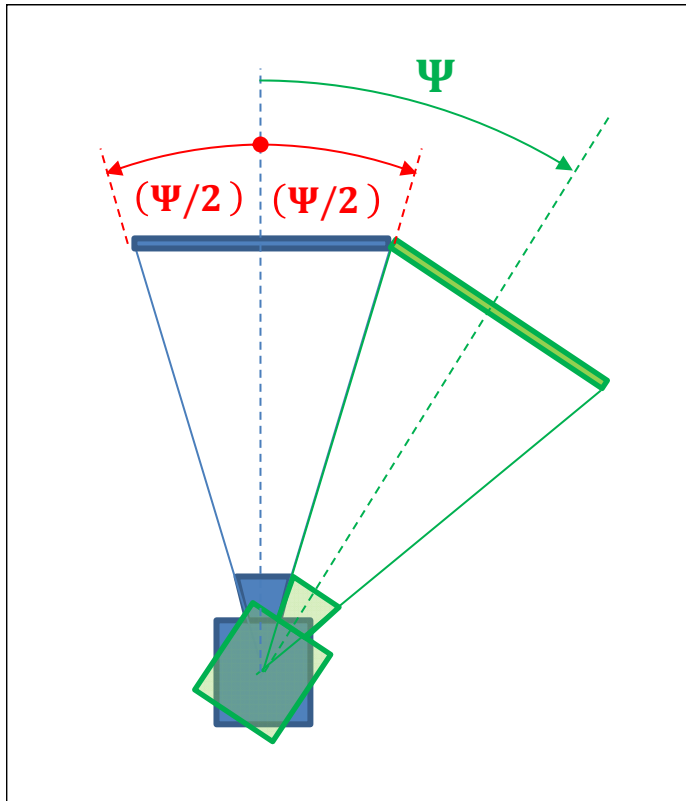


Figure B2. Determining the *HFOV* by rotating a second (green) camera through angle Ψ to match the scene at the boundary of the view from the first (blue) camera.

Experiments with this method indicate that the *HFOV* in *FSX* is a function of the window aspect ratio (width / height), as well as the *FSX* zoom level. Results using a window of aspect ratio of 1.6 and a zoom of 0.3 are shown in Figure B3. In this case, the *HFOV* is 90° and the *VFOV* is 61.8°. Per Equation [B4], *R* in this case would be equal to $w/2$.

Creating the FSX instrument panel “mask” bitmap file

With the value of *R* determined as described above, Equations [B1] and [B3] can be used to convert the (Ψ, Θ) viewing angles of the cockpit window structures into the (h, v) screen coordinates at which they should be drawn in order to be consistent with the outside scenery drawn by *FSX*. Once the (h, v) coordinates are in hand, the bitmap file defining the full-screen instrument panel “mask” can be created.

These bitmaps were created for this *Study* as follows.

1. First, the (h, v) coordinates of the windows were plotted into a graph with boundaries set equal to the horizontal and vertical resolution of the computer screen (i.e., the horizontal scale ranged from $-w/2$ to $+w/2$, and the vertical scale ranged from $-h/2$ to $+h/2$, where *w* is the screen width in pixels and *h* is the screen height in pixels); see Figure B4.
2. An image of the plot created in step 1 was pasted into Microsoft *PowerPoint*, and the graphical tools in *PowerPoint* were used to create a grey background covering the entire plot area, with black-filled polygons depicting the unobstructed areas of the window transparencies (see Figure B5).
3. The *PowerPoint* image was pasted into the *GIMP2* image-manipulation program, and resized to 1024 x 768, as required by *FSX*.
4. The *FastStone Photo Resizer 3.2* program was used to change the color depth of the bitmap to “4 (2 bit).” This step successfully compresses the bitmap into an “8 bit file,” as required by *FSX*.
5. The bitmap is specified in the *FSX panel.cfg* file for the desired airplane model. In addition, the windows that are to use the panel (with camera rotations defined to be consistent with the view created in the bitmap file) are created in the *FSX .FLT* files for the “flight” corresponding to the project. Details concerning configuring the *panel.cfg* and *.FLT* files can be found in the *FSX Software Development Kit (SDK)* documentation, and in Reference 2.

The instrument panel mask constructed per the steps illustrated in Figures B4 and B5 is shown in its finished form within *FSX* in Figure B6.

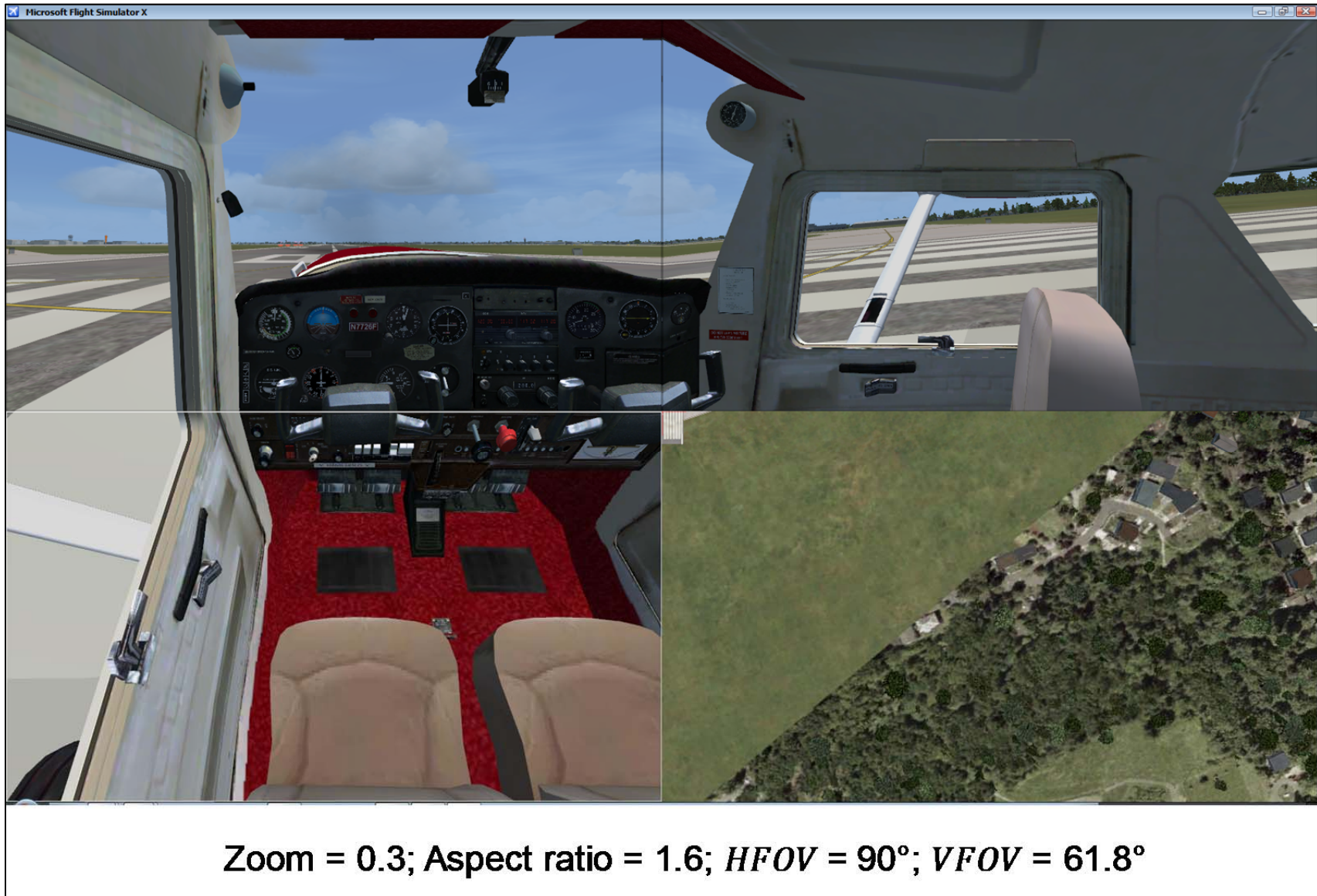


Figure B3. Application of the method for determining the $HFOV$ illustrated in Figure B2.

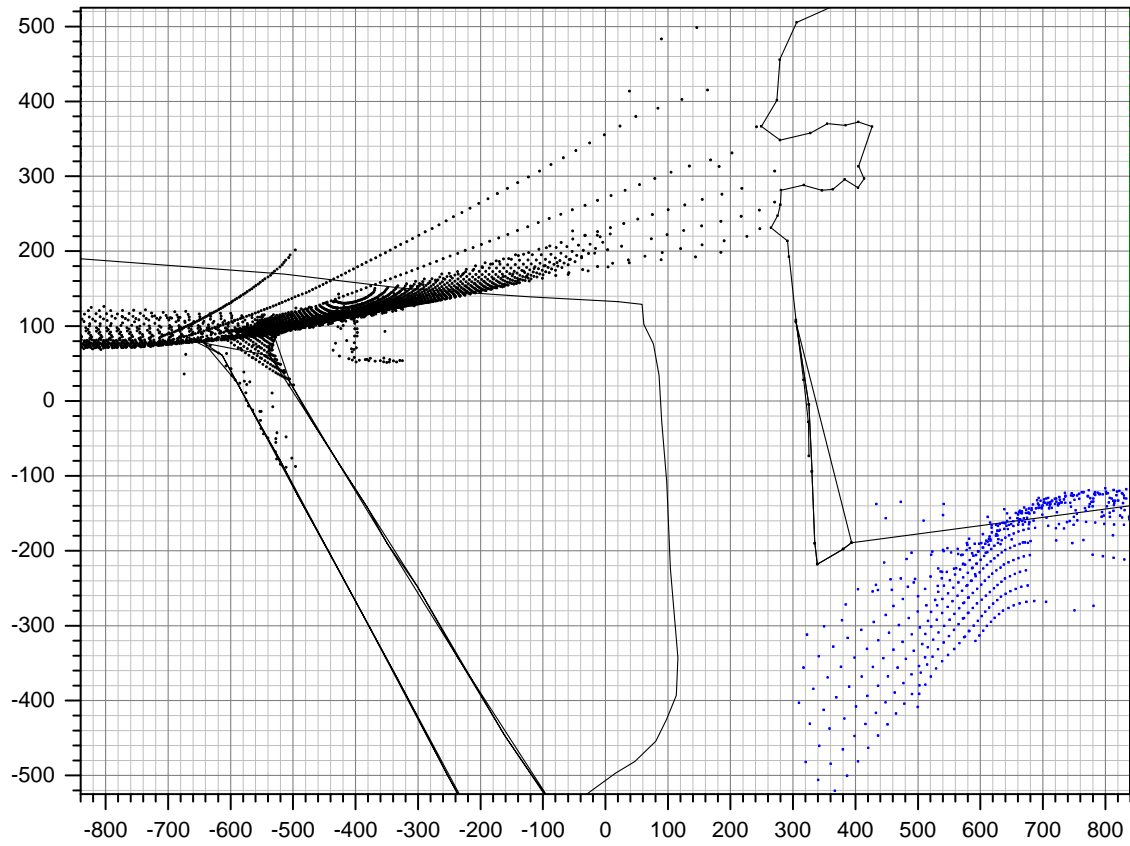


Figure B4. Plot of window v vs. h screen coordinates. The axis scales correspond to screen height and width.

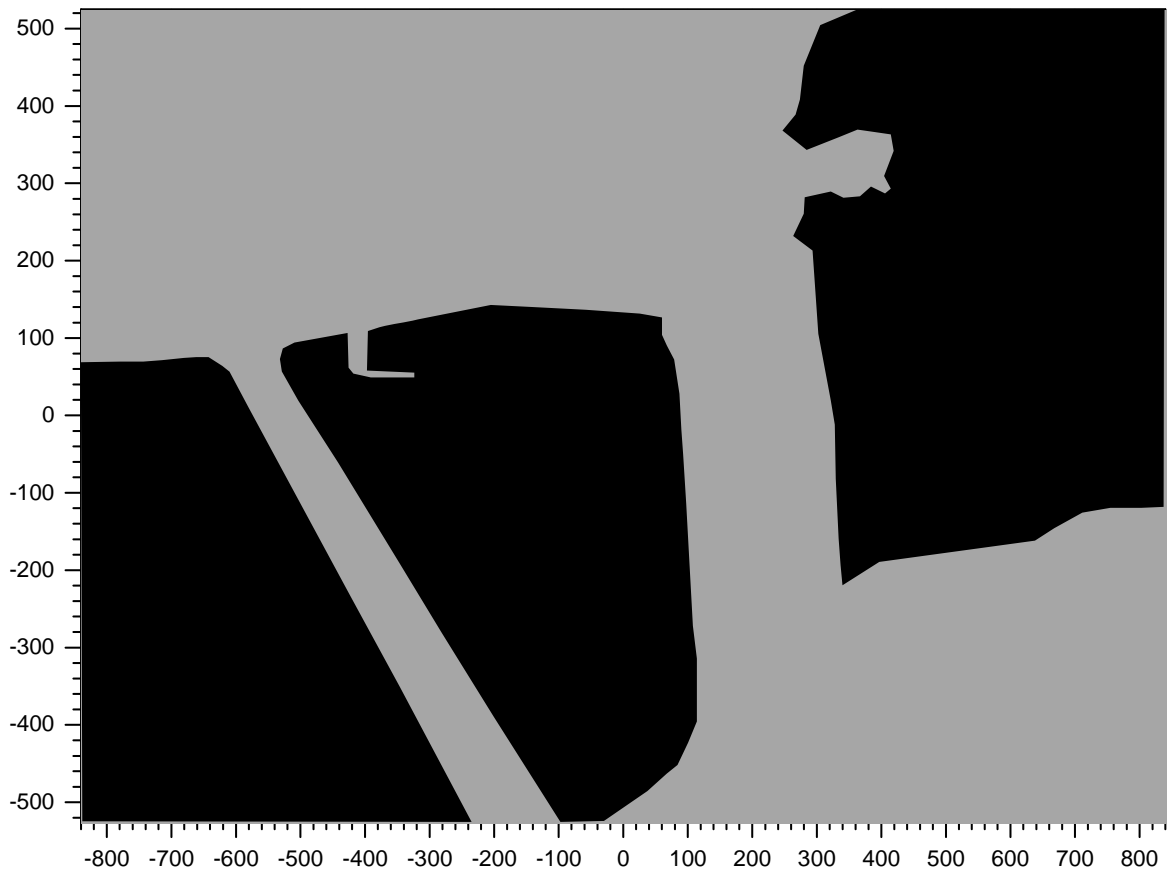


Figure B5. Black color applied to plot of Figure B4 to denote unobstructed window transparencies.

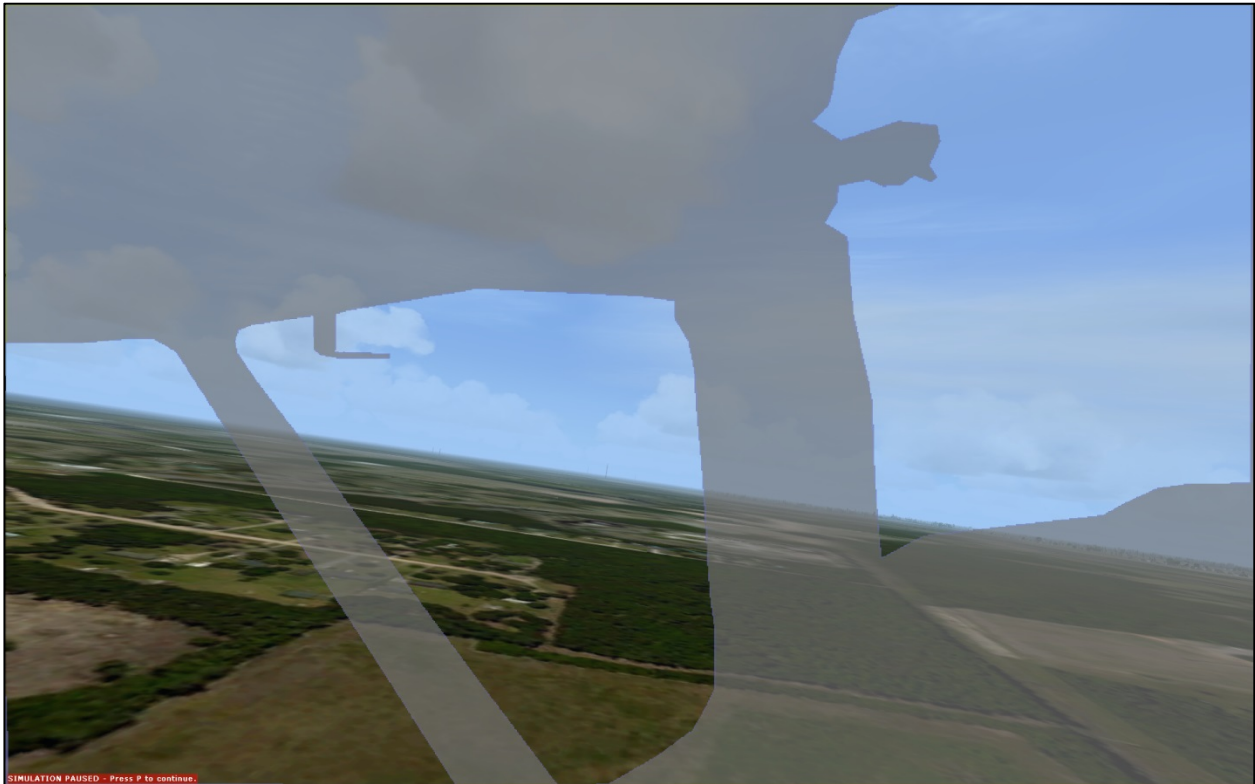


Figure B6. Finished instrument panel mask as it appears in *FSX*, with panel transparency set to 34%.

Joining windows in FSX to create larger field of view

As noted above, the maximum field of view available in a single *FSX* window is 90° , corresponding to the minimum available zoom level of 0.3. In this view, objects beyond an azimuth angle Ψ of $\pm 45^\circ$ (for a camera pointed straight ahead) will be outside the field of view and not visible.

To see objects beyond $\pm 45^\circ$ of azimuth while at the same time preserving a field of view of at least $\pm 45^\circ$ of azimuth about the direction of travel, the view from two co-located cameras can be joined side-by-side, with the second camera pointed in such a way that the boundaries of the fields of view of the cameras coincide at a particular azimuth angle. This method is illustrated in the top two images of Figure B3. In this Figure, the camera in the left image is pointed straight ahead ($\Psi = 0^\circ$), and the right boundary of its field of view is at $\Psi = +45^\circ$. The camera in the right image is rotated to $\Psi = +90^\circ$, and its left boundary is at $+90^\circ - 45^\circ = +45^\circ$ (coinciding with the right boundary of the image on the left). By setting the views from the cameras side-by-side, a continuous field of view from -45° to $+135^\circ$ is obtained.

However, discontinuities (kinks) in straight lines may appear at the boundary of these views when they are viewed side-by-side on a flat surface (such as a computer screen), because the viewer will be viewing both from the same angle, whereas one of the views is intended to be viewed at an angle rotated relative to the other. The discontinuities can be removed if each view is presented on a separate surface (monitor), and then the surfaces are joined at an angle equal to the relative rotation between the cameras (though this may be impractical). The discontinuities are apparent in Figure B3.

To use this method to increase the total field of view, and also use the user-defined instrument panel masks described above, a separate mask must be created for each camera view. In addition, the airplane *model.cfg* FSX file must be modified to comment out the line specifying the airplane interior model, so that this model does not get drawn and the instrument panel masks appear over a scene that only depicts the outside world.

References

1. Diston, Dominic J., *Computational Modeling and Simulation of Aircraft and the Environment, Vol. 1: Platform Kinematics and Synthetic Environment*, p. 58. Copyright © 2009, John Wiley & Sons, Ltd.
2. Hestnes, Ivar, *Visual System Tutorial, Rev. 1.0*. Available at <http://www.google.com/url?sa=t&rct=j&q=&esrc=s&source=web&cd=1&cad=rja&uact=8&ved=0ahUKEwiFkpCX-PDOAhVG7B4KHfVCCtAQFggcMAA&url=http%3A%2F%2Fwww.flightdeck737.be%2Fwp-content%2Fuploads%2F2011%2F03%2FVisual-system-tutorial.pdf&usq=AFQjCNFHJq7T3TRTvT4ylwOAm1PpzJc-Eg>